

NUCLEAR MATTER WITH REALISTIC HAMILTONIANS

BY

ISAAC LAGARIS *of 1981*

Dip., University of Ioannina, 1975
M.S., University of Illinois, 1977

THESIS

Submitted in partial fulfillment of the requirements
for the degree of Doctor of Philosophy in Physics
in the Graduate College of the
University of Illinois at Urbana-Champaign, 1981

Urbana, Illinois

NUCLEAR MATTER WITH REALISTIC HAMILTONIANS

Isaac Lagaris

Department of Physics

University of Illinois at Urbana-Champaign, 1981

ABSTRACT

The determination of the nuclear hamiltonian is a prerequisite for the development of a microscopic theory that would explain the structure and the properties of observed nuclei and neutron stars. The nuclear hamiltonian may contain terms associated with two, three and in general with many particle interactions. In principle it may be possible to derive the nuclear hamiltonian from meson theory (or quark theory if necessary) by eliminating all except the nucleon degrees of freedom. Since even the two-nucleon interaction is not completely understood from this fundamental point of view, the construction of the nuclear hamiltonian at present must be carried out phenomenologically. By studying the properties of two nucleon systems, we obtain realistic models of the two-nucleon interaction in the nuclear hamiltonian. Properties of bound states of many-nucleon systems need to be studied to obtain information about the three and more nucleon interaction.

In this thesis we first review some of the theoretical methods designed to handle the nuclear matter many-body problem. The emphasis is put on the variational theory developed by Pandharipande and Wiringa. This method treats the so called v_6 model, in which the two-nucleon interaction is assumed to have only central, spin, isospin and tensor components, and there are no many nucleon interactions. This model is not realistic; it does not fit most of the experimental data. However the solution of the v_6 problem is the basis on which a more complete theory, capable of handling the realistic two-nucleon potential models can be built.

A realistic v_{14} model of the two-nucleon interaction is obtained by fitting the available two-body data in S, P, D and F waves. This inter-

action has terms that are linear and quadratic in spin orbit and quadratic in the relative orbital angular momentum. The variational theory is extended to treat this realistic interaction model and nuclear matter properties are calculated with it neglecting many-nucleon interactions.

The results of these calculations show that the empirically known properties of nuclear matter, such as its ground state energy, equilibrium density and compressibility, cannot be explained by this nuclear hamiltonian that incorporates only two-body interactions. Results obtained with other realistic two-nucleon interactions also fail to reproduce the empirical nuclear matter properties. Hence we postulate a form for a three-nucleon interaction (TNI), inspired from the meson theory of nuclear interactions. Instead of attempting to develop a variational theory to treat TNI microscopically in nuclear matter, we parametrize the effect of TNI on the energy of nuclear matter with three parameters. These are varied to obtain the empirical energy, density and compressibility of nuclear matter. The results of our calculations show that the TNI contribution to the energy is much smaller than that of the two-body v_{14} interaction, as expected, and thus it may be reasonable to neglect four and more nucleon interactions in the nuclear hamiltonian.

The effective nuclear hamiltonian obtained in this work may be used to study the equation of state of hot and cold nucleon matter, the structure of neutron stars, and the volume part of the nucleon-nucleus optical potential. In the last section, the variational method is extended to study, with this hamiltonian, the equation of state of asymmetric matter.

The calculated symmetry energy is in reasonable agreement with the empirical data, and it is shown that the $(\frac{N-Z}{A})^{n>4}$ terms in the expansion of the energy of asymmetric matter are small.

ACKNOWLEDGMENTS

I wish to thank my advisor, Vijay R. Pandharipande for his patient support throughout this work. Without his guidance this work could not have been completed. To me, he has been more than a teacher. He has been a paternal figure, especially after the death of my father. He and his wife made me feel part of their family during my stay in Illinois, and for this I would like to thank both of them.

I would like to thank the other members of our group; my friends, R. Wiringa, K. Schmidt, B. Friedman, J. Carlson, Q. Usmani and S. Fantoni, for stimulating discussions. Special thanks are due to Dr. Kevin Schmidt for suggesting a recursion relation approach to a problem that appeared in our asymmetric nuclear matter studies.

I also want to thank Professors D. G. Ravenhall, P. Debevec, David Pines, A. Nathan and J. Smith for many helpful discussions. I am also indebted to Professor D. M. Miliotis, who helped me to come to the University of Illinois for graduate studies.

My mother and my late father offered me moral support and encouragement continuously. I wish I could thank them.

I enjoyed the companionship of many friends during my five year stay in Urbana-Champaign. I would like to thank them all and especially Dave Ackerman, Makis Bacahs, Kostas Dovantzis, Nikos Kylafis, Telemachos Mouschovias, Babbis Marinos, Makis Paleologou, Yorgos Papavassilopoulos, Poulikos Prastakos, Theodoros Politis, Grant Richards, George Roumeliotis, Tom Stadel and Lefteris Tsoukalas, for their constant friendship and loyalty.

I am thankful to Ms. Marilena Stone for her superb job and efficiency in typing this thesis.

This research was supported by the NSF Grant PHY78-26582 which is gratefully acknowledged.

TABLE OF CONTENTS

Chapter	Page
I INTRODUCTION.....	1
A. Nuclear Matter.....	1
B. Theoretical Approaches.....	2
C. Brueckner-Bethe-Goldstone Perturbation Theory.	3
D. The Variational Theory of Jastrow ⁷⁾	5
E. The Correlation Operator Method ⁹⁾	6
F. Comparison of Results Obtained with v_6 Models.	8
G. The Nucleon-Nucleon (N-N) Interaction.....	12
H. Three Nucleon Interaction (TNI).....	14
II The v_{14} POTENTIAL.....	16
III NUCLEAR MATTER CALCULATIONS.....	68
A. Euler-Lagrange Equations.....	68
B. Cluster Expansion of the Energy Expectation Value.....	72
C. Calculation of E_6	81
D. The Calculation of E_{LS}	92
E. The Calculation of E_{LS}^O	107
F. Results of Reid and v_{14}^O Models.....	113
IV THREE-NUCLEON INTERACTION CONTRIBUTIONS.....	118
V ASYMMETRIC NUCLEAR MATTER.....	128
A. Statement of the Problem.....	128
B. Results.....	131
C. Calculation of $E_{2B}(\rho, \beta)$	133
D. Calculation of Central Correlation Chains and W_0 (MB).....	143
E. β -Dependence of W_c and W_s	146
REFERENCES.....	150
VITA.....	154

I. INTRODUCTION

A. Nuclear Matter

In the course of attempting to develop a theory of observed nuclei, as a first step one considers nuclear matter (NM). NM is a fictitious infinite and uniform system of neutrons and protons interacting in the absence of the Coulomb field. It is thought to approximate the conditions in the interior of heavy nuclei. If the number of neutrons equals the number of protons in the system, it is called symmetric NM, otherwise it is referred to as asymmetric NM, which is the more general case.

The aim of the theory is to develop a reliable method to calculate the empirically known properties of NM, such as the ground state energy per nucleon, the equilibrium density, the symmetry energy, the compression, modulus etc., starting from a microscopic nuclear hamiltonian, and to provide a starting point for a microscopic theory of finite nuclei. Once a reliable many-body technique is devised it can also be used to test the various models for the nucleon-nucleon (N-N) interaction, and to study the properties of neutron stars, the only really extended system known to exist.

NM is characterized by its energy and the equilibrium density. The semiempirical mass formula for the energy per nucleon:

$$E = -\alpha_1 + \alpha_2 \left(\frac{N-Z}{A}\right)^2 + \alpha_3 A^{-1/3} + \frac{3e^2}{5r_0} Z^2 A^{-4/3} + \dots \quad (1.1)$$

shows that in the absence of Coulomb forces and in the limit $A \rightarrow \infty$ the energy per nucleon of NM is determined by the volume and the symmetry terms α_1 and α_2 . Typical values¹⁾ for α_1 are 15-16 MeV and 28-40 MeV for α_2 . The equilibrium density extracted from electron scattering experiments

is about .15-.16 nucleons/fm³.

A good theory should be able to calculate the equation of state $E = E(\rho, \beta)$ (β being the symmetry or polarization parameter $\beta = \frac{N-Z}{A}$) from any given hamiltonian. For $\beta=0$ (symmetric NM) the occurrence of a minimum in $E = E(\rho, \beta=0)$ will indicate both the equilibrium density ρ_0 and the ground state energy α_1 per nucleon.

The symmetry energy is obtained from:

$$E_{\text{sym}} = \frac{1}{2} \left. \frac{\partial^2 E(\rho, \beta)}{\partial \beta^2} \right|_{\beta=0, \rho=\rho_0} \quad (1.2)$$

The compression modulus:

$$K = 9 \rho^2 \left. \frac{\partial^2 E(\rho, \beta=0)}{\partial \rho^2} \right|_{\rho=\rho_0} \quad (1.3)$$

can also be calculated from the equation of state. Empirically²⁾ K is believed to be in the range of 210-250 MeV.

In principle it should also be possible to calculate many other properties of interest, such as the surface energy coefficient α_3 , the effective mass $m^*(\rho)$ etc., from the nuclear hamiltonian. However in this work we study only the $E(\rho, \beta)$.

B. Theoretical Approaches

The three primary techniques for solving many-body problems of the nature posed by NM or liquid helium are Monte Carlo³⁾ solution of the Schrödinger equation, Brueckner-Bethe-Goldstone (BBG) perturbation theory,^{4,5,6)} and the variational methods.⁷⁻¹¹⁾ These three approaches differ significantly in their goals, strength and limitations.

The Monte Carlo method calculates the ground state energy for a finite number of particles in a box with periodic boundary conditions

subject only to statistical sampling errors. To date, however, it has only been implemented for bosons, interacting with central two-body potentials. Hence it will not be described here.

The BBG approach originated by Brueckner et al.¹²⁾ and formulated by Goldstone¹³⁾ is a low density expansion whose convergence properties are still not rigorously established. It may be useful at NM densities, but its application to denser systems, like liquid helium or neutron star matter appears to be very difficult.

Variational theories do not have the density limitations of the BBG theory; on the other hand they have the drawback of calculating an upper bound and not the actual ground state energy itself. It is believed, however, that physically sensible trial wavefunctions will yield a bound reasonably close to the true minimum. Variational theories were under intensive development during the last few years, and by now the technical difficulties of the calculation seem to have been overcome.

C. Brueckner-Bethe-Goldstone Perturbation Theory

The hamiltonian is written in the following fashion:

$$H = H_0 + H_1 \quad (1.4)$$

where: $(T_i = -\frac{\hbar^2}{2m} \nabla_i^2$ denotes the kinetic energy operator)

$$H_0 = \sum_i (T_i + V_i) \quad , \quad (1.5)$$

$$H_1 = \sum_{i < j} v_{ij} - \sum_i V_i \quad . \quad (1.6)$$

The one-body Schrödinger equation:

$$(T + V)\phi_k = \epsilon_k \phi_k \quad (1.7)$$

defines the single particle energies ϵ_k and wavefunctions ϕ_k . Define the many-body non-interacting and interacting ground states and energies

as:

$$H_0 |\phi\rangle = E_0 |\phi\rangle, \quad (1.8)$$

$$H |\psi\rangle = (E_0 + \Delta E) |\psi\rangle. \quad (1.9)$$

Goldstone's theorem states that:¹³⁾

$$|\psi\rangle = |\phi\rangle - \frac{Q}{H_0 - E_0} H_1 |\psi\rangle, \quad (1.10)$$

with

$$Q = 1 - |\phi\rangle\langle\phi|, \quad (1.11)$$

so

$$\Delta E = \langle\phi|H_1|\psi\rangle. \quad (1.12)$$

One constructs the two-body reaction matrix:

$$\langle k_1 k_2 | G | p_1 p_2 \rangle = \langle k_1 k_2 | v | p_1 p_2 \rangle - \sum_{\substack{k' > k_F \\ p' > k_F}} \frac{\langle k_1 k_2 | v | k' p' \rangle \langle k' p' | G | p_1 p_2 \rangle}{\epsilon_{k'} + \epsilon_{p'} - \epsilon_{p_1} - \epsilon_{p_2}} \quad (1.13)$$

where:

$$\langle k_1 k_2 | v | p_1 p_2 \rangle \equiv \iint \phi_{k_1}^*(r_1) \phi_{k_2}^*(r_2) v(r_1, r_2) \phi_{p_1}(r_1) \phi_{p_2}(r_2) dr_1^3 dr_2^3. \quad (1.14)$$

The usual Hartree-Fock choice for the one-body potential is:

$$\langle k | V | k \rangle = \sum_{k' < k_F} [\langle k k' | v | k k' \rangle - \langle k' k | v | k k' \rangle]. \quad (1.15)$$

Brueckner¹²⁾ replaced v with the reaction matrix G in the matrix elements of (1.15) to obtain the one-body potential in equation (1.5). If one defines the two-body "uncorrelated" function

$$\phi_{12} = e^{-\frac{1}{2}(\vec{k}_1 - \vec{k}_2) \cdot \vec{r}_{12}} \quad (1.16)$$

and a two-body correlated function as:

$$v\psi_{12} = G\phi_{12} \quad (1.17)$$

then the "wound integral" κ :

$$\kappa = \rho \int |\phi_{12} - \psi_{12}|^2 dr_{12}^3 \quad (1.18)$$

estimates the probability that there is an unoccupied state below the Fermi surface. At NM density, with the Reid potential,¹⁴⁾ $\kappa \approx .15$. Brandow¹⁵⁾ has given arguments indicating that the contributions of BBG diagrams may be classified in powers of κ by the number of independent hole lines. The ground state energy up to two-body level is given by:

$$E = T_f + \frac{1}{2} \sum_{\substack{k < k_F \\ k' < k_F}} [\langle kk' | G | kk' \rangle - \langle k'k | G | kk' \rangle] \quad (1.19)$$

where T_f is the Fermi gas kinetic energy.

The contribution of three-body clusters is much more difficult to calculate, since in this case one obtains the required G-matrices by solving three-body Fadeev equations.^{16,17)} Day¹⁸⁾ and others¹⁹⁾ have also approximately estimated the contribution of four-body clusters, without solving the necessary four-body equations. Their results indicate that the hole-line expansion converges roughly in powers of κ . However κ increases as one considers three and four hole-line diagrams as well as it increases with ρ , a fact that limits the method to low densities.

D. The Variational Theory of Jastrow⁷⁾

The variational wavefunction in this theory ψ_J is taken to be of the form:

$$\psi_J = \prod_{i < j} f_J(r_{ij}) \Phi(\rho) . \quad (1.20)$$

The f_J is simply a function of the interparticle distance r and is usually parametrized in some way. The parameters are then varied to minimize the

variational energy E_J ,

$$E_J = \frac{\langle \psi_J | H | \psi_J \rangle}{\langle \psi_J | \psi_J \rangle} \quad (1.21)$$

The minimum of E_J gives an upper bound for E . E_J can be evaluated exactly with a Monte-Carlo integration. It can also be expanded in Mayer-cluster-diagrams which can be summed with chain summation techniques. The most popular technique uses the method of hypernetted chains (HNC). This method was developed by van Leeuwen et al.²⁰⁾ for Bose systems and was extended by Fantoni and Rosati²¹⁾ for Fermi systems (FHNC). HNC calculations in a wide variety of simple Bose systems by V. R. Pandharipande and K. E. Schmidt⁸⁾ show excellent agreement with the exact Monte-Carlo integrations.

The basic shortcomings of the choice (1.20) for ψ_J are that it does not allow for momentum dependence appropriate to interacting systems, the complicated operator dependence indicated by the N-N interactions, and does it allow for three or more body correlations. However, the simple Jastrow studies have been useful in providing a starting point for other more sophisticated many-body techniques one of which is described below.

E. The Correlation Operator Method⁹⁾

In this method the trial wavefunction has the form:

$$\psi = [S \prod_{i < j} F_{ij}] \phi \quad (1.22)$$

The presence of the symmetrizer S , is required because in general the two-body correlation operators F_{ij} and F_{jk} do not commute. The form of the correlation operator is dictated by the interaction Hamiltonian. The N-N interaction has strong central, spin, isospin, tensor and spin orbit components, and hence one expects that the correlation operator,

appropriate for NM calculations, should also display a similar structure.

It is taken to be:

$$F_{ij} = \sum_{p=1}^8 f^P(r_{ij}) O_{ij}^P \quad (1.23)$$

where the operators $O_{12}^{p=1,8}$ are:

$$O_{12}^{p=1,8} = 1, \sigma_{12}, \tau_{12}, \sigma_{12}\tau_{12}, t_{12}, t_{12}\tau_{12}, b_{12}, b_{12}\tau_{12} \quad (1.24)$$

$$\sigma_{12} = \vec{\sigma}_1 \cdot \vec{\sigma}_2, \quad \tau_{12} = \vec{\tau}_1 \cdot \vec{\tau}_2, \quad (1.25)$$

$$t_{12} = \frac{3\vec{\sigma}_1 \cdot \vec{r}_{12} \vec{\sigma}_2 \cdot \vec{r}_{12}}{r_{12}^2} - \vec{\sigma}_1 \cdot \vec{\sigma}_2, \quad (1.26)$$

$$b_{12} = \frac{1}{2} (\vec{\sigma}_1 + \vec{\sigma}_2) \cdot \vec{L}_{12}. \quad (1.27)$$

Here $\vec{\sigma}$ and $\vec{\tau}$ are Pauli matrices for spin and isospin respectively and \vec{L}_{12} is the relative orbital angular momentum between particles 1 and 2.

In principle the f^P 's should be determined by minimizing the energy expectation value:

$$E = \frac{\langle \psi | H | \psi \rangle}{\langle \psi | \psi \rangle}. \quad (1.28)$$

However, in practice the f^P 's are described by a few variational parameters, such as d , d_t , α , which vary the range and the strength of the correlations and the energy expectation value is minimized with respect to variations in d , d_t , α .

Bethe²²⁾ suggested in 1977 that the many-body theory of NM should be developed in a series of steps by considering homework potentials that

successively incorporate more and more sophistication. Pandharipande and Wiringa in a series of papers²³⁻²⁶⁾ carried out the calculation for the so called v_6 problem. This is a homework problem in which the N-N interaction is truncated to include only the first six operators $O_{12}^{p=1,6}$ of (1.24). In their work, the correlation operator is chosen to have the same operatorial structure with the potential, i.e.:

$$F_{ij} = \sum_{p=1}^6 f^p(r_{ij}) O_{ij}^p \quad (1.29)$$

An overview of the operator correlation method as applied to v_6 models is given in Section 3. In the present work, the correlation operator method is generalized to treat the v_8 homework problem. In this problem the potential has the eight operator components $O_{12}^{p=1,8}$ of (1.34) and so does the correlation operator, which is then given by (1.23). Additional techniques necessary to treat the spin-orbit operators have been developed and they are presented in Section 3, along with the details of the many-body calculation. Realistic potential models have additional operator components and they are treated semiperturbatively as presented in Section 3.

The many-body theory as formulated by Pandharipande and Wiringa is capable of treating symmetric NM, and neutron matter. This theory is extended to handle the more general problem of asymmetric NM. This is considered in Section 5, where the equation of state for asymmetric NM is obtained and the symmetry energy is calculated.

F. Comparison of Results Obtained with v_6 Models

At this point it is appropriate to compare the results that different many-body approaches yield for the v_6 homework problem. The equations of

state calculated with i) the Brueckner-Bethe-Goldstone (BBG), perturbation theory, that includes two, three and estimates of four body cluster contributions to the energy, ii) the correlation operator method with the symmetrized product prescription (SP), and iii) the theory developed by Owen,²⁷⁾ denoted by (IP), are shown in Fig. 1. Owen's theory uses, the so-called independent pair wavefunction (ψ_{IP}) which is given by:

$$\psi_{IP} = \prod_{i<j} f_{ij}^c [1 + \sum_{i<j} u_{ij} + \sum_{\substack{i<j,k \\ j \neq k < l}} u_{ij} u_{kl} + \dots] \phi \quad (1.30)$$

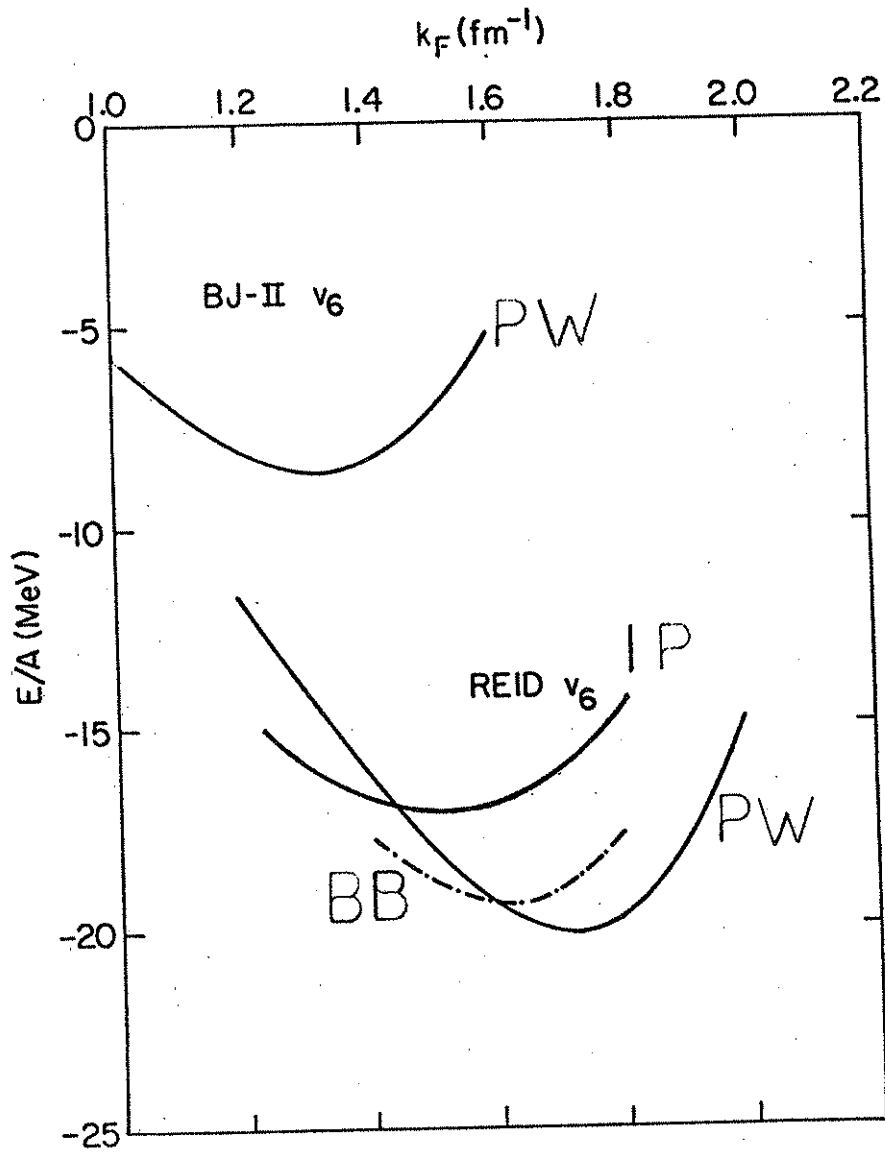
where:

$$u_{ij} = \sum_{p>1} [f^p(r_{ij})/f^c(r_{ij})] O_{ij}^p. \quad (1.31)$$

The SP wavefunction contains terms such as $\frac{1}{2} \sum_{ijk} \{u_{ij}, u_{jk}\}$ which are absent from ψ_{IP} . The lack of these terms in ψ_{IP} makes the evaluation of the Hamiltonian expectation value a lot easier.⁹⁾

Figure 1 shows that the IP curve lays above the BBG and the SP curves. This is to be expected since the ψ_{IP} is physically less plausible. It has been shown by variational calculations for the ground state energy of the ${}^3\text{H}$ nucleus²⁹⁾ that the use of the independent pair wavefunction yields energies $\sim 15\%$ higher than those obtained using the symmetrized product wavefunction. It seems that BBG theory and the SP variational theory for the v_6 problem are in excellent agreement. The error in the BBG calculation is ± 1.5 MeV at $k_F = 1.6 \text{ fm}^{-1}$. The error in the SP calculation has two origins. The error in the calculation of the energy is ± 1 MeV at $k_F = 1.7 \text{ fm}^{-1}$. However ψ_{SP} is not general enough, for example, it does not contain many-body correlations, so it only yields our upper bound, which could be about 1 MeV above the true minimum.²¹⁾





G. The Nucleon-Nucleon (N-N) Interaction

To our present understanding the N-N interaction has a long range part which is quite well described by the one pion exchange (OPE) process, an intermediate range part that is argued to result from the two-pion exchange (TPE) process with nucleon resonances as intermediate states, and a short range part about which very little is known. In most cases it is treated phenomenologically. Meson theories tend to attribute this part to the exchanges of heavier mesons (ρ, ω); also it is conceivable that this short range part is influenced by the quark structure of the nucleons. However neither meson theory nor the theory of quantum chromodynamics has been successful in modeling the N-N interaction, so at present one must resort to phenomenological potentials that fit the experimental data and are consistent with our fundamental knowledge of strong interactions.

A simple approach to construct potential models has been followed by Reid.¹⁴⁾ He decomposes his potential in J, T and S channels, where J, T and S are the total angular momentum, the isospin and spin of the interacting pair of particles. For S=0 his potential is simply a function of the interparticle distance r for every J and T.

$$v_{12}(J=L, T, S=0) = v_{J,T}(r_{12}) . \quad (1.32)$$

In S=1 channels his potential assumes the form:

$$v_{12}(J, T, S=1) = v_{J,T}^c(r_{12}) + v_{J,T}^t(r_{12})t_{12} + v_{J,T}^b(r_{12})b_{12} . \quad (1.33)$$

The various v's are parameterized and these parameters are determined by fitting the available experimental data channel by channel.

Alternatively the potential may be written as an operator:

$$V_{12} = \sum_{p=1}^8 v^p(r_{12}) O_{12}^p + \dots \text{ other terms } (L^2, (L \cdot S)^2, \nabla^2, \dots) . \quad (1.34)$$

The existence of the first eight operator components is uniquely indicated by the two-body scattering data, while the "other terms" are not. They may be chosen in many different ways. In this approach one considers the four (T,S) channels, and the data for all possible J values belonging to a T,S channel, are fitted simultaneously.

Variational many-body theories, by construction, need the operator representation of the N-N interaction in order to perform calculations. On the other hand BBG theory calculations use the N-N interaction in J,T,S channels. The advantage of the operator representation is that it can always be trivially decomposed in J,T,S channels and hence is employable by both theories. The channel representation cannot always be trivially, if at all, converted to an operator form.

In Section 2 we present a v_{12} model obtained from the Reid potentials in T,S,J channels. In addition to the standard eight operators of (1.34), it includes four L^2 dependent terms, denoted by:

$$O_{12}^{p=9,12} = q_{12}, q_{12}^\sigma, q_{12}^\tau, q_{12}^\sigma q_{12}^\tau \quad (1.35)$$

where q_{12} is a shorthand notation for the L_{12}^2 operator.

This model does not fit ${}^3D_{2,3}$ and 3F_J phase shifts quantitatively, and so it is not very realistic. A realistic model, known as the Paris interaction, was obtained by the Paris group.³⁰⁾ Unfortunately, as reported in Section 2, it is very difficult to treat it with our variational many-body theory. In the course of this work we constructed a realistic v_{14} potential model convenient for variational many-body calculations. This model has in addition to the twelve operator components of the v_{12}

model, two quadratic spin-orbit terms:

$$O_{12}^{p=13,14} = b_{12}^2, b_{12}^2 \tau_{12}. \quad (1.36)$$

It fits the scattering data in S,P,D and F waves up to 425 MeV. It is discussed in Section 2.

H. Three Nucleon Interaction (TNI)

The possibility that there are many-body forces between nucleons was proposed almost as soon as the meson theory of N-N interactions became known.³¹⁾ The subject was developed in terms of meson exchange theory in the 1950's and saw a revival in the late 1960's with the realization that current algebra techniques could be applied to the problem.³²⁾

An N-body potential is a term, in the potential energy of N bodies, which is an irreducible function of the coordinates of the N-particles. Irreducible in the sense that it cannot be written as a sum of functions of the coordinates of less than N particles. Naturally the case of three-body interactions was the one that attracted the most attention and effort. Some plausible processes that lead to a three-body potential are mentioned in Section 4. Microscopic NM calculations involving three-body terms in the nuclear Hamiltonian have been performed in the past, most of them in the framework of Bruckner theory.³³⁾ In these calculations the TNI is treated essentially in first order perturbation theory.

The results of NM calculations with realistic models given in Section 3, indicate that the two-body interactions alone are incapable of reproducing the empirical properties of NM, and that many-body interactions should be included in the nuclear Hamiltonian. This indication is also supported from studies on light nuclei,²⁹⁾ where if only two-body

interactions are considered, it seems to be impossible to explain their density distribution.

In Section 4, we parametrize the effect of a TNI on the NM energy, and adjust the parameters so that the empirical equation of state is obtained. Techniques required to treat the TNI in a non-perturbative, variational microscopic calculation are still under development.

II. THE v_{14} POTENTIAL

Recently we constructed a realistic potential to model the N-N interaction. Our goals in constructing this potential are:

- i) To obtain an interaction operator that fits well the data, and that is simple enough for variational many-body calculations.
- ii) Since such a potential is bound to have more than the standard eight operator components. The terms associated with $O^{p>8}$ should be weak, so that they can be treated semi-perturbatively.
- iii) The tensor part of this interaction should be weaker than that of the Reid potential. This is indicated from the analysis of the deuteron photodisintegration experimental data.³³⁾

This potential is written as:

$$v_{ij} = \sum_{p=1}^{14} v^p(r_{ij}) O_{ij}^p \quad (2.1)$$

where $v^p(r_{ij})$ are functions of the interparticle distance r_{ij} and $O_{ij}^{p=1,14}$ are the operators given by equations (1.24), (1.35) and (1.36).

The two nucleon interaction is written as:

$$v_{ij} = \sum_{p=1}^{14} (v_{\pi}^p(r_{ij}) + v_I^p(r_{ij}) + v_S^p(r_{ij})) O_{ij}^p \quad (2.2)$$

The one pion exchange potential (OPEP) $v_{\pi}^p(r_{ij})$ ³⁴⁾ is non-zero only for $p=\sigma\tau$ and $t\tau$:

$$v_{\pi}^{\sigma\tau}(r) = 3.488 \frac{e^{-.7r}}{.7r} (1 - e^{-cr^2}) \quad (2.3)$$

$$v_{\pi}^{t\tau}(r) = 3.488 \left(1 + \frac{3}{.7r} + \frac{3}{(.7r)^2}\right) \frac{e^{-.7r}}{.7r} (1 - e^{-cr^2})^2 \quad (2.4a)$$

$$\equiv 3.448 T_{\pi}(r) . \quad (2.4b)$$

The $1/r$ and $1/r^3$ singularities of the OPEP are removed, and the cutoff parameter c is determined by fitting the phaseshifts. Green and Haapakoski³⁵⁾ have recommended the $(1 - e^{-cr})^2$ cutoff arguing that it simulates the effect of ρ -exchange interaction. We have cutoff the Yukawa shaped $v_{\pi}^{\sigma\tau}(r)$ purely because the quark model suggests that the nucleon is not a point source, and so the two-nucleon interaction should not have a $1/r$ behavior at small r .

The $v_I^P(r)$ is attributed to two-pion exchange (TPE) processes with nucleon isobars in intermediate states. The tensor part of the OPEP is much stronger than the $\sigma\tau$ part. So the radial dependence of the TPEP should approximately be given by $T_{\pi}^2(r)$ and we take:

$$v_I^P(r) = I^P T_{\pi}^2(r) . \quad (2.5)$$

This choice of v_I also makes it simpler to introduce effects of three nucleon interactions, as discussed in Section 4. The strengths I^P are determined by fitting the phase shifts.

Traditionally the short range interaction $v_S^P(r_{ij})$ is attributed to ω, ρ exchange, and taken to have a Yukawa shape. However, since the believed size of nucleon is at least of the order of the Compton wave length of ω and ρ mesons, the Yukawa shape will be very much modified. Hence we take the $v_S^P(r_{ij})$ to be a sum of two Woods-Saxon potentials:

$$v_S^P(r) = S^P W(r) + S'^P W'(r) , \quad (2.6)$$

$$W(r) = (1 + \exp((r-R)/a))^{-1} , \quad (2.7)$$

$$W'(r) = (1 + \exp((r-R')/a'))^{-1} . \quad (2.8)$$

It is possible to obtain reasonable fits to the scattering data with $S^1P = 0$ for all p except b and $b\tau$. The spin-orbit potential in $T=1$ states has to need a smaller range than that of the central core to fit the scattering data. Hence we need the $W'(r)$ terms for $p=b$ and $b\tau$. We note that the parameterization of our interaction has similarities with that used by Hamada and Johnston³⁶⁾ and by Brussel, Kerman and Ruben.³⁷⁾

The values of the parameters are determined by fitting the neutron-proton phase shifts obtained by Arndt, Hackman and Roper³⁸⁾ by energy dependent analysis. Consideration was given to 1) phases obtained by energy independent analysis, 2) a more recent analysis by Arndt³⁹⁾ of $E1$ in 3S_1 - 3D_1 channel, and 3) the recent analysis of Bugg et al.,⁴⁰⁾ particularly in regions where energy dependent and independent analysis give different phases. The phase shifts up to 425 lab energy are fitted; not because we believe that a nonrelativistic model is adequate at such energies, but because if one wants to correct for effects of relativistic kinematics⁴¹⁾ it may be useful to start from a nonrelativistic potential that indeed fits the scattering data.

There is some evidence that the N-N interaction has a charge dependence. Since nuclei generally have more neutrons than protons, and neutron stars have mostly neutrons, it may be better to fit the $T=1$ interaction to n-n data. However, n-n data is nonexistent, and so we fit the n-p data. The ${}^3\text{He}$ - ${}^3\text{H}$ mass difference suggests that the n-n interaction is a little more attractive than the p-p,⁴²⁾ and the n-p scattering data also suggests that the n-p interaction is a little more attractive than the p-p. From a practical point of view, one does not have to compute Coulomb functions for fitting the n-p scattering.

In the singlet channels, the v_{14} potential takes the form (we use $v_{T,S}$ to denote potentials in states having pair isospin and spin T,S):

$$v_{T,0} = \sum_{p=c,q} (S_{T,0}^p W(r) + I_{T,0}^p T_{\pi}^2(r)) O^p + v_{\pi,T,0}; \quad (2.9)$$

whereas in triplet states:

$$v_{T,1} = \sum_{p=c,t,b,q,bb} (S_{T,1}^p W(r) + S_{T,1}^{\prime p} W'(r) + I_{T,1}^p T_{\pi}^2(r)) O^p + v_{\pi,T,1}. \quad (2.10)$$

The strengths $S_{T,S}^p$, $S_{T,S}^{\prime p}$ and $I_{T,S}^p$ are determined from the fits, the S^p , $S^{\prime p}$ and I^p are trivially obtained from these. The $S_{T,S}^p$ and $I_{T,S}^p$ are given in Tables I and II, while the complete list of parameters along with S^p and I^p is given in Table III. The I^p and S^p for $p = q, q\sigma, q\tau, q\sigma\tau, bb$ and $bb\tau$ are much smaller than those for $p = c, \sigma, \tau$ and $\sigma\tau$.

We compare our phase shifts with those given by the Paris potential,³⁰⁾ Reid v_{12} and (Bethe Johnson)⁵⁰⁾ BJ-II v_{12} models. The Paris potential has a theoretically plausible two-pion exchange contribution, which we have approximated by $v_I^p(r)O^p$. The Reid and BJ-II v_8 models have their 1S_0 , 3S_1 - 3D_1 , 1P_1 , 3P_2 - 3F_2 potentials in T,S = 1,0;0,1;0,0 and 1,1 states, whereas the v_{12} models have:

$$v_{1,0} = v({}^1S_0) + \frac{1}{6} (v({}^1D_2) - v({}^1S_0)) O^q, \quad (2.11)$$

$$v_{0,1} = v({}^3S_1 - {}^3D_1) + \frac{1}{6} (v({}^1D_2) - v({}^1S_0)) (O^q + 2O^b), \quad (2.12)$$

$$v_{0,0} = v({}^1P_1), \quad (2.13)$$

Table I

Potential strengths in singlet states (MeV).

P	$S_{1,0}^P$	$I_{1,0}^P$	$S_{0,0}^P$	$I_{0,0}^P$
c	2000.	-6.255	8700.	-13.2
q	49.	0	-500.	.6

Table II

Potential strengths in triplet states (MeV).

P	$S_{0,1}^P$	$S_{0,1}^{1P}$	$I_{0,1}^P$	$S_{1,1}^P$	$S_{1,1}^{1P}$	$I_{1,1}^P$
c	2400.	0.	-6.8009	2145.	0.	-4.32
t	0.	0.	.75	0.	0.	-.18
b	80.	0.	0.	0.	-2200.	0.
q	380.	0.	0.	-20.	0.	0.
bb	-230.	0.	-.2	147.5	0.	0.

Table III

Parameters of the v_{14} two-nucleon interaction model.

	$c = 2 \text{ fm}^{-2}$	$R = .5 \text{ fm}$ $R' = .36 \text{ fm}$	$a = .2 \text{ fm}$ $a' = .17 \text{ fm}$
P	I^P	S^P	S^P
c	-5.7030	2575.3	0
σ	.7628	- 366.56	0
τ	.8992	- 466.56	0
$\sigma\tau$	- .2790	402.81	0
t	.0525	0	0
$t\tau$	- .2325	0	0
b	0	20.	-1650.
$b\tau$	0	- 20.	- 550.
q	.0375	37.938	0
$q\sigma$	- .0375	42.063	0
$q\tau$	- .0375	- 40.688	0
$q\sigma\tau$.0375	- 59.313	0
bb	- .05	53.125	0
$bb\tau$.05	94.375	0

$$v_{1,1} = v({}^3P_2 - {}^3F_2). \quad (2.14)$$

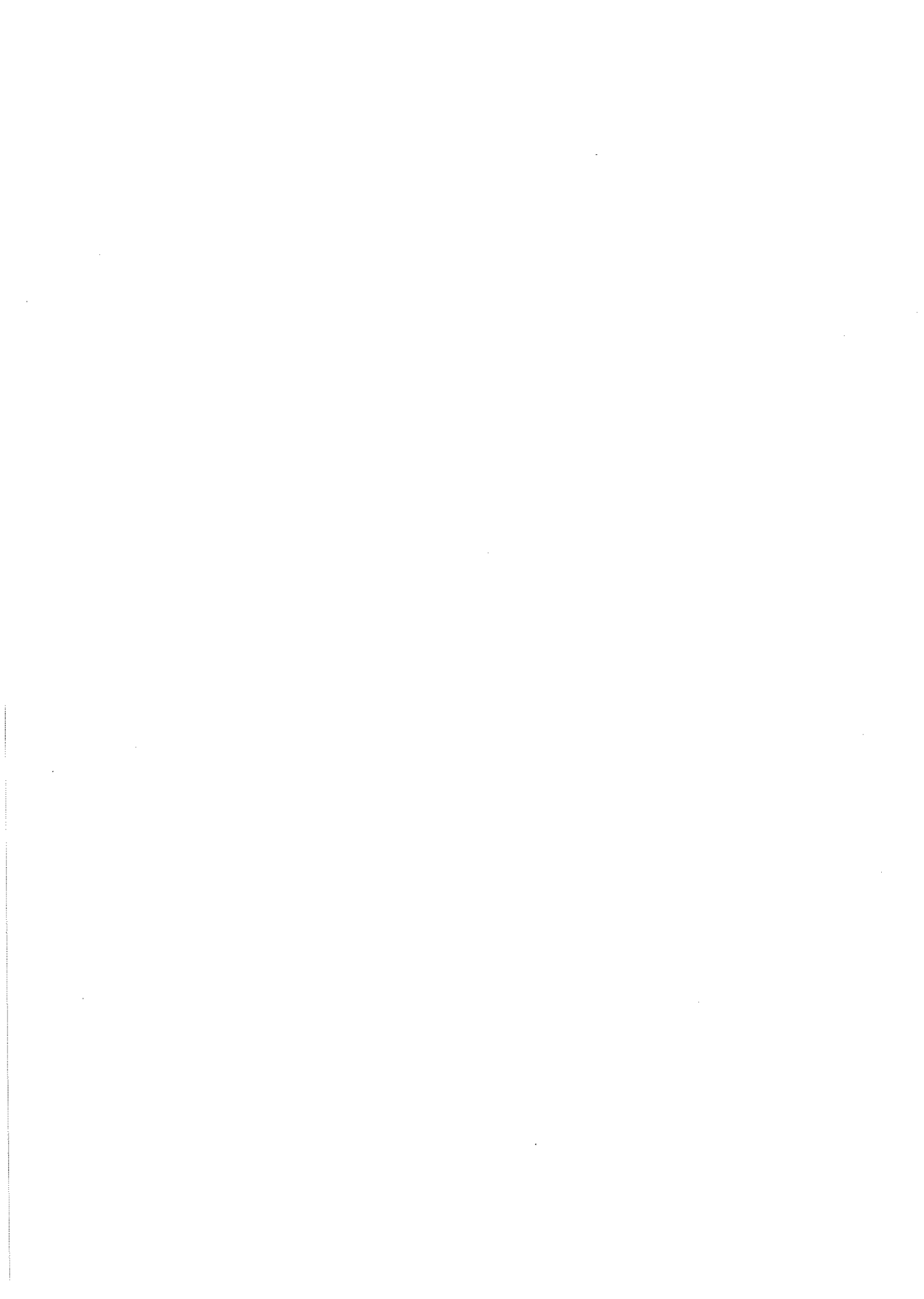
The v_8 models fit the 1S_0 , ${}^3S_1 - {}^3D_1$, 1P_1 and ${}^3P_2 - {}^3F_2$ phases,; the v_{12} models fit these, the 1D_2 , and give a reasonable value for the weighted average of 3D phases:

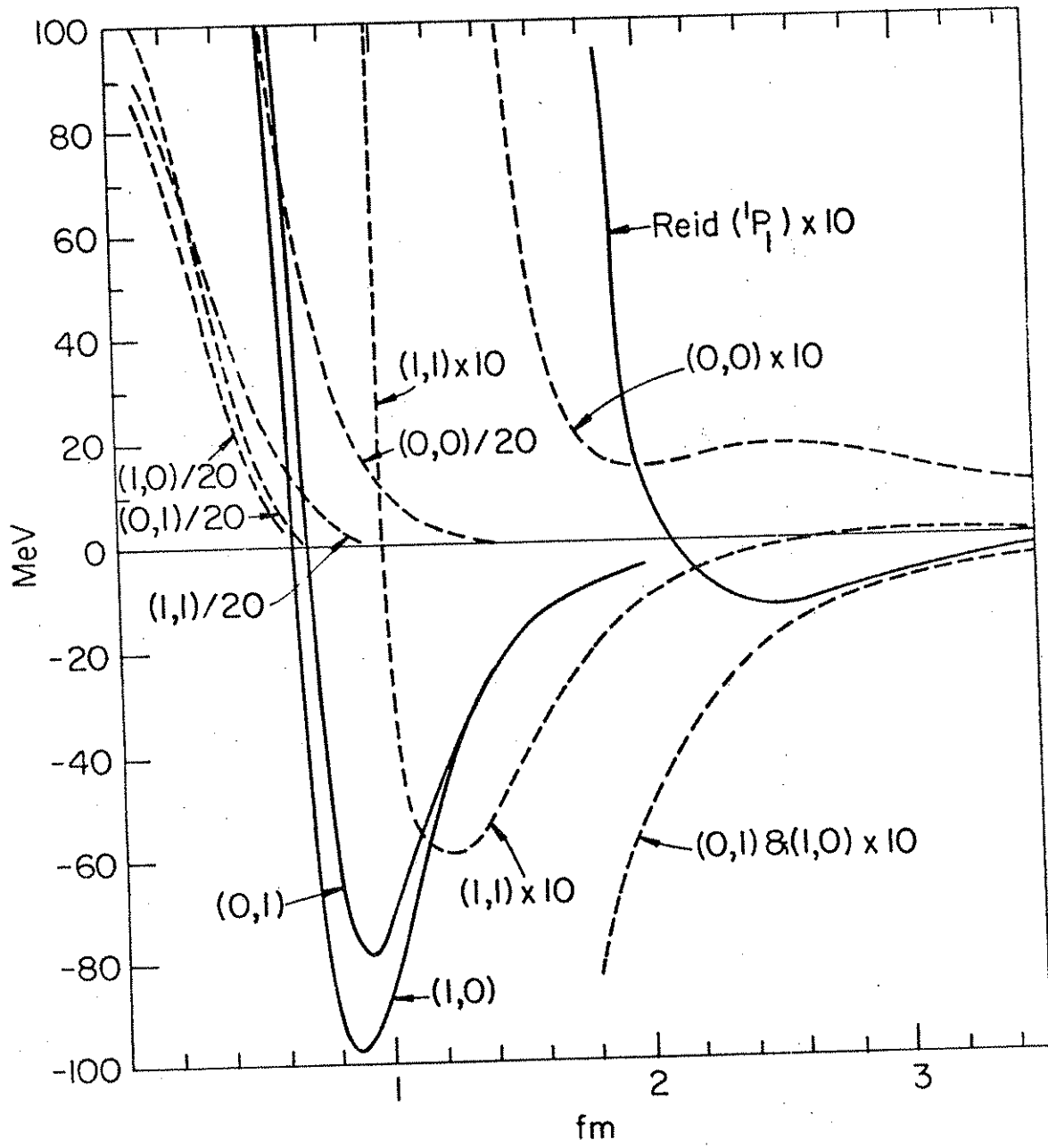
$$\delta_{av}({}^3D) = [3\delta({}^3D_1) + 5\delta({}^3D_2) + 7\delta({}^3D_3)]/15. \quad (2.15)$$

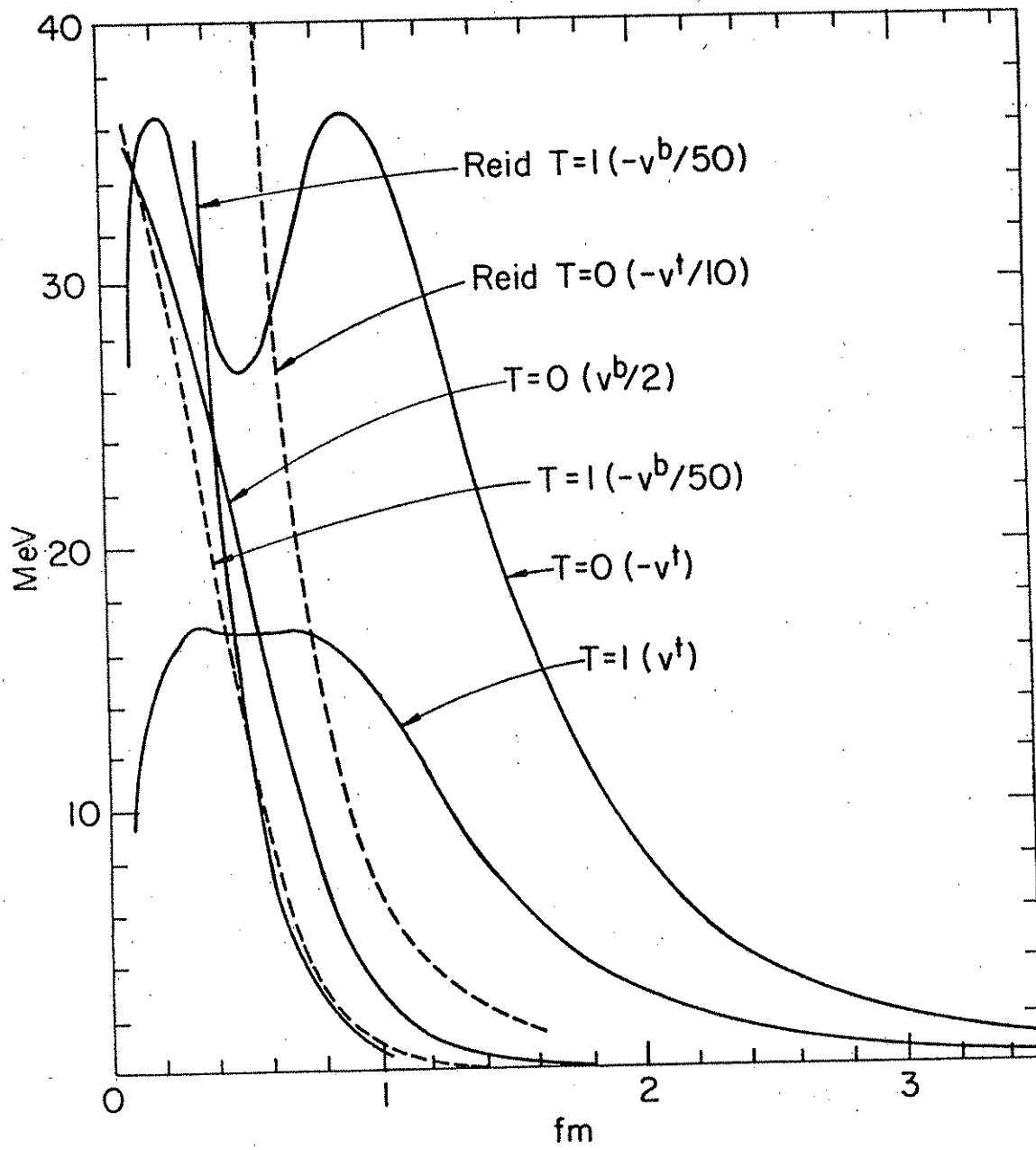
The operator $(0^a + 20^b)$ in Eq. (2.12) gives a zero when operating on 3S_1 and 3D_1 states, and thus the ${}^3S_1 - {}^3D_1$ interaction is unaffected by the added term.

Figures 2-4 show the potentials in T,S channels and compare it with the Reid v_{12} in a couple of cases. Figures 5-20 show the AHR (Arndt, Hackman and Roper)³⁸⁾ energy dependent n-p phase shifts by solid lines and energy dependent p-p phase shifts by dashed lines. The Arndt³⁹⁾ energy dependent EI is shown in Fig. 6 by a broken line. The phases obtained by energy independent analysis by AHR and by Bugg et al.⁴⁰⁾ are respectively shown by I, and †. In T=0 channels these are n-p phases, while in T=1 channels they are p-p. The phases calculated with the present, Paris, Reid v_{12} and BJ-II v_{12} potentials are shown by •, +, x and o respectively. Note that the Paris, Reid and BJ potentials are fitted to the p-p phase shifts in T=1 states, while ours are fitted to the n-p data. There is a very sizable difference between the n-p and p-p 1S_0 phases at high energy.

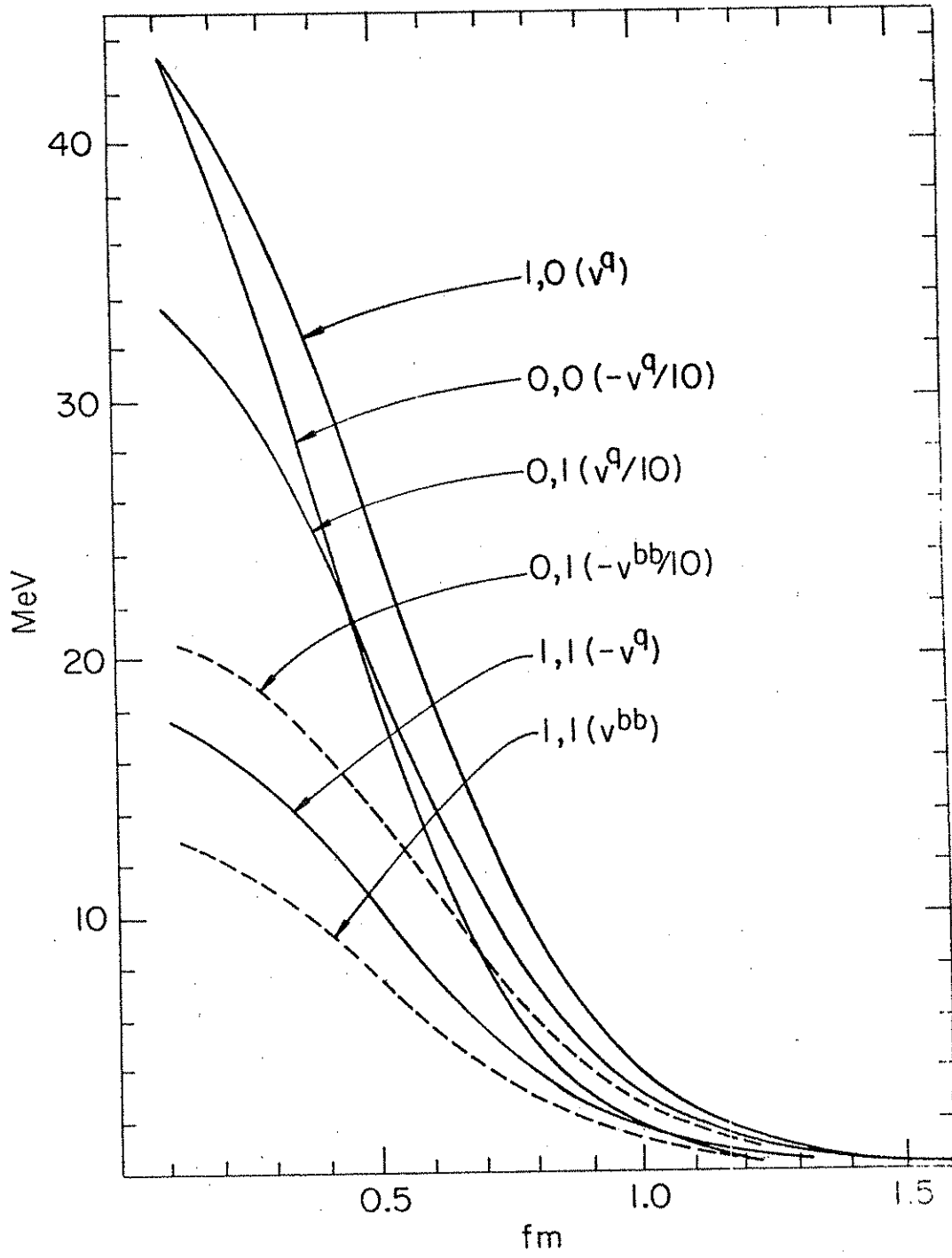
The central potentials in T,S channels (Fig. 2) have the familiar shape. The v^c in 0,0 states does not become negative like Reid's (Fig. 2). The Reid (1P_1) potential gives very bad phase shifts in the 1F_3 state (Fig. 20) and thus is not a proper representative of the T,S = 0,0 inter-



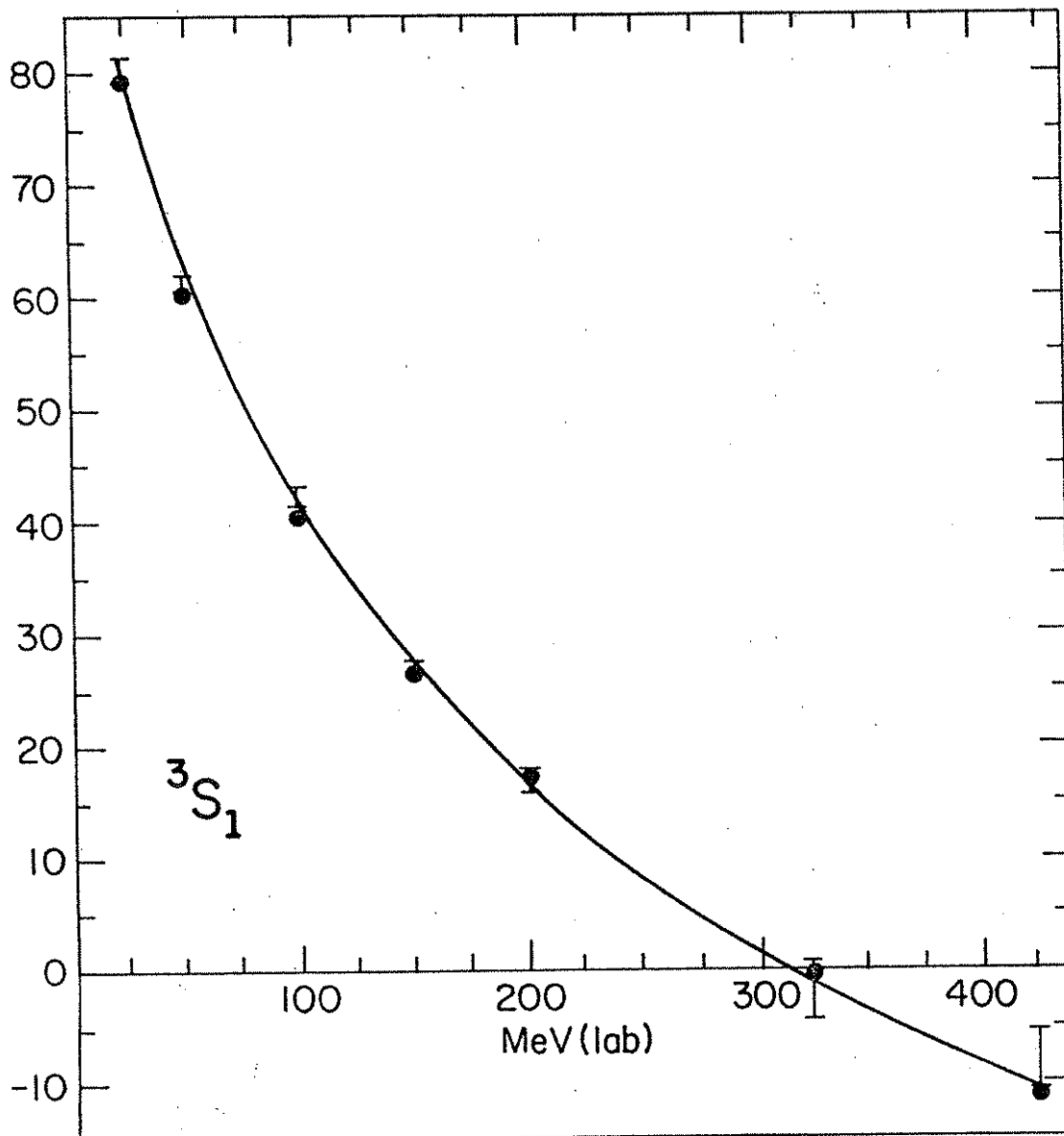




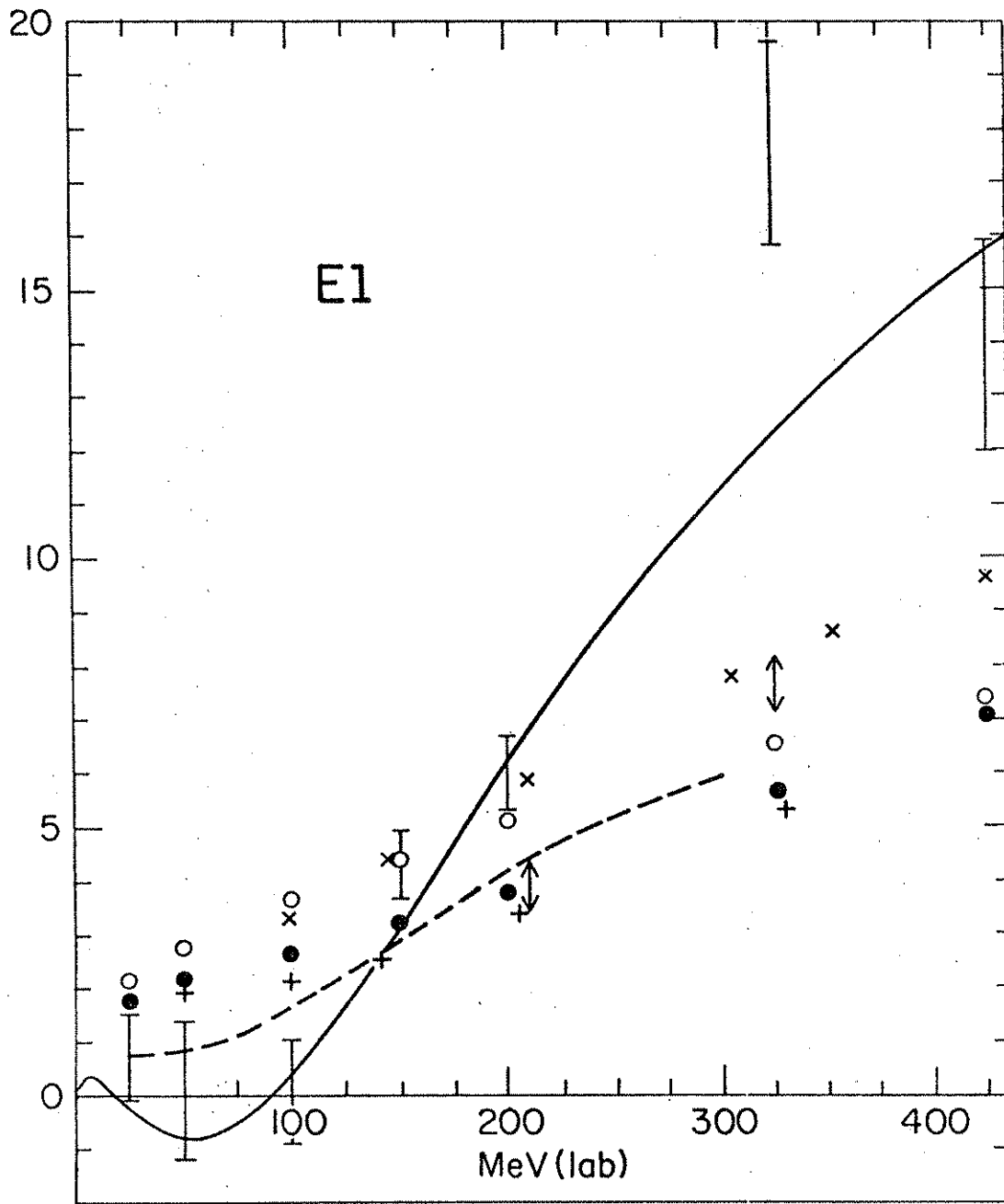


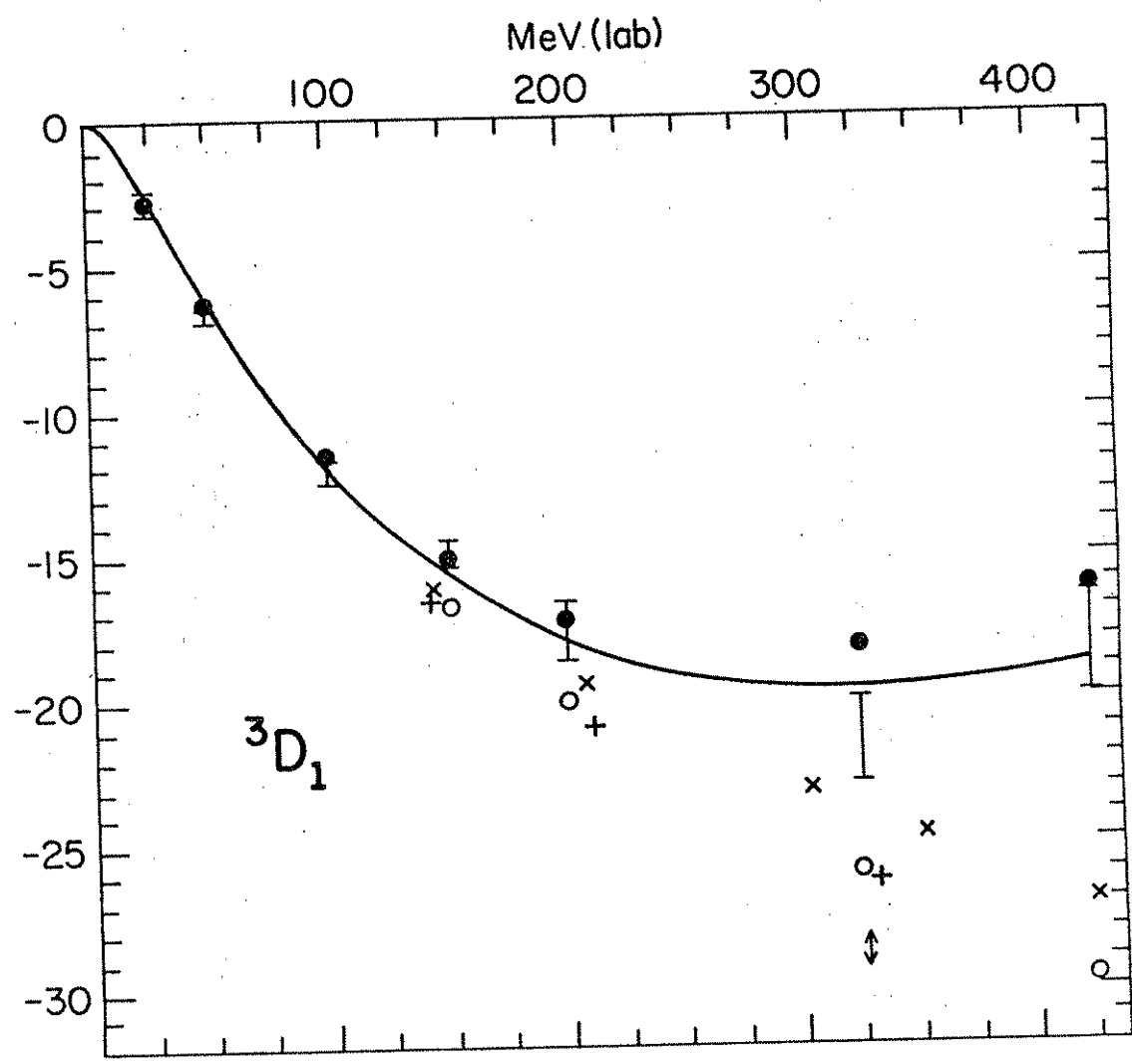


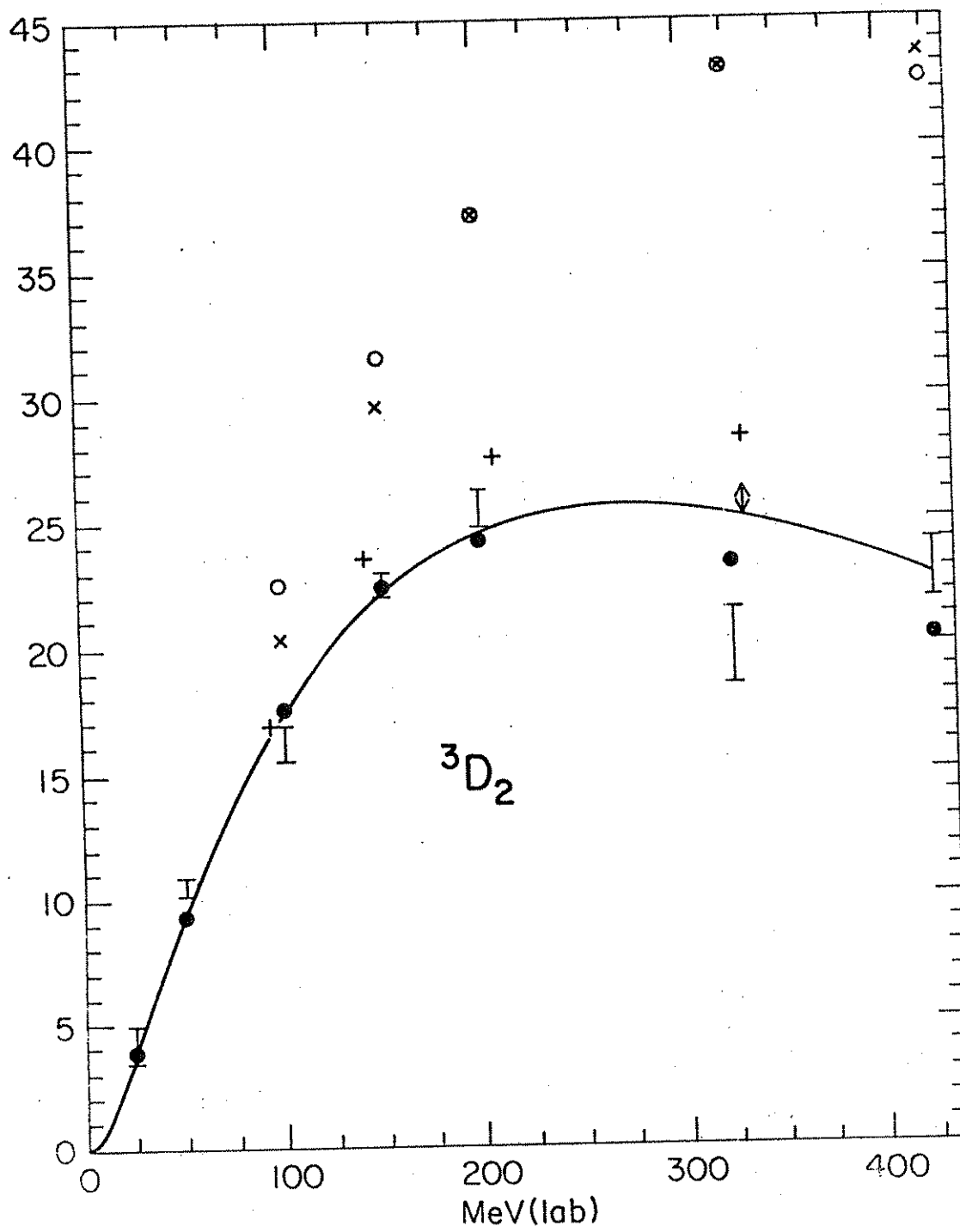


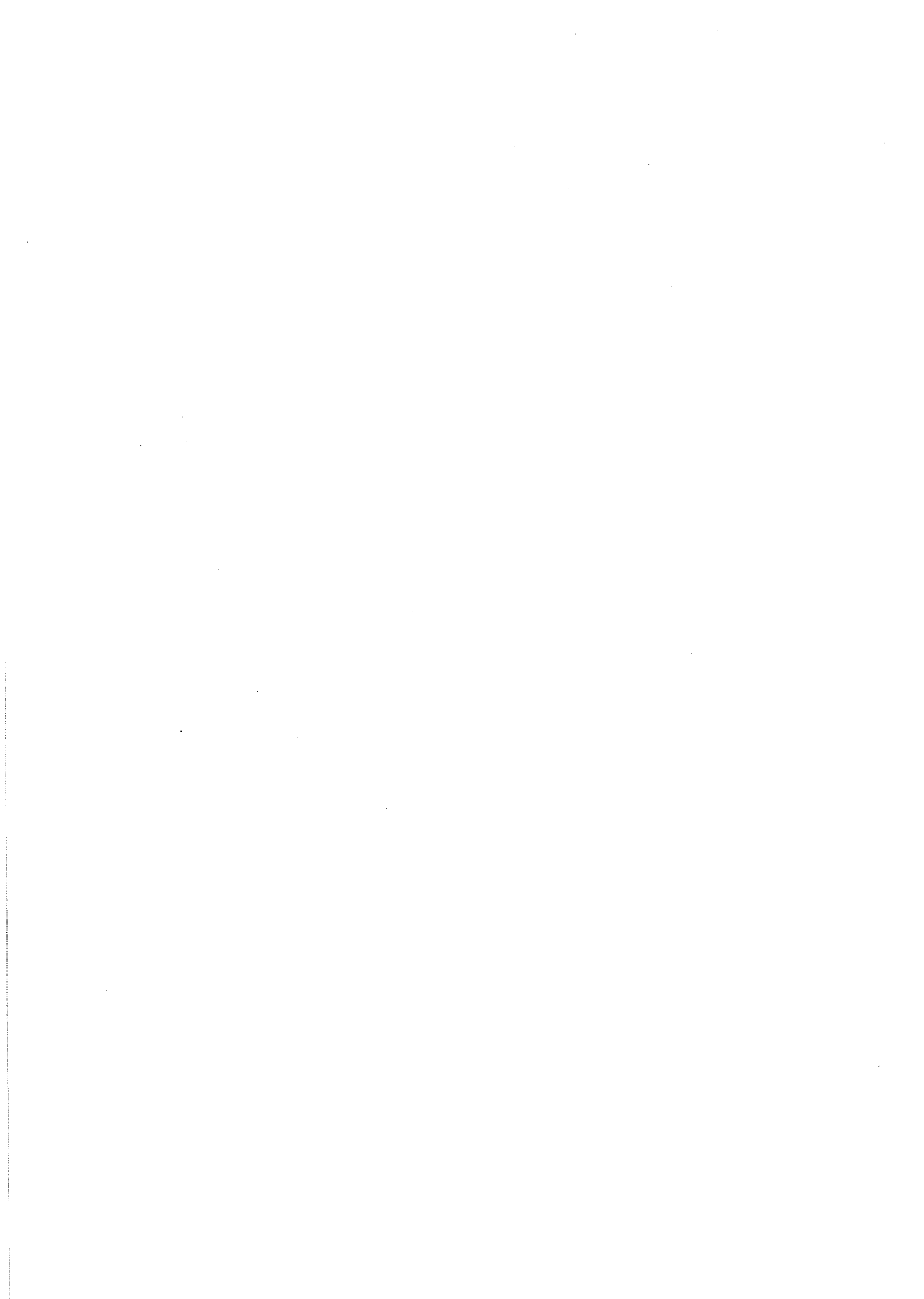


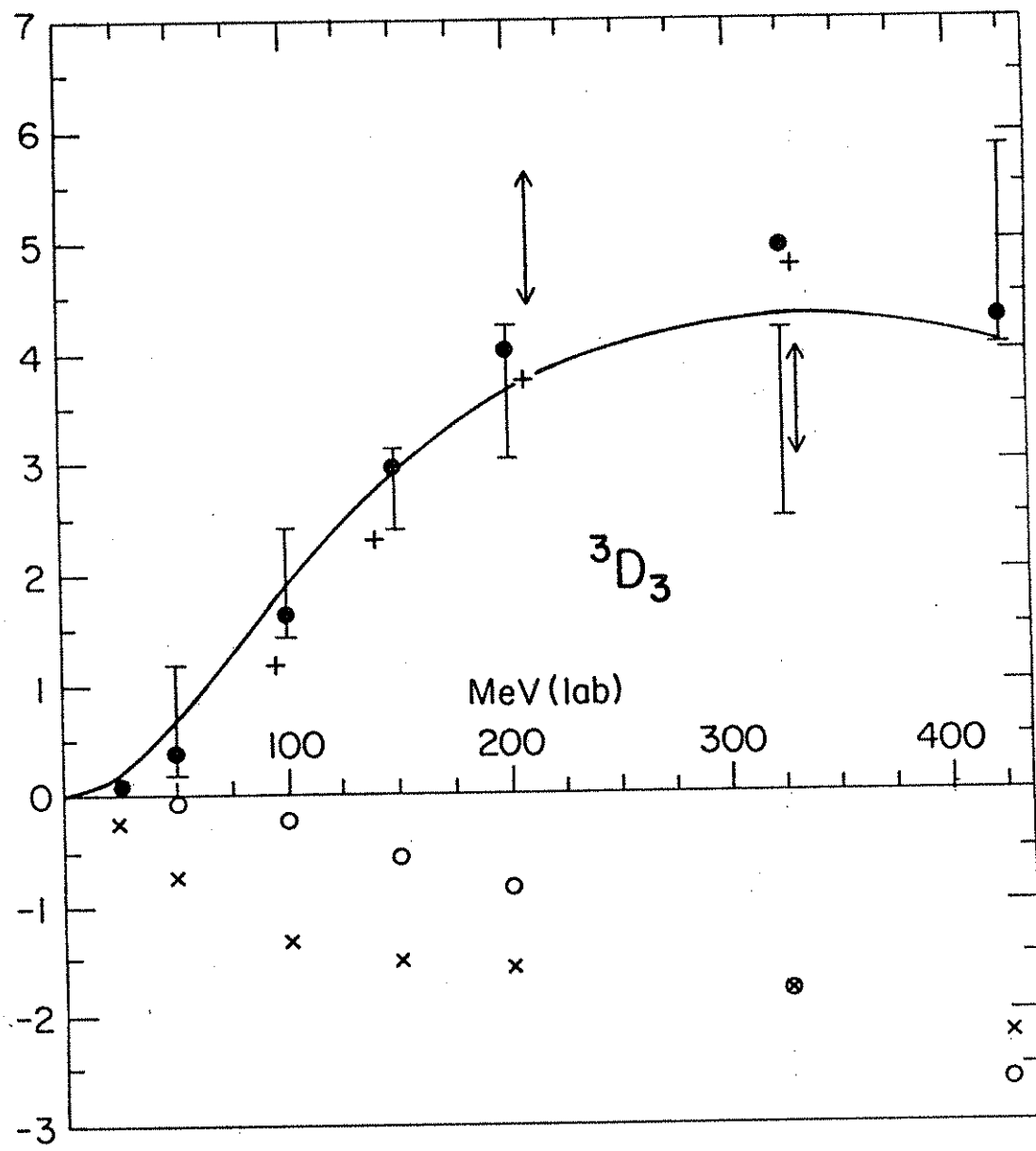




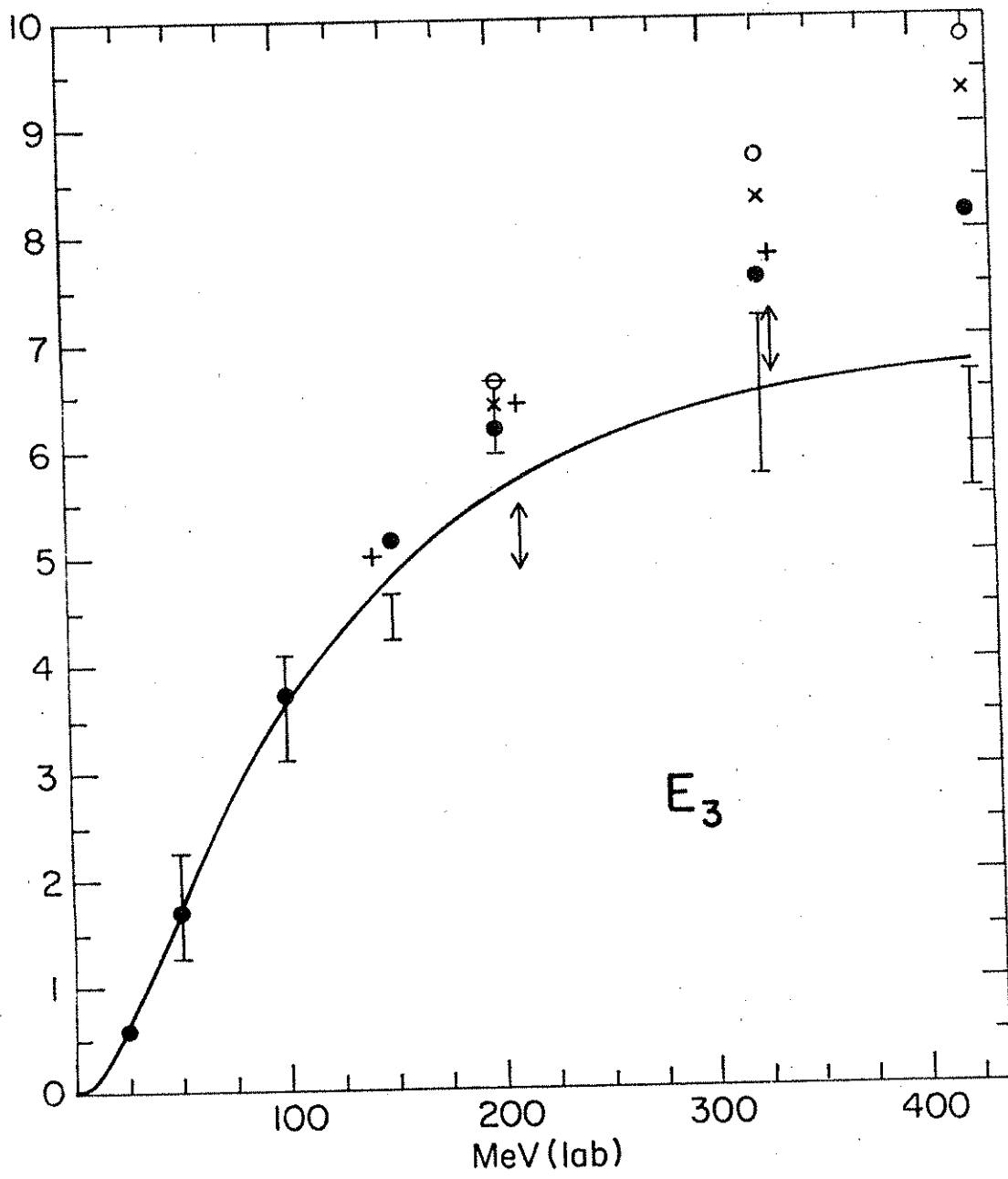


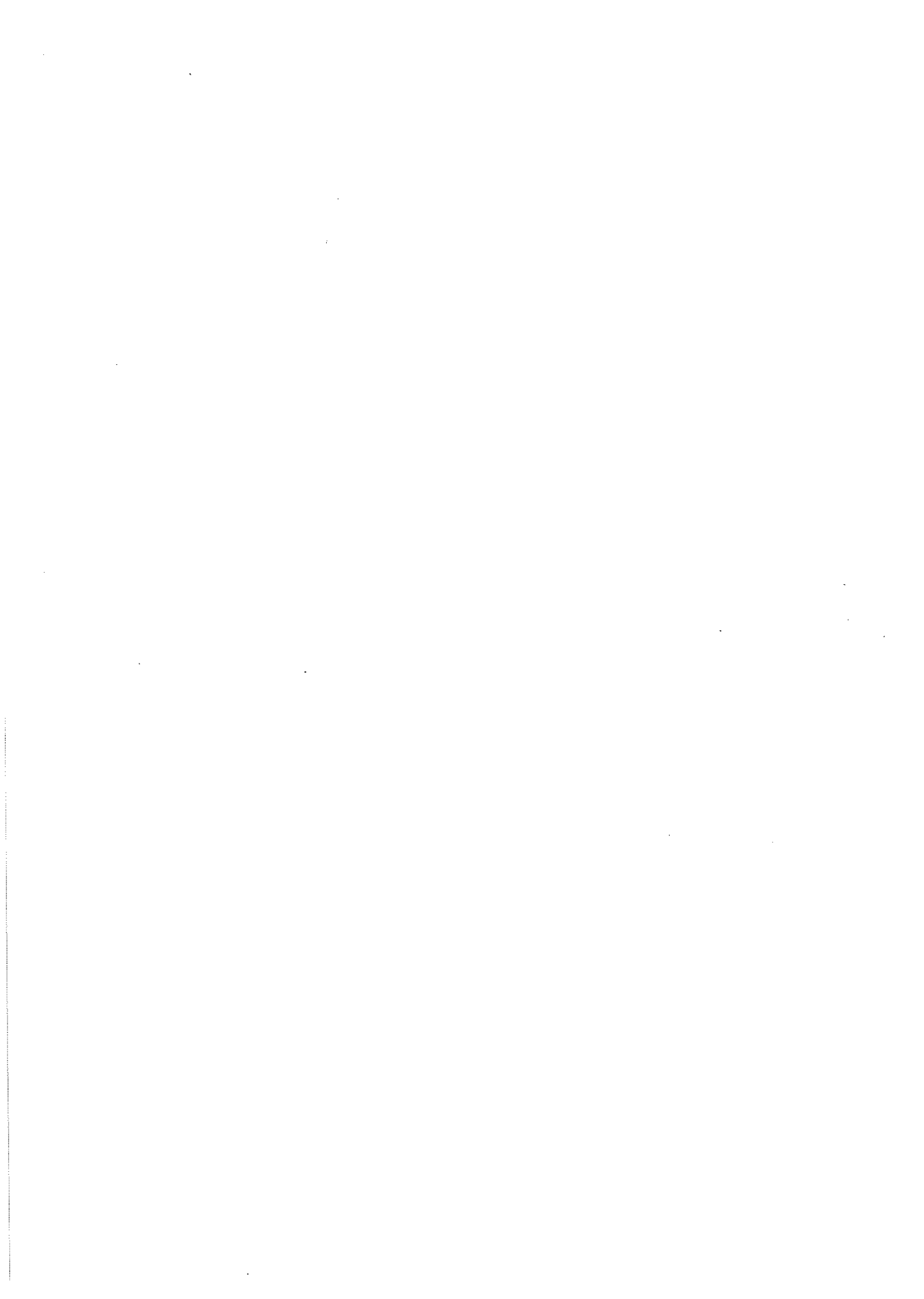


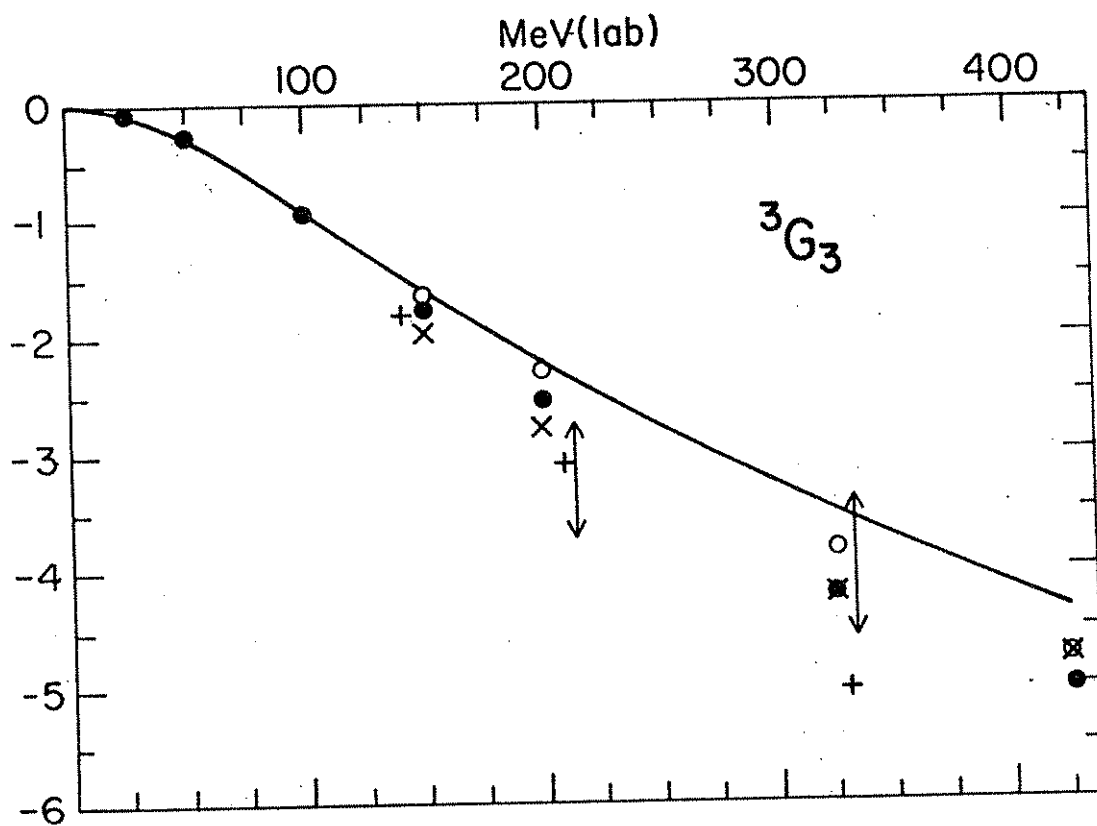




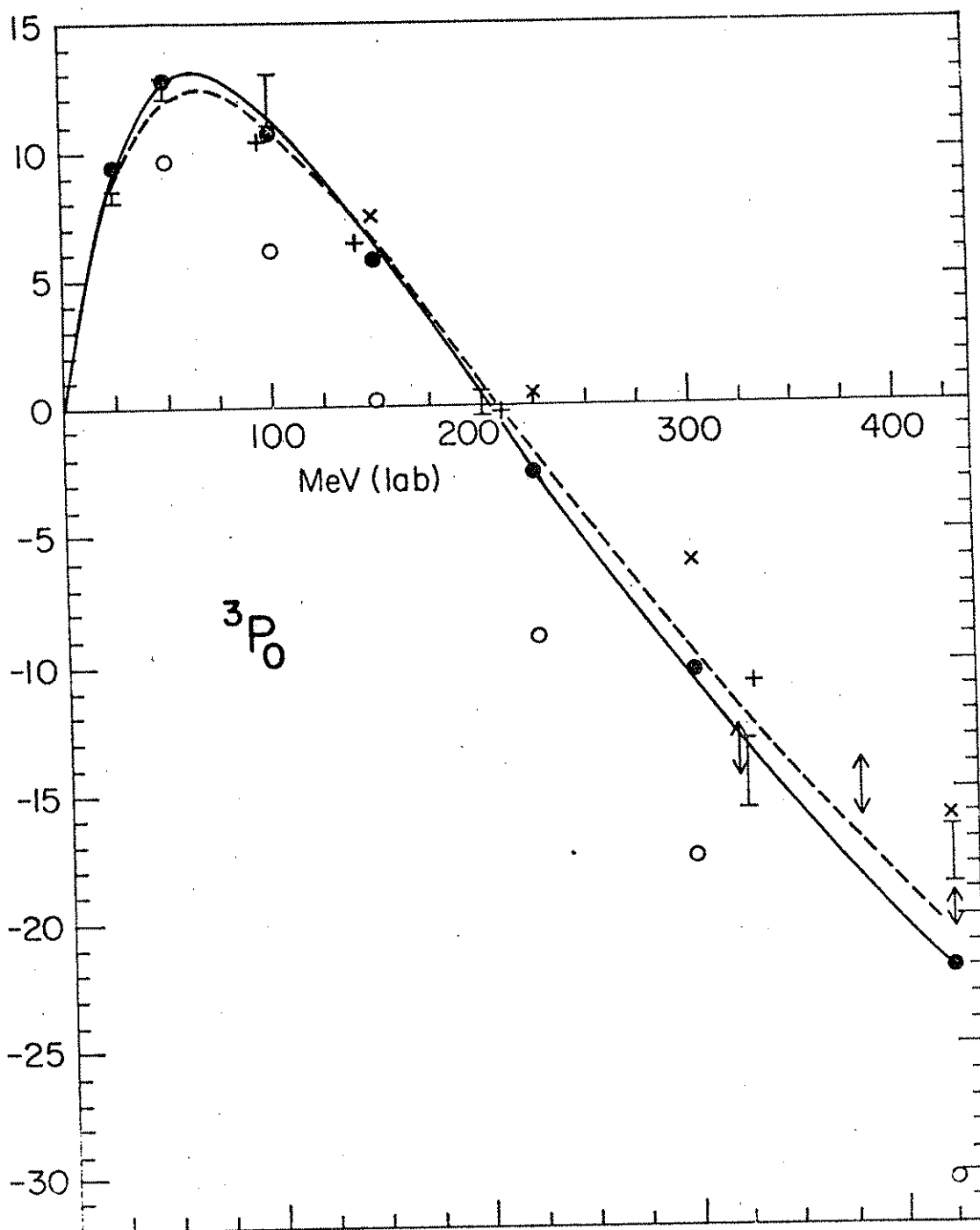


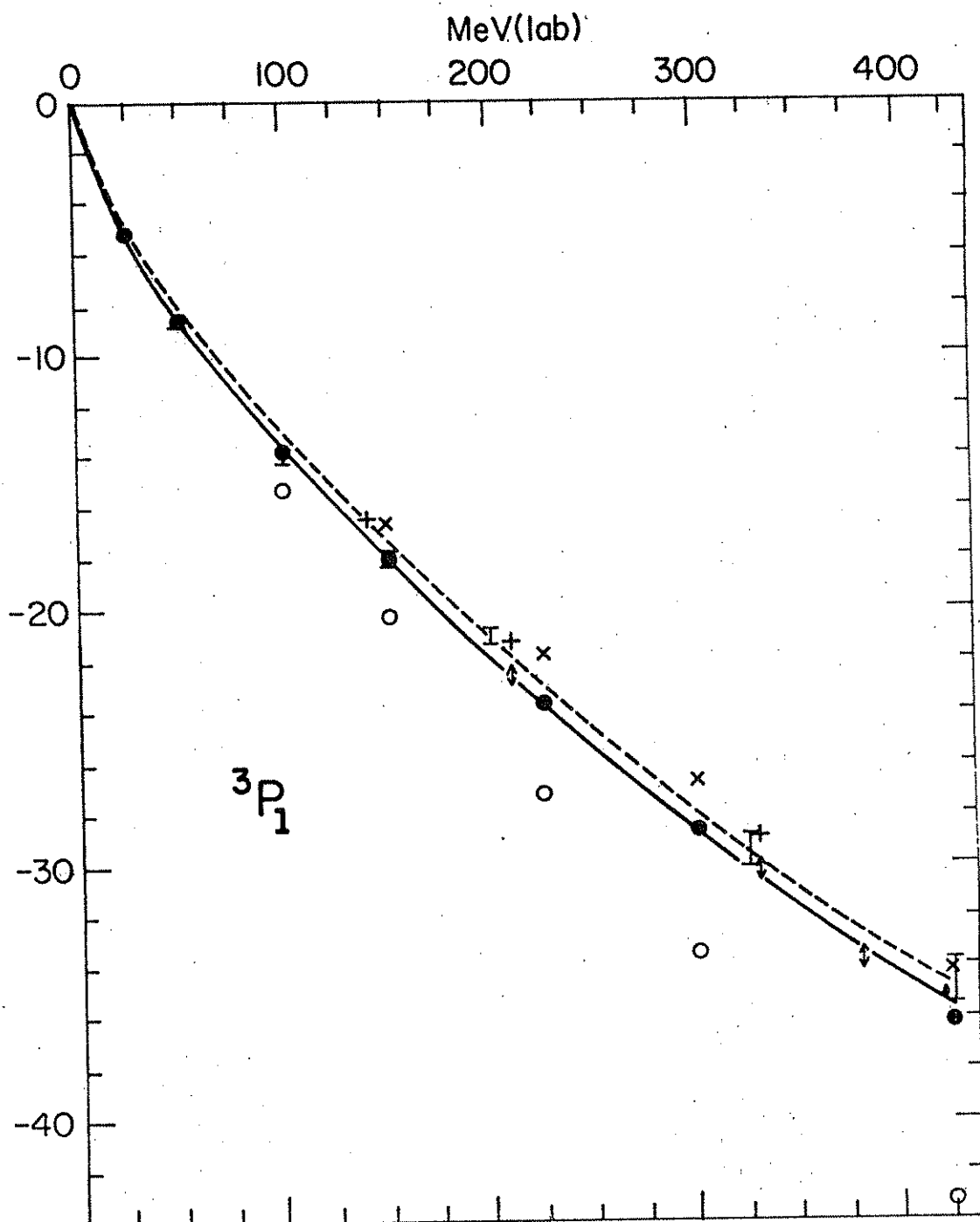




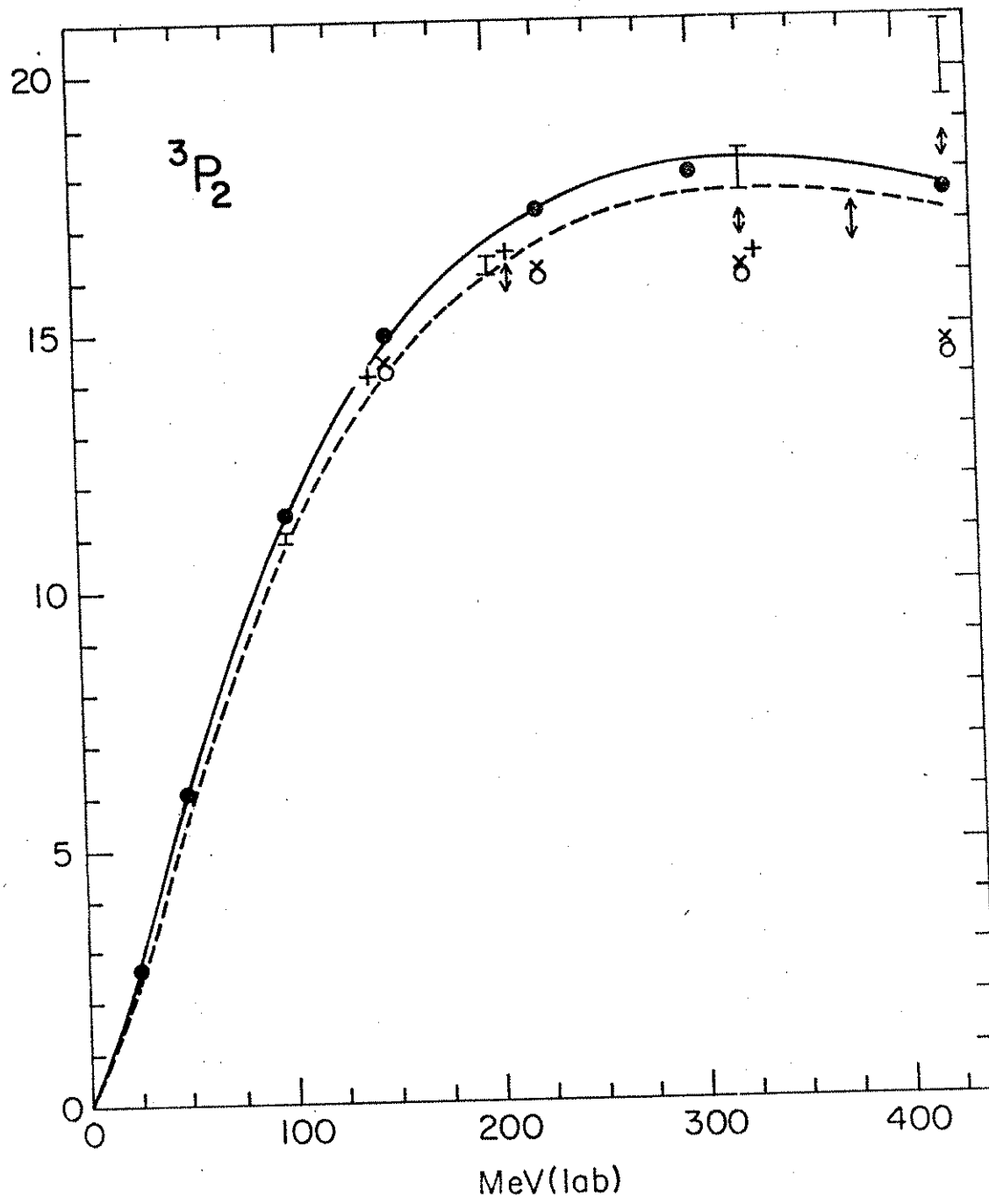


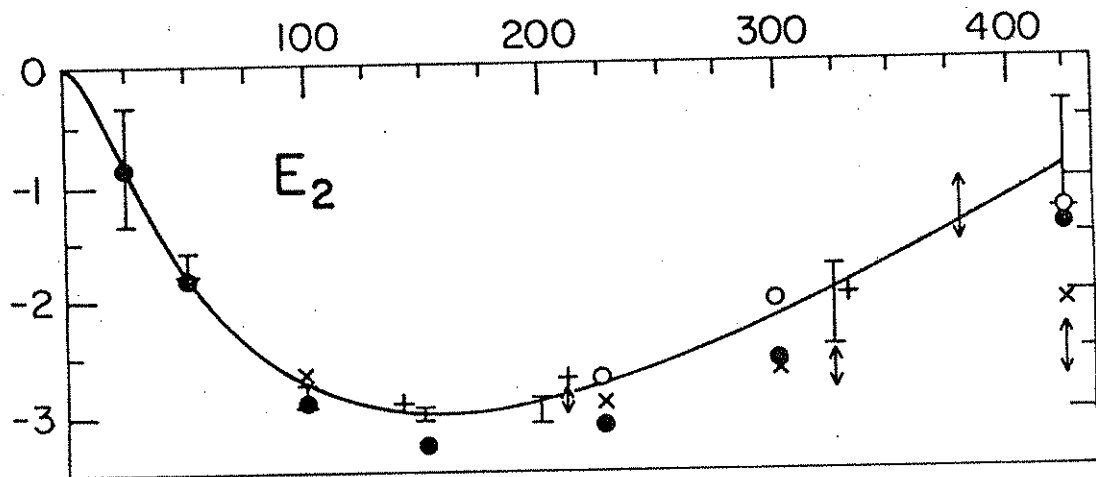
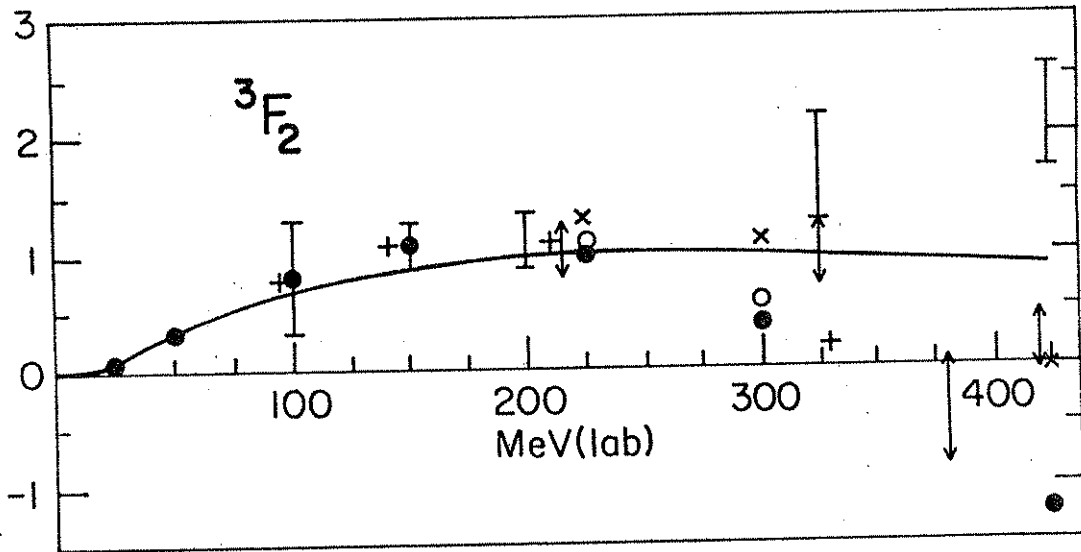


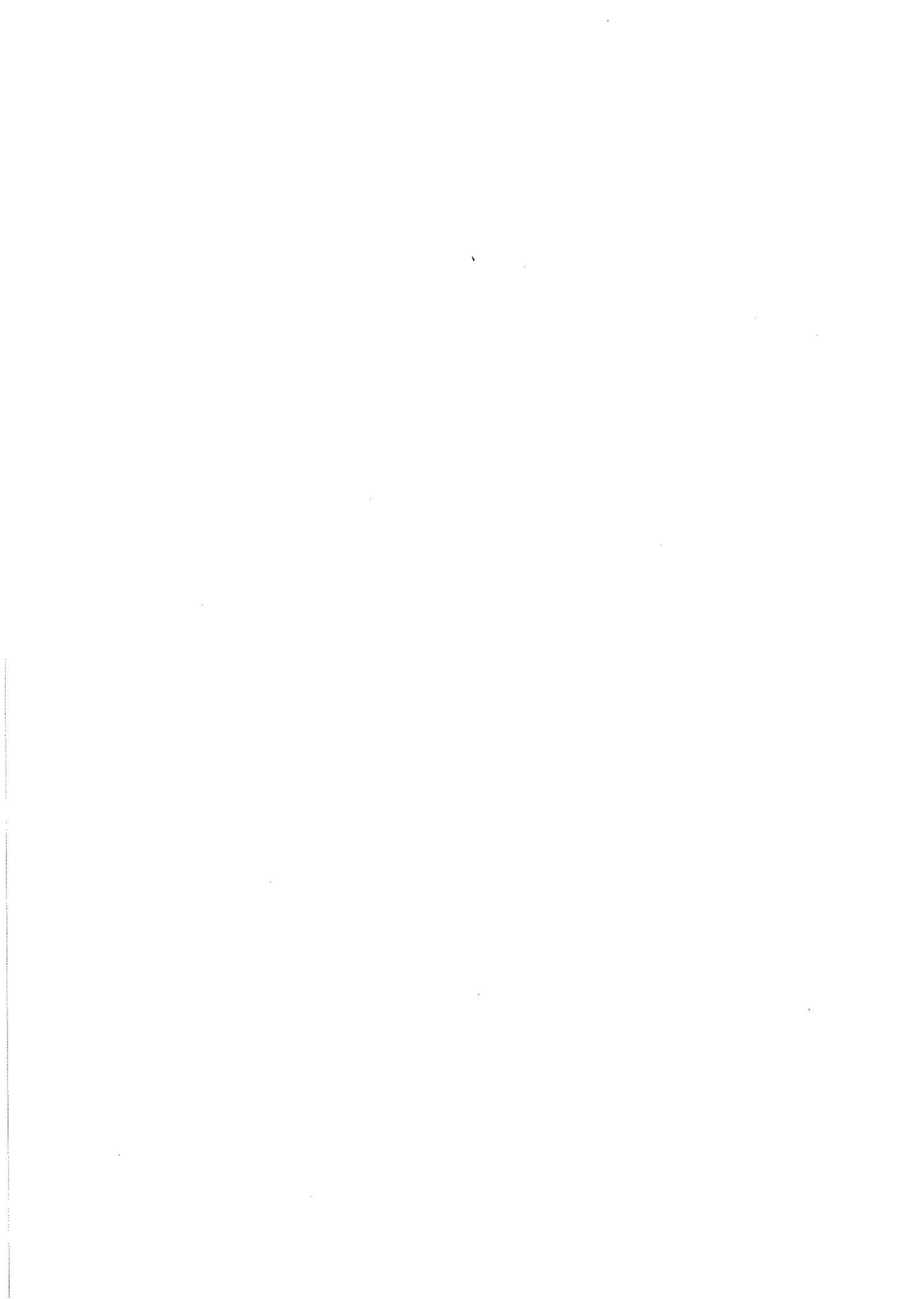


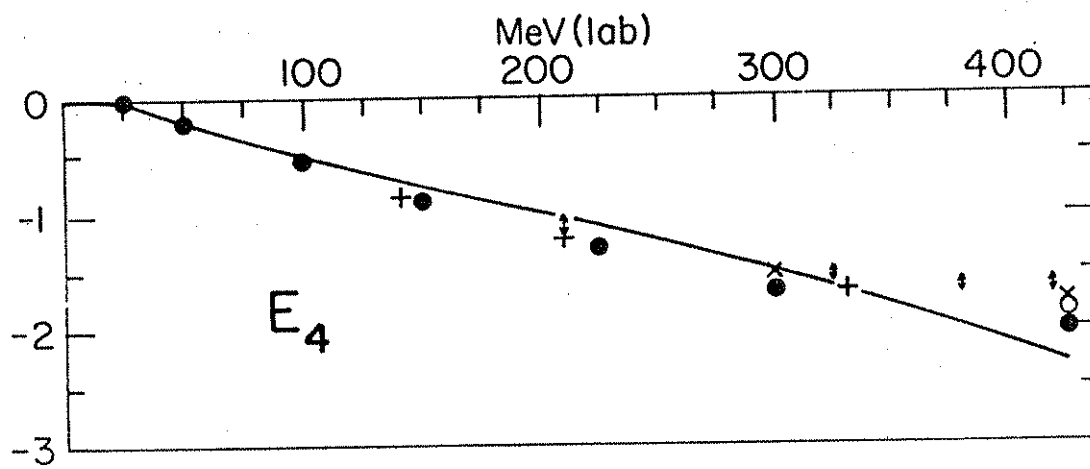
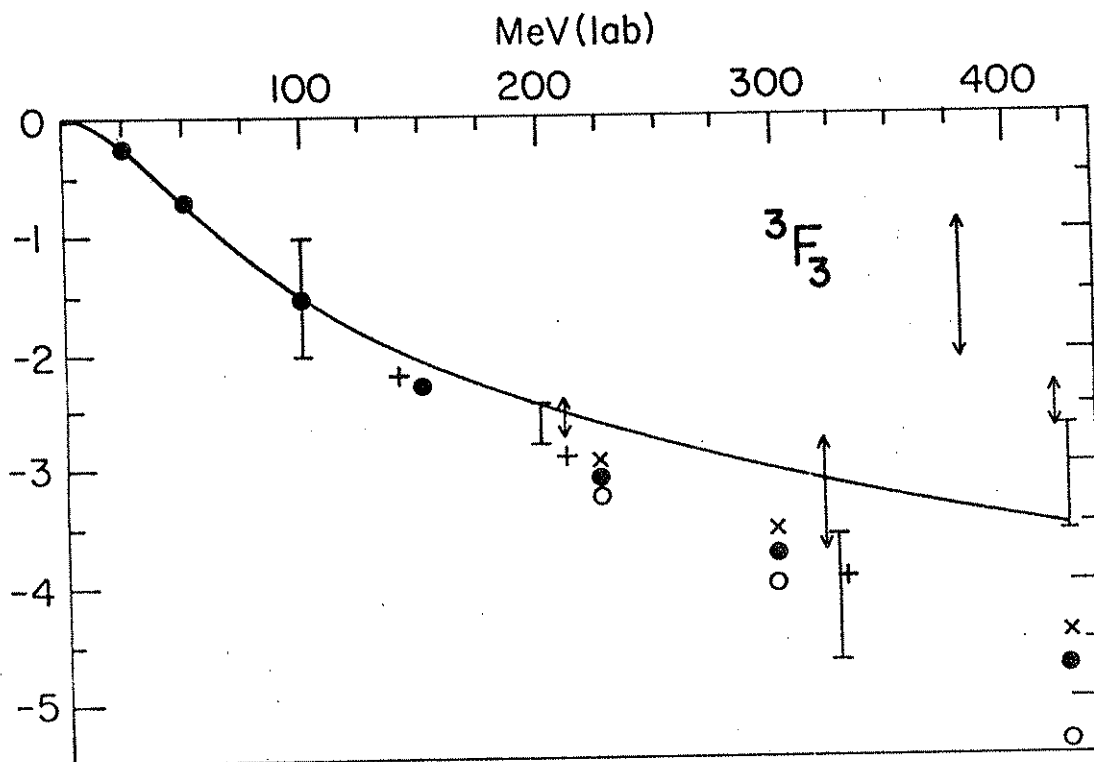


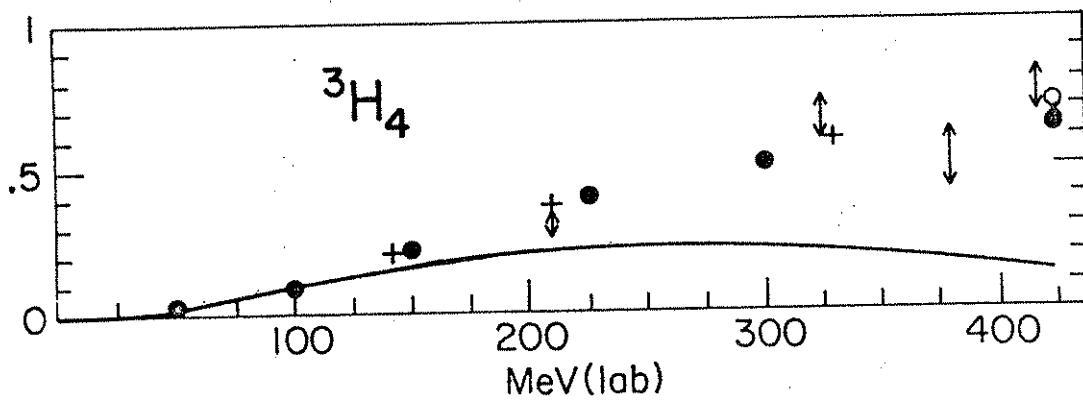
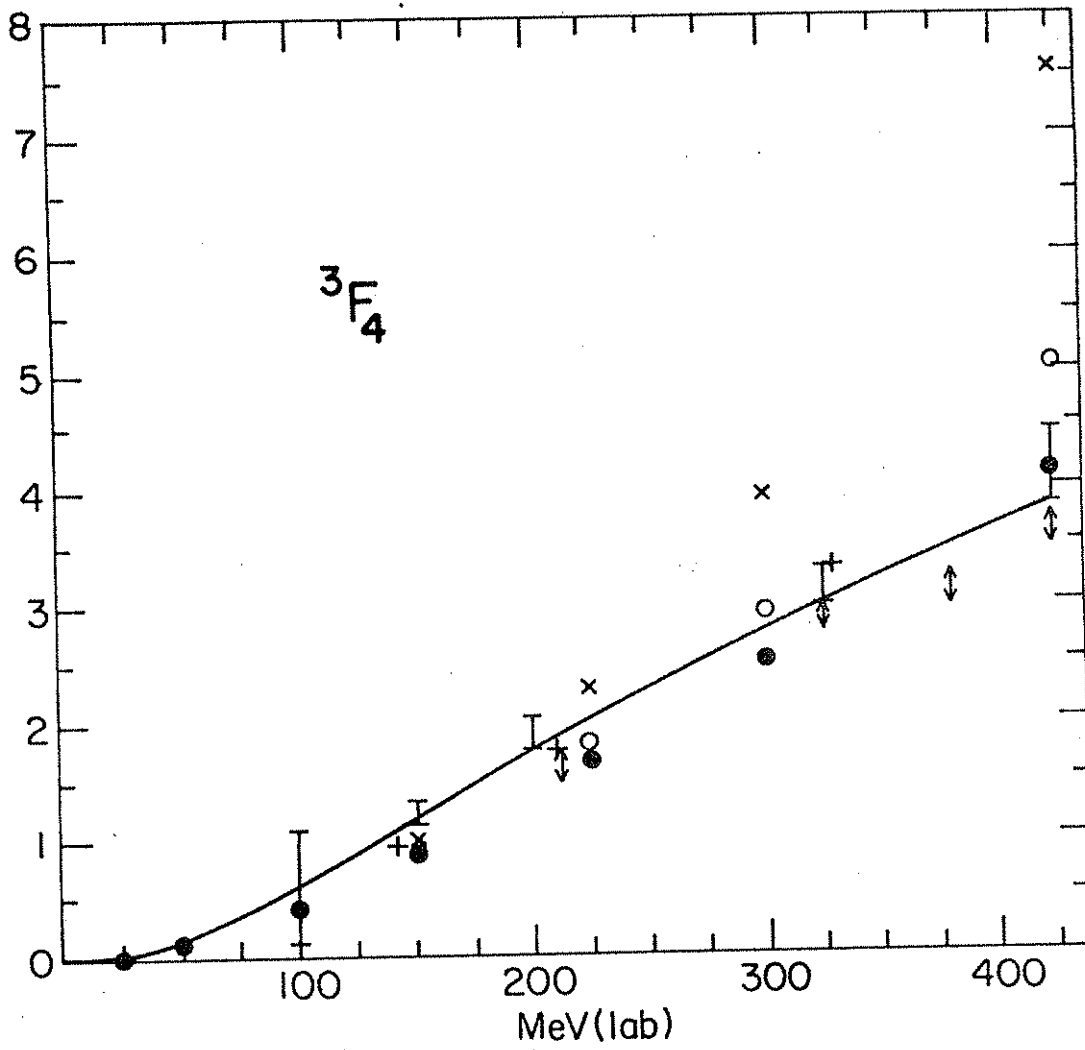


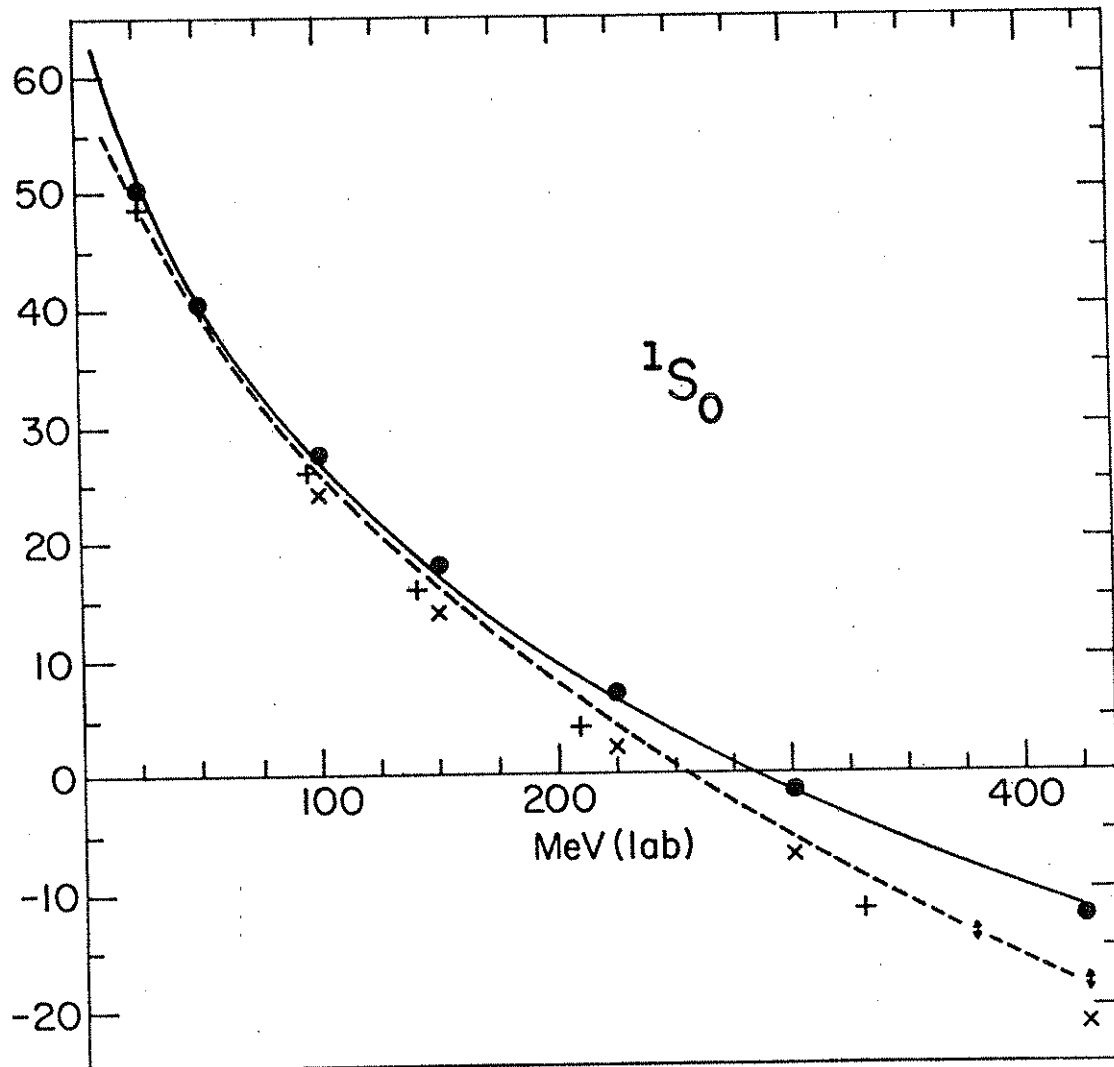


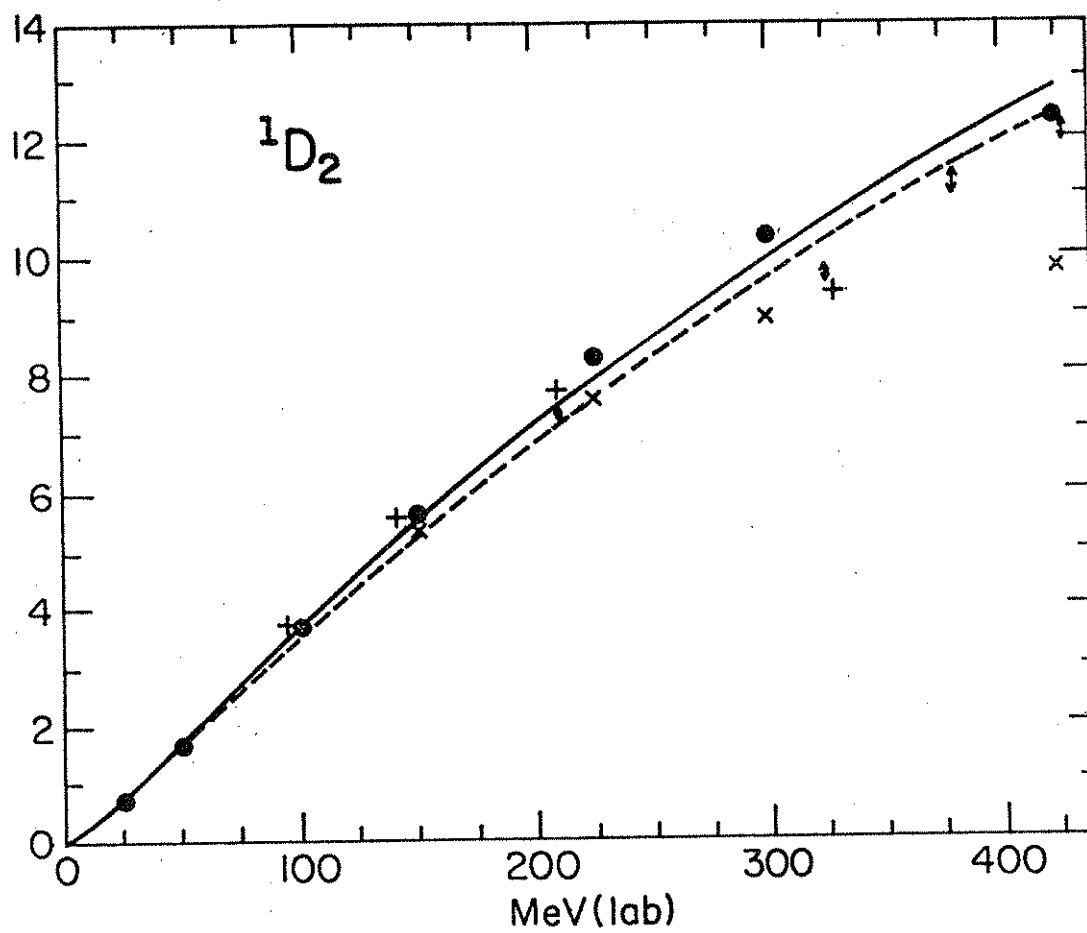




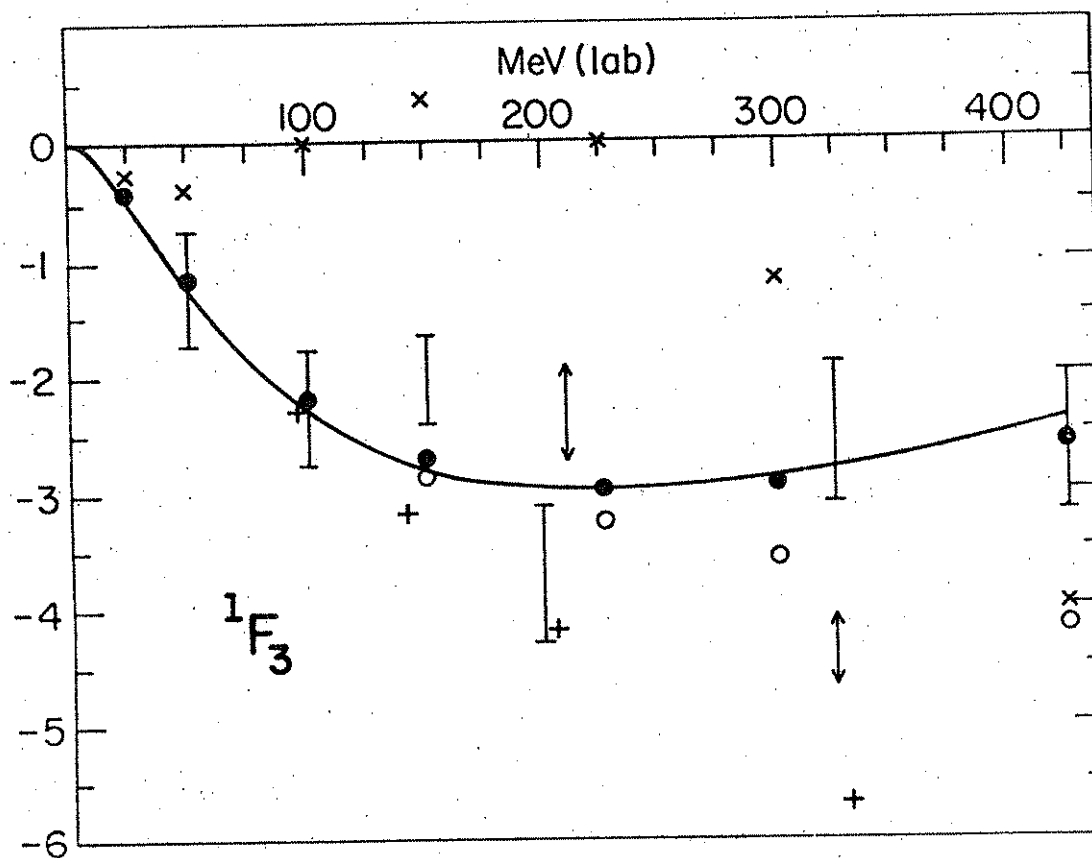
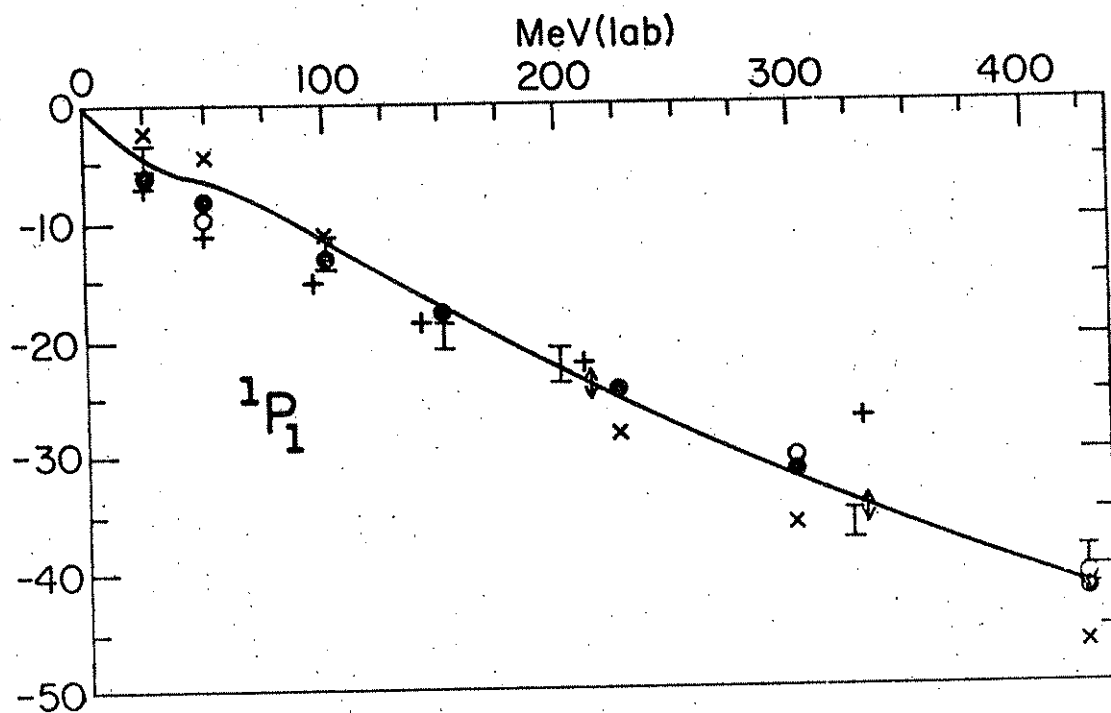












action. Also note from Fig. 2 that the v^c in 0,1 states is almost but not quite as attractive as that in 1,0 states.

The tensor potentials are much weaker than Reid's particularly at $r \leq 1$ fm. They are given by a sum of two terms:

$$v_{T,1}^t = I_{T,1}^t T_\pi^2(r) + 3.488 (4T-3) T_\pi(r) , \quad (2.16)$$

and $T_\pi(r)$ is linear in r at small r . The two terms of $v_{T,1}^t$ have opposite signs, and so the $v_{T,1}^t$ have an unreasonable peak at $\sim .2$ fm. This peak is purely due to our choice of cutoff and should not have any physical significance; neither does it have any effect on the two-nucleon interaction. The Reid v_{12} potential has a very strong tensor force as can be seen from the 3D_1 , 3D_2 and 3D_3 phase shifts shown in Figs. 7-9. The tensor force is attractive in 3D_2 , while repulsive in 3D_1 and 3D_3 states.

The $\vec{L} \cdot \vec{S}$ interaction (Fig. 3) in $T=0$ states is weak, while that in $T=1$ states is comparable with Reid's. The BJ-II v_{12} potential has a very strong $\vec{L} \cdot \vec{S}$ interaction in $T=1$ states, and it fails to explain the scattering data in 3P_0 and 3P_1 states (Figs. 12,13). The Reid v_8 , v_{12} models also do not explain 3P_0 and 3P_1 phases very satisfactorily. The range of the $\vec{L} \cdot \vec{S}$ potential in $T=1$ states has to be shorter than the range of the repulsive core in $T,S = 1,1$ states to i) reproduce the 3P_2 phase shift (Fig. 14) at higher energies, and ii) to prevent the 3F_4 phase (Fig. 17) from becoming too attractive at $E \sim 400$ MeV.

The L^2 and $(\vec{L} \cdot \vec{S})^2$ potentials are shown in Fig. 4. In triplet states the $v_{T,S}^q$ and $v_{T,S}^{bb}$ have opposite signs, and they cancel substantially in the $J = \ell \pm 1$ channels. The $v_{0,1}^q$ and $v_{0,1}^{bb}$ are needed primarily to reduce the large attractive phase shifts in 3D_2 without making the 3D_1

and 3D_3 phases very repulsive. The $v_{1,0}^q$ is well determined by the 1D_2 phase (Fig. 19), and it is quite small. In principle the 3F phases could determine the $v_{1,1}^q$ and $v_{1,1}^{bb}$, but the data on 3F_2 and 3F_3 phases is rather poor. Fortunately the $v_{1,1}^q$ and $v_{1,1}^{bb}$ appear to be very weak. A relatively substantial $v_{0,0}^q$ is needed to fit the 1F_3 phase (Fig. 21), however the data here is not too good.

The data on E1 (Fig. 3) is also poor. If we had chosen an even weaker tensor force in T=0 states, the E1 would have become smaller, and the 3D phases could be fit with weaker $v_{0,1}^q$ and $v_{0,1}^{bb}$. Thus E1 plays an important role in deducing the interaction operator from the scattering data, and a better measurement of it will be most welcome.

In general our phases are not too different from those given by the Paris potential. We seem to do a little better on the spin singlet states and the 3P states, while the data on 3D and 3F states is not accurate enough to choose among the two models. However, it must be noted that the Paris potential is fitted to the scattering data itself whereas ours is fitted only to phase shifts.

The contribution of Δ (33-resonances) to I^c can be estimated in the closure approximation.⁴³⁾ It comes out to ~ -2 , whereas the I^c in our model is -5.7 (Table III). Hence it is suggested that the Δ 's provide only a third or so of the intermediate range attraction. The rest of it must be from other resonances, and the π - π interactions. However it should be pointed out that I^c is not uniquely determined by the data. It is possible to make substantial correlated changes in the parameters I^c , c , R and S^c which leave the phases relatively unaffected. The values of $I^{p \neq c}$ are much smaller than I^c in accord with the isobar model.

The calculated deuteron energy, quadrupole moment, D-state probability, and the asymptotic D to S-state ratio⁴⁴⁾ are given in Table IV, along with their experimental values, and those obtained with the Paris and Reid models. Thanks to the weaker tensor force the D-state percentage is small, but not quite as small as suggested by the photodisintegration data.⁴⁵⁾ The quadrupole moment and the A_D/A_S are both on the lower side, but within experimental limits.

In Fig. 21 we compare the calculated deuteron structure function $A(q^2)$ with the experiment,^{46,47)} and predictions of Paris and Reid models. The $A^2(q)$ is underestimated by $\sim 10\%$ at $q^2 = 6 \text{ fm}^{-2}$, and by $\sim 33\%$ at $q^2 \sim 20$. Of course there is no reason to believe our non-relativistic calculation at $q^2 \geq 10$.

The "dipole" approximation:

$$F_0(q) = 1/(1+aq^2)^2 ; \quad a = .055 \text{ fm}^{-2} \quad (2.17)$$

is used for the proton form factor in the calculation of $A(q^2)$. Using the more realistic $F_0(q)$ of Blatnik and Zovko⁴⁸⁾ will increase our $A^2(q)$ in the $q^2 = 20 \text{ fm}^{-2}$ region by a few percent.

Instead of taking into account the nucleon isobar degrees of freedom by an effective intermediate range attraction $v_1^P(r_{ij})O_{ij}^P$, if they are explicitly included in the deuteron wave function, the $A(q^2)$ will probably be a few percent larger in the $q^2 \sim 10 \text{ fm}^{-2}$ region.⁴⁹⁾ It is also likely that the meson-exchange-current (MEC) contributions will increase $A(q^2)$ somewhat.

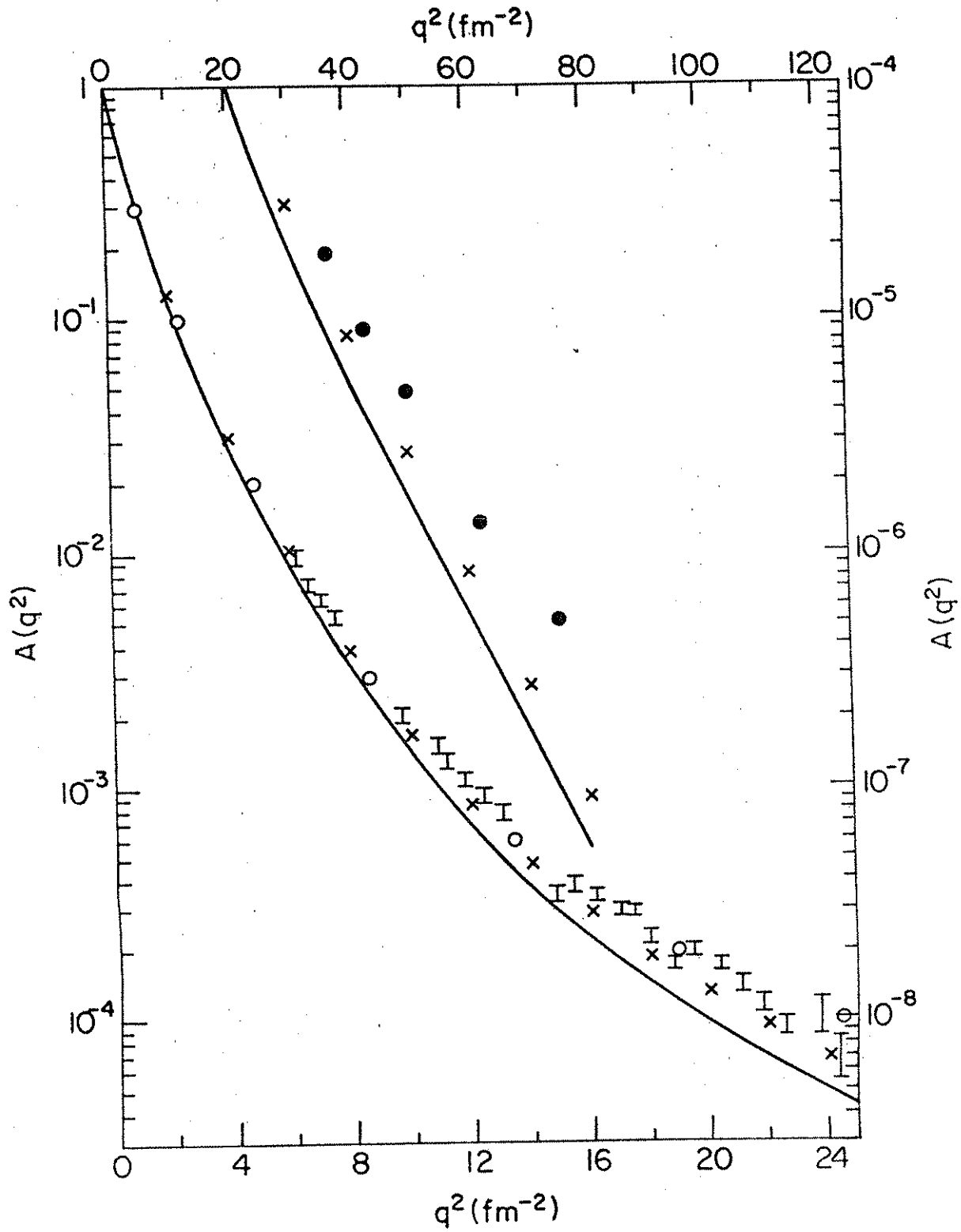
Both Paris and Reid potentials do better on the $A(q^2 \leq 20 \text{ fm}^{-2})$, probably because they have somewhat stronger tensor force than ours. However, the deuteron photodisintegration data^{44,45)} supports a tensor

Table IV

Deuteron Properties

	Present	Paris	Reid	Expt.
E (MeV)	-2.225	-2.225	-2.225	-2.224
Q (fm ²)	0.273	0.279	0.280	0.278 ± .008
D-state (%)	5.2	5.8	6.5	< 5?
A _D /A _S	0.0247	0.0260	0.0262	.0263 ± .0013





force that is even weaker than ours ($P_D < 5\%$). It appears to be rather difficult to simultaneously obtain i) the correct 3D_J phases with weak $v_{0,1}^q$ and $v_{0,1}^{bb}$, ii) the correct $A(q^2 \leq 10 \text{ fm}^{-2})$ and iii) a $P_D \leq 5\%$. In our model we have compromised a little on both P_D and $A(q^2)$ hoping that isobar and meson-exchange-current corrections will have some effect on the interpretation of the electron scattering and photodisintegration data.

III. NUCLEAR MATTER CALCULATIONS

A. Euler-Lagrange Equations

Variational calculations of nuclear matter generally begin by defining a set of correlation functions $f^P(r, d^P, \alpha^P \dots)$ where $d^P, \alpha^P \dots$ are variational parameters. The energy expectation value $E(k_F, d^P, \alpha^P \dots)$ is calculated and minimized with respect to variations in $d^P, \alpha^P \dots$. This approximate procedure is used because the variational problem $\delta E = 0$ with respect to arbitrary variations in f^P is too complex.

In practice the $f^P(r, d^P, \alpha^P, \dots)$ are obtained by minimizing the two-body cluster contribution of an interaction $(\bar{v}-\lambda)$. The interaction \bar{v} is related to the bare interaction:

$$\bar{v}_{ij} = \sum_{p=1,14} \alpha^p v^p(r_{ij}) O_{ij}^p, \quad (3.1)$$

the variational parameters α^p are meant to simulate the quenching of the spin-isospin interactions between particles 1 and 2 due to flipping of the spin and/or isospin of particle 1 or 2 by other particles in matter.²⁶⁾ The $\lambda^p(r)$ are primarily meant to simulate the screening effects in matter. They are determined by the healing distances d^p of $f^p(r_{ij})$; the d^p 's are treated as variational parameters.

For the sake of brevity and clarity we use letters c, σ, τ, t, b and q to represent operators $1, \sigma_i \cdot \sigma_j, \tau_i \cdot \tau_j, S_{ij}, (\vec{L} \cdot \vec{S})_{ij}$ and L_{ij}^2 . So $v^c, v^{\sigma\tau}, v^t, v^{q\tau}, v^{bb}$ respectively denote $v^1, v^4, v^5, v^{11}, v^{13}$, etc. In general minimizing the two-body cluster energy with the interaction $\bar{v}-\lambda$ gives eight coupled equations for the functions $f^{p=1,8}$. If, however, we assume that the healing distances satisfy the relations:

$$d^c = d^\sigma = d^\tau = d^{\sigma\tau} = d_c \quad (3.2)$$

$$d^t = d^{t\tau} = d_t \quad (3.3)$$

$$d^b = d^{b\tau} = d_b \quad (3.4)$$

the equations decouple into four sets, one each for pair spin and isospin $T, S = 1, 0; 1, 1; 0, 0$ and $0, 1$. At least in v_6 models $2 \cdot 2$ is found to be a reasonable assumption.²⁶⁾

It is convenient to define T, S channel functions:

$$x_{T,S}^c = x^c + (4S-3)x^\sigma + (4T-3)x^\tau + (4S-3)(4T-3)x^{\sigma\tau}, \quad (3.5)$$

$$x_{T,S}^q = x^q + (4S-3)x^{q\sigma} + (4T-3)x^{q\tau} + (4S-3)(4T-3)x^{q\sigma\tau}, \quad (3.6)$$

$$x_{T,S}^y = x^y + (4T-3)x^{y\tau}, \quad y = t, b \text{ and } bb. \quad (3.7)$$

In the above equations x can be v, \bar{v} or f . The $x_{T,S}^y$ are relevant only in the $S=1$ channels. The "uncorrelated ϕ 's" are defined as:

$$\phi_{T,S}^c(r) = \{1 - (-1)^{T+S} \ell^2(k_F r)\}^{1/2}, \quad (3.8)$$

$$\phi_{T,S}^q(r) = \left\{ \frac{1}{5} k_F^2 r^2 - (-1)^{T+S} r \ell(k_F r) \ell'(k_F r) \right\}^{1/2}, \quad (3.9)$$

$$\phi_{T,S}^{qq}(r) = \left\{ \frac{12}{175} k_F^4 r^4 + \frac{2}{5} k_F^2 r^2 - (-1)^{T+S} \frac{1}{2} (r \cdot \nabla)^2 \ell^2(k_F r) \right\}^{1/2}, \quad (3.10)$$

$$\ell(x) = 3(\sin(x) - x \cos(x))/x^3. \quad (3.11)$$

They give the expectation values of operators $1, L^2$ and L^4 with Fermi gas wavefunctions:

$$\frac{1}{A} \langle \phi | \sum_{i < j} x_{T,S}^p(r_{ij}) O_{ij}^p | \phi \rangle = \rho \frac{(2S+1)(2T+1)}{32} \int d^3r x_{T,S}^p(r) (\phi_{T,S}^p(r))^2. \quad (3.12)$$

Here A is the number of nucleons, and $p = c, q$ or qq .

It is simple to calculate the two-body cluster energy C_2 as a sum of four terms, each coming from a T,S channel:

$$C_2 = \sum_{T,S} C_{2,T,S} \quad (3.13)$$

The $C_{2,T,S}$ are functions of $\bar{v}_{T,S}^p$ and $f_{T,S}^{p'}$; $p=c$ and q , and $p'=c$ in $S=0$ states, while $p = c,t,b,q$ and bb , and $p' = c,t$ and b in $S=1$ states.

Minimizing the $C_{2,T,S}$ gives us the Euler-Lagrange (EL) equation for the $f_{T,0}^c$ in singlet states:

$$\left\{ -\frac{\hbar^2}{m} [\nabla^2 + 2(\phi_{T,0}^c)^{-1} \nabla \phi_{T,0}^c \cdot \nabla] + \bar{v}_{T,0}^c - \lambda_{T,0}^c + (\phi_{T,0}^c)^{-2} (\phi_{T,0}^q)^2 \bar{v}_{T,0}^q \right\} f_{T,0}^c = 0, \quad (3.14)$$

and a set of coupled EL equations for the $f_{T,1}^c$, $f_{T,1}^t$ and $f_{T,1}^b$ in triplet states:

$$\begin{aligned} & \left\{ -\frac{\hbar^2}{m} [\nabla^2 + 2(\phi_{T,1}^c)^{-1} \nabla \phi_{T,1}^c \cdot \nabla] + \bar{v}_{T,1}^c - \lambda_{T,1}^c + (\phi_{T,1}^c)^{-2} (\phi_{T,1}^q)^2 (\bar{v}_{T,1}^q + \frac{2}{3} \bar{v}_{T,1}^{bb}) \right\} f_{T,1}^c \\ & + \left\{ 8(\bar{v}_{T,1}^t - \lambda_{T,1}^t) - (\phi_{T,1}^c)^{-2} (\phi_{T,1}^q)^2 \frac{2}{3} \bar{v}_{T,1}^{bb} \right\} f_{T,1}^t \\ & + \frac{2}{3} (\bar{v}_{T,1}^b - \lambda_{T,1}^b - \frac{1}{2} \bar{v}_{T,1}^{bb}) (\phi_{T,1}^c)^{-2} (\phi_{T,1}^q)^2 f_{T,1}^b = 0, \end{aligned} \quad (3.15)$$

$$\begin{aligned} & \left\{ -\frac{\hbar^2}{m} [\nabla^2 + 2(\phi_{T,1}^c)^{-1} \nabla \phi_{T,1}^c - \frac{6}{r}] + \bar{v}_{T,1}^c - \lambda_{T,1}^c - 2(\bar{v}_{T,1}^t - \lambda_{T,1}^t) - 3(\bar{v}_{T,1}^b - \lambda_{T,1}^b) \right. \\ & \left. + 6\bar{v}_{T,1}^q + 9\bar{v}_{T,1}^{bb} + (\bar{v}_{T,1}^q + \frac{5}{6} \bar{v}_{T,1}^{bb}) (\phi_{T,1}^c)^{-2} (\phi_{T,1}^q)^2 \right\} f_{T,1}^t \\ & + \left\{ \bar{v}_{T,1}^t - \lambda_{T,1}^t - \frac{1}{12} (\phi_{T,1}^c)^{-2} (\phi_{T,1}^q)^2 \bar{v}_{T,1}^{bb} \right\} f_{T,1}^c \\ & - \frac{1}{12} (\bar{v}_{T,1}^b - \lambda_{T,1}^b - 2\bar{v}_{T,1}^{bb}) (\phi_{T,1}^c)^{-2} (\phi_{T,1}^q)^2 f_{T,1}^b = 0, \end{aligned} \quad (3.16)$$

$$\begin{aligned}
& \left\{ -\frac{\hbar^2}{m} [\nabla^2 + 2(\phi_{T,1}^q)^{-1} \nabla \phi_{T,1}^q \cdot \nabla] + \bar{v}_{T,1}^c - \lambda_{T,1}^c - \bar{v}_{T,1}^t + \lambda_{T,1}^t - \frac{1}{2} (\bar{v}_{T,1}^b - \lambda_{T,1}^b) \right. \\
& + (\phi_{T,1}^q)^{-2} (\phi_{T,1}^{qq})^2 (\bar{v}_{T,1}^q + \bar{v}_{T,1}^{bb}) \} f_{T,1}^b + (\bar{v}_{T,1}^b - \lambda_{T,1}^b - \frac{1}{2} \bar{v}_{T,1}^{bb}) f_{T,1}^c \\
& - (\bar{v}_{T,1}^b - \lambda_{T,1}^b - 2\bar{v}_{T,1}^{bb}) f_{T,1}^t = 0 .
\end{aligned} \tag{3.17}$$

The $\lambda_{T,S}^P$ are chosen to satisfy the imposed constraints on the $f_{T,S}^P$:

$$f_{T,S}^c(r > d_c) = 1 , \tag{3.18}$$

$$f_{T,S}^t(r > d_t) = 0 , \tag{3.19}$$

$$f_{T,S}^b(r > d_b) = 0 . \tag{3.20}$$

For the sake of brevity we assume $d_t \geq d_b \geq d_c$, a condition satisfied by the equilibrium values, and obtain:

$$\lambda_{T,1}^t(r > d_t) = \bar{v}_{T,1}^t - \frac{1}{12} (\phi_{T,1}^c)^{-2} (\phi_{T,1}^q)^2 \bar{v}^{bb} , \tag{3.21}$$

$$\lambda_{T,1}^b(r > d_b) = \bar{v}_{T,1}^b - \frac{1}{2} \bar{v}^{bb} (1 - 4 f^t) (1 - f^t)^{-1} , \tag{3.22}$$

$$\begin{aligned}
\lambda_{T,1}^c(r > d_c) = & \bar{v}_{T,1}^c + (\phi_{T,1}^c)^{-2} (\phi_{T,1}^q)^2 (\bar{v}_{T,1}^q + \frac{2}{3} \bar{v}_{T,1}^{bb}) + 8 (\bar{v}_{T,1}^t - \lambda_{T,1}^t) f_{T,1}^t \\
& - \frac{2}{3} (\phi_{T,1}^c)^{-2} (\phi_{T,1}^q)^2 \{ \frac{-bb}{v_{T,1}} f_{T,1}^t - (\bar{v}_{T,1}^b - \lambda_{T,1}^b - \frac{1}{2} \bar{v}_{T,1}^{bb}) f_{T,1}^b \} ,
\end{aligned} \tag{3.23}$$

$$\lambda_{T,0}^c(r > d_c) = \bar{v}_{T,0}^c + (\phi_{T,0}^c)^{-2} (\phi_{T,0}^q)^2 \bar{v}_{T,0}^q . \tag{3.24}$$

The $\lambda_{T,S}^P(r < d_p)$ are constants chosen so as to make the gradients

$$f_{T,S}^P = 0 \text{ at } r = d_p .$$

The nuclear-matter $E(k_F, d^P, \alpha^P, \dots)$ is calculated and minimized with respect to variations in d^P, α^P, \dots . The unspecified variational parameters could be the β^P used in ref. 9 or any other relevant choice.

B. Cluster Expansion of the Energy Expectation Value

Pandharipande and Wiringa⁹⁾ (PW), have derived a diagrammatic cluster expansion for the expectation value of the energy:

$$E = \frac{1}{A} \frac{\int \mathcal{A}(\Pi\phi_a^*) S[\Pi_{a<b} F_{ab}^+] H S[\Pi_{a<b} F_{ab}] (\Pi\phi_a) d\tau}{\int \mathcal{A}(\Pi\phi_a^*) S[\Pi_{a<b} F_{ab}^+] S[\Pi_{a<b} F_{ab}] (\Pi\phi_a) d\tau} \quad (3.25)$$

where for simplicity they antisymmetrize only the left hand side ψ^* .






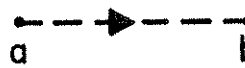



Since for an infinite system the exact evaluation of (3.25) is impossible, it is approximated by expanding the ΠF^2 in the integrals in the numerator and denominator, in powers of the short range functions:

$$F_{12}^C = f_{12}^C - 1, \quad F_{12}^{P>1} = 2f_{12}^P f_{12}^C \quad \text{and} \quad f_{12}^{P>1} f_{12}^{Q>1} \quad (3.26)$$

This expansion can be represented by generalized Mayer diagrams using the elements shown in Fig. 22. The elements 1-3 represent "passive" correlations, while elements 5-9 depict the operation of H. The interaction line 5 includes terms in which ∇_a^2 and ∇_b^2 operate on the F_{ab} . The derivative lines 6-9 are needed to calculate kinetic contributions having $\nabla_a F_{ab} \cdot \nabla_a F_{ac}$ and $\nabla_a F_{ab} \cdot \nabla_a \phi$.

A typical diagram representing one of the integrals in the expansion will have points labeled by i, j, \dots , each one standing for the coordinates $\vec{r}_i, \vec{r}_j, \dots$, of particles i, j, \dots . An integration over all $\vec{r}_i, \vec{r}_j, \dots$, is implied. The points are connected by elements shown in Fig. 22, that represent the functions of r_{ij} in the integrand.

Since ψ^* is antisymmetrized we need to keep track of the plane wave states occupied by the particles in ψ^* . For this we use solid lines

1		F_{ab}^c
2		$F_{ab}^{p>l} O_{ab}^p$
3		$f_{ab}^{p>l} f_{ab}^{q>l} O_{ab}^p O_{ab}^q$
4		$e^{i\vec{k}_a \cdot (\vec{r}_a - \vec{r}_b)} (l_{ab})$
5		$f_{ab}^p H_{ab}^q f_{ab}^l O_{ab}^p O_{ab}^q O_{ab}^l$
6		$\nabla_a F_{ab}^c$
7		$\nabla_a (F_{ab}^{p>l} O_{ab}^p)$
8		$\nabla_a (f_{ab}^{p>l} f_{ab}^{q>l} O_{ab}^p O_{ab}^q)$
9		$i\vec{k}_a e^{i\vec{k}_a \cdot (\vec{r}_a - \vec{r}_b)} (\nabla_a l_{ab})$

with directions, which are called exchange lines (4th and 9th elements in Fig. 22). By convention the particles 1,2,...,A occupy states k_1, k_2, \dots, k_A in ψ . Those terms in the Slater determinant $\prod_a e^{-i\vec{k}_a \cdot \vec{r}_a}$ of ψ^* where the particles remain in the same states are called direct, and their diagrams contain no exchange lines. An exchange line going from a to b represents the contribution of a term in ψ^* where particle b occupies state \vec{k}_a . Since each particle must end up in a definite state, all exchange lines must join to form closed loops, and only one exchange line may pass through any point. The total exchange pattern in any exchange diagram will consist of one or more exchange loops.

The wavy lines as well as the interaction lines are labeled according to the operators they carry. The exchange of the spin and isospin of particles a and b can be represented by an operator e_{ab} :

$$e_{ab} = \frac{1}{4}(1 + \sigma_{ab} + \tau_{ab} + \sigma_{ab}\tau_{ab}) . \quad (3.27)$$

An n-particle exchange loop is equivalent to a series of (n-1) two-body exchanges. Thus every such loop has an associated factor of $(-1/4)^{n-1}$, and all but one of the exchange lines has an operator label n to represent $O_{ab}^{n \leq 4}$. Every exchange line also has the $e^{-i\vec{k}_a \cdot \vec{r}_{ab}}$ factor, which on summing over \vec{k}_a gives the Slater function $\ell(k_{F_{ab}})$. The $\vec{\nabla}_a F_{ac} \cdot \vec{\nabla}_a \phi$ terms in the energy expectation value gives zero contribution, unless particle a is exchanged. When this is the case, we get terms having $\nabla_a F_{ac} \cdot i\vec{k}_a e^{i\vec{k}_a \cdot \vec{r}_{ab}}$, whose contribution is given by diagrams having the derivative exchange line. (The 9th element of Fig. 22.)

The contribution of any diagram can be separated into two factors. One is the spatial integral that contains all the functions $F^c, F^{p>1}$,

$f^{p>1} f^{q>1}$, v^q , etc., denoted by the diagrammatic elements. The other is the product of the associated operators.

If a diagram contains at least one pair of points such that there is no path, made up from elements contained in Fig. 22, joining them, the diagram is said to be disconnected, otherwise it is said to be connected. A connected diagram that cannot be reduced to a disconnected one by cutting at a single point is said to be an irreducible diagram; otherwise it is said to be reducible, or separable.

A connected diagram that contains an interaction line or two derivative lines is called an interacting diagram, otherwise it is called non-interacting. Interacting diagrams come only from the numerator of (3.25) while non-interacting diagrams can come either from the numerator or the denominator. There is a countably infinite number of diagrams in each class.

Let $[A]$ be the A^{th} irreducible interacting diagram and $[a]$ be the a^{th} irreducible non-interacting one. By $[Aa]$ we denote the diagram formed when $[A]$ and $[a]$ have no points in common. Clearly this diagram is disconnected. By $\overline{[Aa]}$ we denote the diagram formed when $[A]$ and $[a]$ are articulated at a single point. Clearly this is a separable diagram. Diagrams $\overline{[Aa]}$, $\overline{\overline{[Aa]}}$, ... involving two, three or more articulation points are not considered because they are irreducible interacting diagrams which are already contained in class $[A]$. By $\overline{[A][a]}$ we denote the product of diagrams $[A]$ and $[a]$ which have all but one point labels different.

The derivation of the diagrammatic cluster expansion is given in PW. Here we merely quote the result.

$$E = [A] + \overline{[Aa]} - \overline{[A][a]} + \text{terms having three or more irreducible pieces.} \quad (3.28)$$

The first term is the sum of all irreducible interacting diagrams. The second is the difference between the expectation value of all separable diagrams of the form $\overline{[Aa]}$, and $\overline{[A]}\overline{[a]}$ is the product of the expectation values of the two associated separated diagrams. (In the matrix element associated with a diagram, the exchange operators implied from the exchange lines, if any, should appear to the very left, since their existence is due to the antisymmetrizer that operates on Φ^* .)

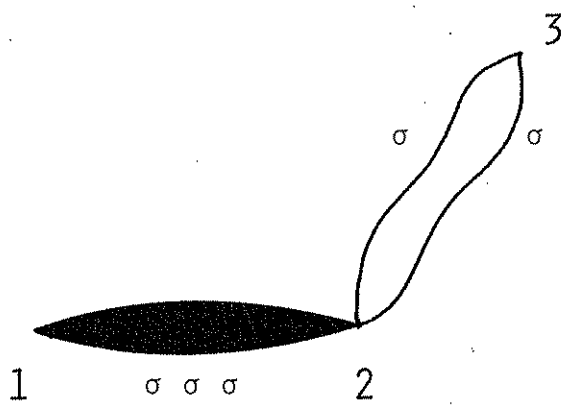
The operators associated with $f^{p>1} = 2f^c f^p$ in an interacting diagram can come either from the left or the right side of the Hamiltonian with equal probability. The operators O^p and O^q associated with $f^{p>1} f^{q>1}$ cannot come from the same side of the Hamiltonian. By convention $O^{p>1}$ is taken always to come from the left and $O^{q>1}$ from the right. In the calculation of the operator of a diagram we must separately symmetrize the product of all the operators coming from correlations to the left of H and to the right of H.

Thus the operator part of a diagram is generally of the type:

$$\sum_i w^i \Pi^i O_{ab}$$

where $\Pi^i O_{ab}$ denotes the product of O_{ab} in a specific order labeled by i , and w^i is the probability for that order to occur. For example the operator part of diagram 23 is:

$$\begin{aligned} & \frac{1}{4} \{ \sigma_{12}, \sigma_{23} \} \sigma_{12} \{ \sigma_{12}, \sigma_{23} \} = \\ & \frac{1}{4} \sigma_{12} \sigma_{23} \sigma_{12} \sigma_{12} \sigma_{23} + \frac{1}{4} \sigma_{23} \sigma_{12} \sigma_{12} \sigma_{12} \sigma_{23} + \\ & \frac{1}{4} \sigma_{12} \sigma_{23} \sigma_{12} \sigma_{23} \sigma_{12} + \frac{1}{4} \sigma_{23} \sigma_{12} \sigma_{12} \sigma_{23} \sigma_{12} \end{aligned} \quad (3.29)$$



The Pauli identity:

$$\vec{\sigma}_1 \cdot \vec{A} \vec{\sigma}_1 \cdot \vec{B} = \vec{A} \cdot \vec{B} + i \vec{\sigma}_1 \cdot (\vec{A} \times \vec{B}) \quad (3.30)$$

can be used to express any operator product as:

$$\pi O_{ab}^P = C + \text{rest} \quad (3.31)$$

where C is an operator independent of spin or isospin (such as $1, L^2, L^4$ etc.), and the rest contains terms in which each $\vec{\sigma}_a$ or $\vec{\tau}_a$ occurs at most once. Since the expectation value of $\vec{\sigma}_a$ or $\vec{\tau}_a$ is zero, the contribution of the operator product in (3.30) is just given by C. Rules to calculate "C-parts" of operator products are given in PW.

The C-parts depend in general upon the order of operators in the product. For example the C-parts of the four terms in Eq. (3.29) are respectively: $6/4$, $-18/4$, $6/4$, and $6/4$. Thus the operator part of the [Aa] diagram 22 is zero. This differs from the product of C-parts of the separated diagrams $\overline{[A][a]}$, which in this case is $(-6) \times 3 = -18$. The radial parts of $\overline{[Aa]}$ and $\overline{[A][a]}$ are identical, but their operator parts may be different, as illustrated above. Notice that in Jastrow theory, where the correlation f_j is purely central, one does not consider $\overline{[Aa]} - \overline{[A][a]}$ terms, because in that case $\overline{[Aa]}$ and $\overline{[A][a]}$ have identical C-parts and thus cancel each other. The cluster expansion of PW then, reduces to the well known irreducible Mayer cluster expansion, where only the irreducible interacting diagrams [A] contribute to the energy expectation value.

It is convenient to decompose E into three parts:

$$E = E_6 + E_{LS} + E_Q \quad (3.32)$$

where E_6 is the sum of all diagrams that do not carry operators $O^{p \geq 7}$. The E_6 is large and is calculated carefully by methods developed by PW. For the sake of completeness we briefly review the calculation of E_6 . E_{LS} is the sum of all diagrams having at least one $\vec{L} \cdot \vec{S}$ line but no v^{9-14} interactions. The calculation of E_{LS} is discussed in Section 3D. The E_Q is the sum of all diagrams carrying v^{9-14} interaction lines and it is discussed in Section 3E. E_Q is just an expectation value of v^{9-14} interactions, however E_{LS} is not a simple expectation value because we can have diagrams with $\vec{L} \cdot \vec{S}$ operators coming from F.

C. Calculation of E_6

The set of the operators $O_{12}^{p=1,6}$ in (1.24) is closed under multiplication, i.e.;

$$O_{12}^i O_{12}^j = \sum_{m=1}^6 K^{ijm} O_{12}^m. \quad (3.33)$$

The matrices K^{ijm} , so defined are given explicitly in PW. The C-part of a product of two operators is then:

$$C(O_{12}^i O_{12}^j) = K^{ij1} \equiv A^i \delta_{ij}, \quad (3.34)$$

$$A^{i=1,6} = 1, 3, 3, 9, 6, 18, \quad \text{and} \quad (3.35)$$

$$C(O_{12}^i O_{12}^j O_{12}^k) = \sum_{m=1}^6 K^{ijm} K^{mkl} = A^k K^{ijk}, \quad \text{etc.} \quad (3.36)$$

Calculation of C-parts for any general many body diagram is quite complicated. PW select classes of important diagrams and calculate their C-parts, using the following two identities:

$$\sum_{\sigma_b, \tau_b} \int d\phi_b O_{ab}^p O_{bc}^q = \sum_{r=1}^6 \int d\phi_b \xi_{abc}^{pqr} O_{ac}^r \quad (3.37)$$

and

$$\frac{1}{4\pi} \int \sin\theta_b d\theta_b d\phi_b \sum_{\sigma_b, \tau_b} O_{ab}^i O_{ac}^j O_{ab}^k = \delta_{ik} A^i (1 + D_{ij}) O_{ac}^j. \quad (3.38)$$

Here θ_b and ϕ_b are the polar and azimuthal angles of the vector \vec{r}_{ab} in a coordinate system where the z-axis is taken to be along the \vec{r}_{ac} direction. Equation (3.37) defines the ξ_{abc}^{pqr} , which are functions of the angles of the triangle (abc), while Eq. (3.38) defines the elements D_{ij} given in PW.

A set of coupled integral equations is used to sum central Fermi hypernetted chains (FHNC) and single operator chains (SOC). Before we review them it is proper to define the two-body distribution function:

$$g(r) = \frac{1}{A\rho} \langle \delta(r - r_{nm}) \rangle \quad (3.39)$$

$g(r)$ gives the probability of finding a particle at a distance r from a chosen particle.

The diagrams for g_{mn} can be classified as composite, nodal and elementary. A nodal point, in a diagram connecting the points m and n , is a point through which all paths connecting m and n must pass. Nodal diagrams, otherwise called chains, are those that have at least one nodal point. Diagrams with no nodal points can either be composite or elementary. Composite diagrams are those that have at least two unconnected paths joining m and n . Diagrams which are neither nodal nor composite are called elementary. A link is defined to be any diagram or diagrammatic element that joins two consecutive nodal points in a nodal diagram. Links then may be, non-interacting diagrammatic elements, composite diagrams and elementary diagrams.

We denote by $G_{xy,ik}^c$ the chain, with central links, that connects the particles i and k which respectively have an exchange nature x and y . The labels xy may be dd , de , ed , ee or cc . The subscript d stands for a "direct" end, e for an "exchange" end and c for a "circular exchange" end. $G_{dd,ik}^c$ thus denotes the sum of all chains in which neither i nor k is exchanged. $G_{de,ik}^c$ is the sum of chains in which k is exchanged with particles in the chain and i is not. $G_{ed,ik}^c$ just reverses the roles of i and k and is numerically equal to $G_{de,ik}^c$. Chains that contribute to $G_{ee,ik}^c$ have both i and k exchanged in independent exchange loops contained in the chains, while chains with an incomplete exchange loop passing through both i and k are included in $G_{cc,ik}^c$. Examples of dd , de , ee and cc chains are given in Fig. 24, diagrams 24.1-23.4.

The links, which in the FHNC approximation do not contain elementary diagrams, are denoted in the same convention as $X_{xy,ik}^c$. However, since a link can be composite, the $X_{ee,ik}^c$ can have both i and k exchanged in the same loop, or in two independent loops within the link.

The end points labeled d , c , and e in chains have zero, one and two exchange lines respectively. Since any point in a diagram contributing to the energy expectation value must have either zero or two exchange lines, we can join $X_{xx',y}^c$ with $X_{y'y,jk}^c$ or $G_{y'y,jk}^c$ at j , only in the combinations $x'y' = dd, de, ed, cc$. For $xy = dd, de, ee$ the FHNC equations, derived first by Fantoni and Rosati,⁶²⁾ become:

$$G_{xy,ik}^c = \sum_{x',y'} \theta[X_{xx',ij}^c; (X_{y'y,jk}^c + G_{y'y,jk}^c)] \quad (3.40)$$

where the sum is over $x'y' = dd, de, ed$. The links X_{xy}^c are given by:

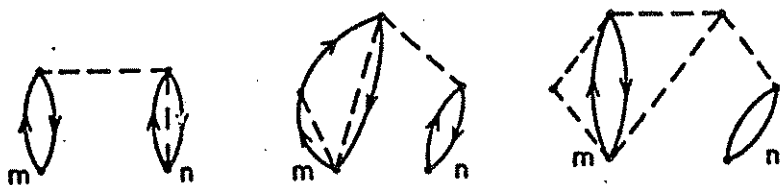
$$X_{dd}^c = f^c \exp[G_{dd}^c] - 1 - G_{dd}^c \quad (3.41)$$



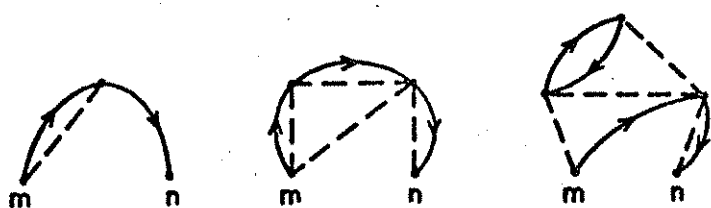
24.1



24.2



24.3



24.4

$$X_{de}^c = f^c G_{de}^c \exp(G_{dd}^c) - G_{de}^c \quad (3.42)$$

$$X_{ee}^c = f^c [G_{de}^c + G_{ee}^c - L^2/4] \exp[G_{dd}^c] - G_{ee}^c \quad (3.43)$$

where:

$$L = -\ell + 4 G_{cc}^c .$$

The G_{cc}^c chain equation is:

$$G_{cc,ik}^c = \theta[X_{cc,ij}^c; (X_{cc} + L/4)_{jk}] \quad (3.44)$$

$$X_{cc}^c = \{f^c \exp[G_{dd}^c] - 1\}L/4 . \quad (3.45)$$

Here θ is the integral operator given by:

$$\theta[X_{ij}^c; Y_{jk}^c] = \rho \int d^3 r_j X_{ij}^c Y_{jk}^c . \quad (3.46)$$

For the SOC case PW exploit equation (3.37) repeatedly to treat the operator links. They define the integral operator:

$$\theta_{ijk}^{pqr}(X_y^p; Y_{jk}^q) \equiv \rho \int \epsilon_{ijk}^{pqr} X_{ij}^p Y_{jk}^q d^3 r_j , \quad (3.47)$$

and the direct functions:

$$h^p = f^p + f^c G_{dd}^p \quad (3.48)$$

$$h^c = \exp(G_{dd}^c) \quad (3.49)$$

In (3.48) G_{dd}^p is the dd chain associated with the operator denoted by p.

The links then are given by:

$$X_{dd}^p = h^p h^c - G_{dd}^p \quad (3.50)$$

$$X_{de}^p = X_{ed}^p = (h^p G_{de}^c + f^c G_{de}^p) h^c - G_{de}^p \quad (3.51)$$

$$x_{ee}^P = [h^P(G_{de}^c + G_{ee}^c) + f^c(-L^2\Delta^P/4 + G_{ee}^P + 2G_{de}^P G_{de}^c)]h^c - G_{ee}^P. \quad (3.52)$$

The SOC equations for $xy = dd, de, \text{ and } ee$ are then:

$$G_{xy,ik}^r = \sum_{x'y'} \sum_{pq} \theta_{ijk}^{pqr}(x_{xx',ij}^p; [X+G]_{y'y,jk}^q) \quad (3.53)$$

where $x'y'$ take the values dd, de, ed .

The treatment of G_{cc}^P chain is somewhat more complex, and may be found in Ref. 9. PW also improve the SOC equations by vertex corrections at nodal points. These corrections take into account contributions of simple separable diagrams such as $([\overline{Aa}] - [\overline{A}][\overline{a}])$, in which the nodal point of the SOC is an articulation point.

The energy expectation value is expressed as a sum of five terms,

$$E = T_F + W + W_F + U + U_F \quad (3.54)$$

according to the different parts of ψ that the Hamiltonian acts upon.

When ∇_m^2 operates only on ϕ_m we get the Fermi gas kinetic energy

$T_F = .3 \frac{\hbar^2}{m} K_F^2$. The other terms must be evaluated through the diagrammatic

cluster expansion. The W includes the potential energy and kinetic

energy terms having $\nabla_{m mn}^2$. It is given by the sum of all diagrams having

the interaction line pqr (of Fig. 22), containing the operator H_{mn}^q ,

$$H_{mn}^c = -\frac{\hbar^2}{m} \nabla_{mn}^2 + v_{mn}^c, \quad (3.55)$$

$$H_{mn}^{q>1} = v_{mn}^q, \quad (3.56)$$

sandwiched between f_{mn}^p and f_{mn}^r , with the ∇_{mn}^2 in H_{mn}^c operating only on

f_{mn}^r . The v represents the sum of kinetic energy terms $\vec{\nabla}_m f_{mn} \cdot \vec{\nabla}_m f_{mo}$ ($o \neq n$).

Kinetic energy terms $\vec{\nabla}_m^F \cdot \vec{\nabla}_m \phi_m$ are counted in W_F and U_F . They only contribute when particle m is exchanged. If the exchange pattern of the diagram is such that a $\nabla_{m\ mn}^l$ element appears, the diagram is included in W_F , whereas those having a $\nabla_{m\ mo}^l$ element contribute to U_F .

The W diagrams in the FHNC/SOC approximation may be further subdivided as:

$$W = W_o + W_s + W_c + W_{cs} \quad (3.57)$$

W_o is the sum of all diagrams that do not have an operator chain connecting point m and n . Central correlation chains do not affect the operator algebra and there may be any number of them in a W diagram of any class. W_c diagrams have one SOC connecting n and m , while W_s diagrams have a separable single operator ring (SOR) attached at either vertex m or n . The W_{cs} have both an SOC between m and n and a separable SOR at m or n . Figure 25 illustrates the diagrammatic topology of W_o , W_s , W_c and W_{cs} .

PW calculate exactly the W_o , W_s and W_c and they estimate the small W_{cs} diagrams. The expressions for the five terms of (3.57) can be found in PW, and hence they are not quoted here.

A glance at Table V reveals that the dominant repulsive term is the Fermi gas kinetic energy T_F , whereas the dominant attraction comes from the E_6 two-body terms. The second important repulsive term seems to come from the separable (W_s) diagrams, and its magnitude, for the v_{14} model is roughly 10% of the E_6 two-body contribution. W_o (MB), which includes the two-body diagrams "dressed" with central chains in the FHNC approximation, is the second important attractive term, and its magnitude rises rapidly with the density. At NM density its magnitude is comparable

Table V

Contributions to Nuclear Matter Energy in MeV/A.

Potential	v_{14}	v_{14}	v_{14}	Reid- v_{12}
k_F	1.13	1.33	1.6	1.6
$d(\text{fm})$	2.53	2.15	1.79	1.79
$d_t(\text{fm})$	4.04	3.44	2.86	2.86
α	0.8	0.8	0.8	0.8
T_F	15.89	22.01	31.85	31.85
E_6 : 2-body	-30.91	-40.06	-53.42	-51.67
E_6 : $W_o(\text{MB})$	-0.45	-3.14	-7.47	-7.85
E_6 : W_c	2.33	3.12	3.30	-0.64
E_6 : W_s	3.51	4.44	5.74	8.33
E_6 : W_{cs}	-0.31	-0.30	-0.13	0.40
E_6 : $W_F(\text{MB}) + U_F$	0.35	0.25	0.46	0.89
E_6 : U	0.14	0.14	1.09	1.13
E_6 : Total	-9.56	-13.56	-18.58	-17.57
E_{LS} : 2-body	-1.24	-2.34	-4.75	-3.67
E_{LS} : MB	0.13	0.07	-0.40	-0.24
E_Q : 2-body	0.22	1.10	3.55	2.19
E_Q : MB	0.72	1.35	3.00	2.19
E : Total	-9.71	-13.40	-17.19	-17.11



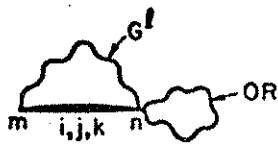
W_0 25.1



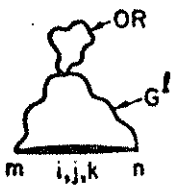
W_c 25.2



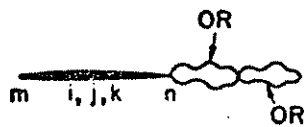
W_s 25.3



W_{cs} 25.4



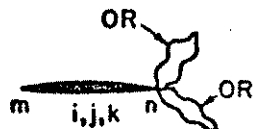
25.5



25.6



25.7



25.8

to that of W_s . For the v_{14} model, W_c is repulsive and increases slowly with the density; however it is small and attractive in the Reid v_{12} model. W_{cs} is very small and reduces W_c by $\sim 10\%$ in the v_{14} model. The combined contribution of $W_F(\text{MB})$, v_F and v is repulsive and at NM density it is just 10% of the W_s contribution.

Earlier calculations, reviewed by Bethe⁴⁾ indicated that the NM energy is sensitive to the strength of the tensor force. These calculations were mostly done at the two-body cluster level. However, our calculations, with the v_{14} and Reid v_{12} models, which differ significantly in the strengths of their tensor potentials, show that this may not be true. The stronger tensor force generates larger repulsive W_s contributions but it also gives more attractive W_c contributions so that the net effect on the NM energy is very small.

There are two major approximations involved in the FHNC/SOC scheme. First is the assumption that the major contribution of passive non-central correlations can be taken into account with single operator chains. Second is that separable diagrams having many operator rings at a common articulation point are smaller than those having only two. These two approximations have been recently studied by Wiringa²⁶⁾ by calculating the leading corrections. The corrections are found to be quite small ($\sim 10\%$) compared to the leading terms. Moreover they tend to cancel out, and the net change in the $E(\rho)$ of the Reid v_6 model due to these corrections is estimated to be ≤ 0.5 MeV at $k_F < 1.6 \text{ fm}^{-1}$.²⁶⁾

D. The Calculation of E_{LS}

Before we go on to calculate the contribution to the energy of the relevant diagrams, let us first dwell on the operator algebra necessary

to carry out this calculation. It is convenient to use the following generalization of the tensor and spin-orbit operators to calculate the various C-parts, encountered in the v_8 problem. Let \vec{A}, \vec{B}, \dots be the vector operators \vec{r}, \vec{v} and \vec{L} . Then define:

$$\alpha_{12}(\vec{A}, \vec{B}) = \frac{3}{2}[\vec{\sigma}_1 \cdot \vec{A} \vec{\sigma}_2 \cdot \vec{B} + \vec{\sigma}_2 \cdot \vec{A} \vec{\sigma}_1 \cdot \vec{B}] - \vec{A} \cdot \vec{B} \sigma_{12} \quad (3.58)$$

$$\beta_{12}(\vec{A}) = \frac{1}{2}[\vec{\sigma}_1 + \vec{\sigma}_2] \cdot \vec{A} \quad (3.59)$$

Note that $b_{12} = \beta_{12}(\vec{L})$ and $t_{12} = \frac{1}{2} \alpha_{12}(\vec{r}_{12}, \vec{r}_{12})$. (3.60)

It can be verified that $\alpha_{12}(\vec{A}, \vec{B}) = \alpha_{12}(\vec{B}, \vec{A})$ in spite of the fact that the operators \vec{A}, \vec{B} do not commute. It may also be verified that the operators: $1, \sigma, \tau, \sigma\tau, \beta(\vec{A}), \beta(\vec{A})\tau, \alpha(A, B)$, and $\alpha(A, B)\tau$ do form a closed set under multiplication. Some of the useful products of these operators are given below:

$$\sigma_{12} \beta_{12}(\vec{A}) = \beta_{12}(\vec{A}) \sigma_{12} = \beta_{12}(\vec{A}) \quad (3.61)$$

$$\sigma_{12} \alpha_{12}(\vec{A}, \vec{B}) = \alpha_{12}(\vec{A}, \vec{B}) \sigma_{12} = \alpha_{12}(\vec{A}, \vec{B}) \quad (3.62)$$

$$b_{12}^2 = \frac{1}{2} L_{12}^2 + \frac{1}{6} \sigma_{12} L_{12}^2 - \frac{1}{2} b_{12} + \frac{1}{6} \alpha_{12}(\vec{L}, \vec{L}) \quad (3.63)$$

$$b_{12} t_{12} = -b_{12} - 3t_{12} + \alpha_{12}(\vec{r}, \vec{v}) - t_{12} \vec{r} \cdot \vec{v} \quad (3.64)$$

$$t_{12} b_{12} = -b_{12} - \alpha_{12}(\vec{r}, \vec{v}) + t_{12} \vec{r} \cdot \vec{v} \quad (3.65)$$

Since the operators $\beta_{12}(\vec{A})$ have two terms, one linear in $\vec{\sigma}_1$ and the other linear in $\vec{\sigma}_2$, while $\alpha_{12}(\vec{A}, \vec{B})$ is linear in both $\vec{\sigma}_1$ and $\vec{\sigma}_2$, only products of the form $\beta_{12}(\vec{A})\beta_{12}(\vec{B})$ and $\alpha_{12}(\vec{A}, \vec{B})\alpha_{12}(\vec{C}, \vec{D})$ can have a non-vanishing C-part. Some useful C-parts are quoted below:

$$C(tbt) = -18, \quad C(bbb) = -\frac{1}{4} L^2 \quad \text{and:} \quad (3.66)$$

$$C(bb) = -C(tbb) = -C(btb) = \frac{1}{2} L^2. \quad (3.67)$$

All other required C-parts are trivially obtained from the above with the help of the identities (3.61)-(3.65) and the rules given in Section 3C. The direct and exchange W_0 two-body contributions to the energy are then given by:

$$\sum_{i,j,k} \frac{1}{2} \rho \int d^3 r_{12} \langle C[f_{12}^i o_{12}^i H_{12}^j o_{12}^j f_{12}^k o_{12}^k] \rangle_{\text{dir}} \quad (3.68)$$

and

$$\sum_{n=1,4} \sum_{i,j,k} -\frac{1}{8} \rho \int d^3 r_{12} \langle C[o_{12}^n f_{12}^i o_{12}^i H_{12}^j o_{12}^j f_{12}^k o_{12}^k] \rangle_{\text{ex}} \quad (3.69)$$

where:

$$\langle X_{12} \rangle_{\text{dir}} = \left(\frac{3}{4\pi k_F} \right)^2 \int dk_1^3 dk_2^3 \phi_{21}^* X_{12} \phi_{12} \quad (3.70)$$

$$\langle X_{12} \rangle_{\text{ex}} = \left(\frac{3}{4\pi k_f} \right)^2 \int dk_1^3 dk_2^3 \phi_{21}^* X_{12} \phi_{12} \quad (3.71)$$

with

$$\phi_{12} = \exp(ik_1 \cdot r_1 + ik_2 \cdot r_2) \quad (3.72)$$

and

$$\phi_{21} = \exp(ik_1 \cdot r_2 + ik_2 \cdot r_1) \quad (3.73)$$

The contribution to E_{LS} energy comes from terms in which at least one of the indices i, j, k is associated with a spin-orbit operator. C-parts of products involving at most three b operators are either numerical constants or the L^2 operator multiplied with a numerical factor. The direct and exchange expectation values of L^2 needed to carry out the calculation described above, are given in Table VI. The Hamiltonian component H_{12}^j

Table VI

	$\langle L^n \rangle$	
n	$\langle L^n \rangle_{\text{dir.}}$	$\langle L^n \rangle_{\text{ex.}}$
0	1	ℓ^2
2	$\frac{1}{5} k_F^2 r^2$	$r \ell \ell'$
t	$\frac{12}{175} k_F^4 r^4 + \frac{2}{5} k_F^2 r^2$	$\frac{1}{2} (r \cdot \nabla)^2 \ell^2$

can be written as:

$$H_{12}^j = v_{12}^j - \delta_{jc} \frac{\hbar^2}{m} \nabla_{12}^2 . \quad (3.74)$$

We can separate the ∇^2 term in H^C , and by commuting it out we obtain the following useful relations that eases the calculation of (3.68) and (3.69).

$$\begin{aligned} C(f_{12}^i O_{12}^i H_{12}^j O_{12}^j f_{12}^k O_{12}^k) = \\ [f_{12}^i H_{12}^j f_{12}^k] C(O_{12}^i O_{12}^j O_{12}^k) - \delta_{jc} \frac{\hbar^2}{m} [2f_{12}^i C(O_{12}^i (\nabla_{12} f_{12}^k) \cdot (\nabla_{12} O_{12}^k))] \\ + f_{12}^i f_{12}^k C(O_{12}^i \nabla_{12}^2 O_{12}^k)] , \end{aligned} \quad (3.75)$$

$$\nabla_{12}^2 b_{12} = 0, \quad \text{and} \quad (\nabla_{12} f_{12}^k) \cdot (\nabla_{12} b_{12}) = \frac{f_{12}^{k'}}{r_{12}} b_{12} . \quad (3.76)$$

The W_F contribution comes from terms $(\nabla_{1F} F_{12}) \cdot \nabla_{1F} \phi_1$. W_F contributes only when particle 1 is exchanged, since $\vec{\nabla}_1 \phi_1$ is proportional to \vec{k}_1 which in the direct case vanishes upon angular integration. The two-body W_F contribution to E_{LS} can be shown, after some operator algebra to be:

$$\frac{\hbar^2}{8m} \rho \int [(f_{12}^b + 3f_{12}^{b\tau}) f_{12}^{b'} + 3(f_{12}^b - f_{12}^{b\tau}) f_{12}^{b\tau'}] [r_{12}^{\ell_{12} \ell_{12}''} + r_{12}^{\ell_{12}' 2 - \ell_{12} \ell_{12}'}] d^3 r_{12} . \quad (3.77)$$

Here primes denote derivatives with respect to r_{12} . Two-body contributions to E_{LS} are much smaller than those in E_6 , as shown in Table VII. This may appear surprising in view of the large magnitudes of v^b and f^b (Fig. 28). However the important E_{LS} contributions have a C-part of $\sim \frac{1}{2} L^2$ which gives a factor of $\sim \frac{1}{10} k_f^2 r^2$. At $r < 1$ fm where f^b and v^b are

Table VII

	Reid V-8	$k_F = 1.77$
	E_6	E_{LS}
T_F	38.98	0.
$W_O - 2 \text{ body}$	-56.10	-3.47
$W_F - 2 \text{ body}$	- 3.69	-0.17
W_s	11.54	-0.22
$W_O - MB$	- 9.69	-0.29
$W_c + W_{cs}$	- 2.78	0.29
$W_F - MB$	- 1.32	- N.C.
U_F	2.94	- N.C.
U	2.84	- N.C.
Total	-17.28	-3.86

appreciable it cuts down all LS contributions. At high densities though, ($k_f \geq 5 \text{ fm}^{-1}$) the E_{LS} contributions may be comparable to those of E_6 .

Since the two-body is in general an order of magnitude bigger than the many-body contribution, we expect the E_{LS-MB} to be quite small. So we estimate it by calculating only the leading three-body corrections.

The general expression for the direct three-body contribution of W_s , corresponding to the diagram 26.1 is given by:

$$\sum_{i,j,k,p,q} \rho^2 \int d^3r_{nm} d^3r_{m1} < \frac{1}{4} C[(f_{mn}^i O_{mn}^i, f_{m1}^p O_{m1}^p) H_{mn}^j O_{mn}^j (f_{mn}^k O_{mn}^k, f_{m1}^q O_{m1}^q)] - C[f_{mn}^i O_{mn}^i H_{mn}^j O_{mn}^j f_{m1}^k O_{m1}^k] C[f_{m1}^p O_{m1}^p f_{m1}^q O_{m1}^q] >_{dir} \quad (3.78)$$

where,

$$\langle X_{m1} \rangle_{dir} = \left(\frac{3}{4\pi k_F^3} \right)^3 \int d^3k_m d^3k_n d^3k_1 \phi_{mnl}^* X_{mnl} \phi_{mnl} \quad (3.79)$$

with

$$\phi_{mnl} = \exp(ik_m \cdot r_m + ik_n \cdot r_n + ik_1 \cdot r_1) \quad (3.80)$$

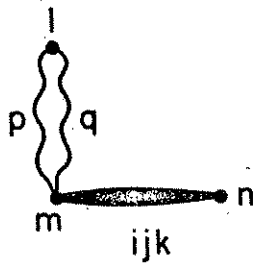
The exchange diagrams 26.2 and 26.3 will have apart from the relevant spin-isospin exchange operators the expectation values: $\langle X_{mnl} \rangle_{ex,m1}$ and $\langle X_{mnl} \rangle_{ex,mn}$ which involve the functions ϕ_{1nm}^* and ϕ_{nml}^* respectively.

$$\phi_{1nm} = \exp(ik_m \cdot r_1 + ik_n \cdot r_n + ik_1 \cdot r_m) \quad (3.81)$$

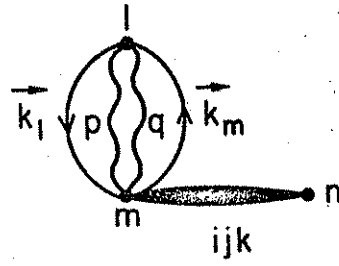
and

$$\phi_{nml} = \exp(ik_m \cdot r_n + ik_n \cdot r_m + ik_1 \cdot r_1) \quad (3.82)$$

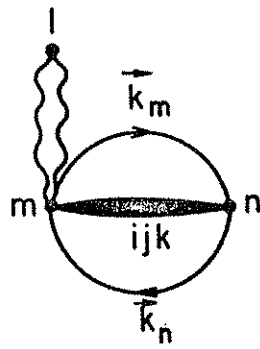
The "f-part" of our E_{LS} diagram contains terms in which a \vec{V} coming from an $\vec{L} \cdot \vec{S}$ operator acts on correlations F , while the "k-part" includes



26.1



26.2



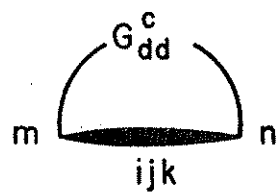
26.3

terms in which the $\vec{\nabla}$ acts upon ϕ . The f- and k-parts of E_{LS} are generally comparable in magnitude since the kinetic energy due to correlations is comparable to the Fermi kinetic energy. For example in Reid v_8 model at $k_F = 1.77 \text{ fm}^{-1}$ the f- and k-parts of three-body $\vec{L} \cdot \vec{S} W_s$ diagrams are -1.54 and 1.32 MeV respectively.

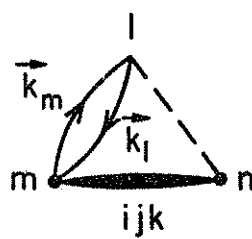
In the present calculation, terms having both b_{mn} and b_{ml} operators have been ignored, since their estimated order of magnitude is very small. Also neglected is the contribution coming from four and more body separable terms, since they should be a small fraction of the calculated three-body W_s contribution to E_{LS} . The W_s terms contribute very little to the E_{LS} . This is due to cancellations that occur between the f- and the k-parts.

In v_6 models the magnitude of the contribution of chain diagrams is typically a tenth of the two-body energy. Accordingly we may expect the contribution of chain diagrams to E_{LS} to be of the order of 0.5 MeV and thus not too important. The k-part of the chain diagrams is calculated but their f-part is not. However, we may expect that the neglected f-part of chain diagrams to be comparable to the calculated k-part. In this sense the present calculation of the contribution of chain diagrams to E_{LS} is just an order of magnitude estimate. The E_{LS} diagrams with central chains (W_0 -MB) are illustrated in Figs. 27.1-4. The k-part of diagrams of the type 27.1,3 having one or more G_{dd}^c chains are calculated by inserting $e^{G_{dd}^c} - 1$ in the integrands of the two-body W_0 diagrams.

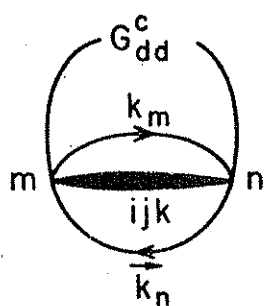
Similarly the terms of diagrams 27.2,4 containing only \vec{k}_n are obtained by respectively inserting G_{de}^c and G_{cc}^c in the two-body integrals. The terms having \vec{k}_m give derivatives of ρ_{ml} , and they have to be calculated explicitly as three-body integrals. The k-part of many W_0 -MB diagrams is



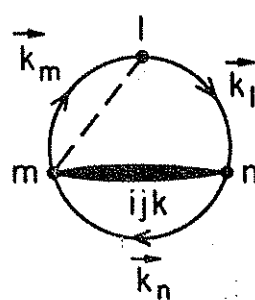
27.1



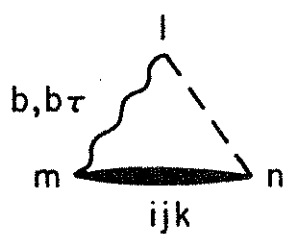
27.2



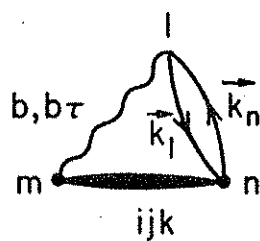
27.3



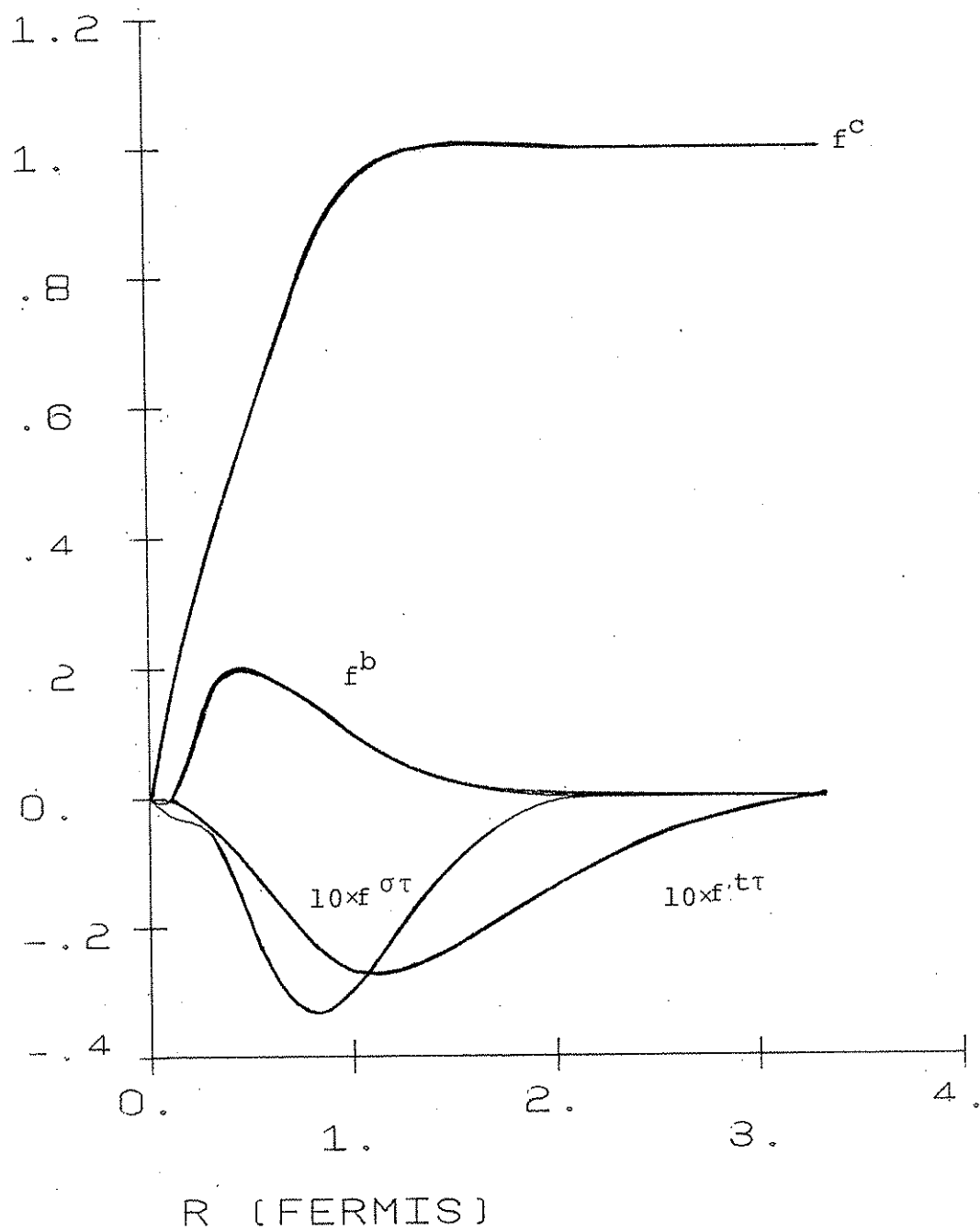
27.4



27.5



27.6



summed by dressing diagrams 27.2 and 27.4 by G_{dd}^c chains. The total estimated W_0 -MB contribution to E_{LS} is quite small and it is given in Table VII.

The contribution of W-diagrams having operator chains is called W_c . Of these we first consider those that have b_{mn} operators and a $G_{mn}^{p=2,6}$ chain. We may generate the leading terms of such diagrams by replacing an $f^{p=2,6}$ in the two-body f_{H}^{ijk} integrals by $f_{G^p}^c$. The $f_{G^p}^c$ are in general much smaller than f^p , and so the W_c is typically $\sim 10\%$ of the two-body W_0 . Two-body calculations indicate that we only need to consider the $ijk = (t\tau)b(t\tau)$ terms and replace $f^{t\tau}$ with $f_{G^{t\tau}}^c$. However since $G^{t\tau}$ are much smaller than the $f^{t\tau}$, the contribution of these diagrams would be negligible.

Diagrams having b links in the chains can also contribute to W_c . Of these we only estimate 27.5 and 27.6, which are the leading three-body terms in $G^{p=7,8}$. Two-body calculations show that the important diagrams to dress with $G^{p=7,8}$ are those with interaction line indices $ijk = bcc, cbc, ccb$.

The contribution of the k-part of diagram 27.5 with $p=b$ and $ijk = cbc$ is for example:

$$\frac{1}{40} k_f^{2,2} \int (v_{f^c}^{bc^2})_{mn} (2f_{f^b}^c)_{ml} r_{mn} r_{ml} \cos\theta_m d^3r_{mn} d^3r_{ml} \quad (3.83)$$

The diagrams 27.5-6 can also be dressed by G_{dd}^c chains, the contribution of their k-parts is given in Table VII, as the order of magnitude estimate of the E_{LS} part of W_c . The W_F two-body contribution is in general much bigger than the many-body kinetic terms, W_{F-MB} , U_F and U . Since the W_F contribution to E_{LS} is tiny (Table VII) we have totally neglected

contributions of W_F -MB, U_F and U to E_{LS} .

E. The Calculation of E_Q

The E_Q is given by:

$$E_Q = \frac{1}{A} \langle \psi | \sum_{i < j} \sum_{p=q}^{14} v^p(r_{ij}) O_{ij}^p | \psi \rangle / \langle \psi | \psi \rangle$$

This at first sight is first order perturbation theory. However the potentials $v^{p=9,14}$ have been considered through the Euler-Lagrange equations in determining the wave function ψ , and so the treatment is semi-perturbative. The contribution of two-body direct diagrams (Fig. 29.1) to E_Q is given by:

$$\sum_{i=1,8} \sum_{j=9,14} \sum_{k=1,8} \frac{1}{2} \rho \int d^3r \langle C(f_{12}^i O_{12}^i v_{12}^j O_{12}^j f_{12}^k O_{12}^k) \rangle_{dir} \quad (3.84)$$

$$\langle X_{12} \rangle_{dir} = \left(\frac{3}{4\pi k_F} \right)^2 \int d^3k_1 \int d^3k_2 \phi_{12}^* X_{12} \phi_{12} \quad (3.85)$$

$$\phi_{12} = \exp(i(\vec{k}_1 \cdot \vec{r}_1 + \vec{k}_2 \cdot \vec{r}_2)) \quad (3.86)$$

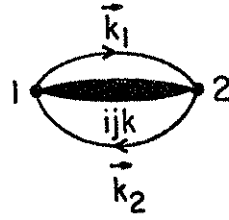
The C-part of the product in Eq. (3.84) can be written as a sum of three terms:

$$C(f_{12}^i O_{12}^i v_{12}^j O_{12}^j f_{12}^k O_{12}^k) = Z_0^d(r_{12}, ijk) + Z_2^d(r_{12}, ijk) L_{12}^2 + Z_4^d(r_{12}, ijk) L_{12}^4 \quad (3.87)$$

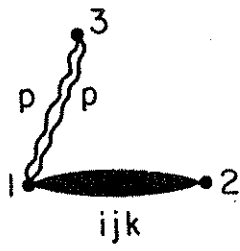
It is relatively easy to calculate the Z_0^d , Z_2^d and Z_4^d . First, we recall that the C-part of a product of operators can be trivially factored into two parts, one each for spin and isospin operators. Secondly products such as $O_{ij}^\sigma O_{ij}^t$, $O_{ij}^\sigma O_{ij}^\sigma$ etc. can be reduced to sums of terms



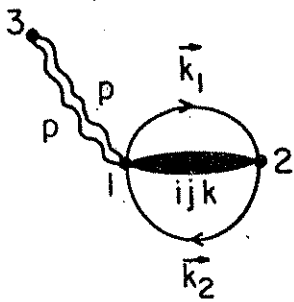
29.1



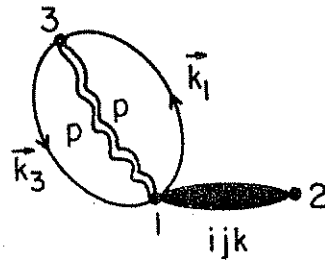
29.2



29.3



29.4



29.5

having operators $1, 0^\sigma, 0^t$ and 0^b . Hence, relatively few new C-parts are needed to calculate the $Z^{d'}$ s, and these are given below:

$$m, n = c, \sigma, t \text{ and } b, \quad (3.88)$$

$$C(0_{12}^m L_{12}^2 0_{12}^n) = \delta_{mn} (36\delta_{nt} + (1-\delta_{nb}) A_{L_{12}}^n + \frac{1}{2} \delta_{nb} L_{12}^4), \quad (3.89)$$

$$C(0_{12}^m (\vec{L} \cdot \vec{S})_{12}^2 0_{12}^n) = 54 \delta_{mt} \delta_{nt} + Q_{mn} L_{12}^2 + \frac{1}{2} \delta_{mb} \delta_{nb} L_{12}^4 \quad (3.90)$$

$$Q_{mn} = \begin{array}{cccc} 1/2 & 1/2 & -1/2 & -1/4 \\ 1/2 & 1/2 & -1/2 & -1/4 \\ -1/2 & -1/2 & 5 & 1 \\ -1/4 & -1/4 & 1 & 0 \end{array} \quad (3.91)$$

The values of $\langle L^n \rangle_{\text{dir}}$ are given in Table VI.

The contribution of two-body exchange diagrams (29.2) is given by:

$$\sum_{n=1,4} \sum_{i=1,8} \sum_{j=9,14} \sum_{k=1,8} -\frac{1}{8} \rho \int d^3 r \langle C(0_{12}^n f_{12}^i 0_{12}^j v_{12}^j 0_{12}^k f_{12}^k) \rangle_{\text{ex}}, \quad (3.92)$$

$$\langle X_{12} \rangle_{\text{ex}} = \left(\frac{3}{4\pi k_F} \right)^2 \int d^3 k_1 \int d^3 k_2 \phi_{21}^* X_{12} \phi_{12}, \quad (3.93)$$

$$\phi_{21} = \exp(i(\vec{k}_1 \cdot \vec{r}_2 + \vec{k}_2 \cdot \vec{r}_1)). \quad (3.94)$$

The C-part of the product in Eq. (3.88) can also be expressed in the form (3.87); the $Z_n^e(r_{12}, ijk)$ are calculated using equations (3.88-91), and $\langle L^n \rangle_{\text{ex}}$ are given in Table VI.

Contributions of two-body clusters to W_Q in the v_{14} model of nuclear

matter at $k_F = 1.6 \text{ fm}^{-1}$ are given in Table VIII. They are not too large; the total two-body contribution at $k_F = 1.6 \text{ fm}^{-1}$ is $\sim -54 \text{ MeV/A}$. The main many-body diagram contributing to E_Q is expected to be the separable diagram 29.3 of Fig. 29. We calculate only the main term of this diagram in which i and $k = c$. Its contribution is given by:

$$\frac{1}{4} \rho^2 \int (f_{12}^c)^2 (v_{12}^9 + \frac{1}{2} v_{12}^{13}) r_{12}^2 d^3 r_{12} \\ \times \frac{2}{3} \sum_{p=1,6} A^p \int f_{13}^p (-v_{13}^2 f_{13}^p + (\delta_{p5} + \delta_{p6}) \frac{6}{r_{13}^2} f^p) d^3 r_{13} . \quad (3.95)$$

We neglect the rather small contribution of terms having $p = b, b$ to diagram 29.3. The contribution of 29.3 calculated with these approximations is given in Table VIII.

One can understand the magnitude of the contribution of 29.3 as follows: The interaction energy of v^{9-14} interactions is roughly proportional to the average value of k^2 ; k is the momentum of the particle. It is thus proportional to the expectation value of the kinetic energy. The total kinetic energy in the liquid is made up of two terms, the Fermi gas kinetic energy T_F , and the kinetic energy due to correlations T_c . At $k_F = 1.6 \text{ fm}^{-1}$ these terms are respectively 31.85 MeV/A and 25.54 MeV/A . The two-body diagrams get their contributions from T_F , and the $6(f^{t,tt})^2/r^2$ term of T_c , while the three-body diagrams get their contributions only from T_c .

The contributions of separable exchange diagrams 29.4 and 29.5 are calculated only for $v^{j=9,12}$. These are quite small (Table VIII). The contribution of chain diagrams to W_Q is neglected; it could be $\sim .5 \text{ MeV}$ in magnitude, and that is approximately the accuracy of our W_Q calculation.

Table VIII

Contributions (in MeV/A) of diagrams shown in fig. 1 to v_{14} model
of nuclear matter at $k_F = 1.6 \text{ fm}^{-1}$

<u>Diagram</u>	<u>Interaction</u>	<u>Contribution</u>
1.1	p = 9-12	5.28
1.1	p = 13-14	-1.11
1.2	p = 9-12	-1.88
1.2	p = 13-14	1.26
1.3	p = 9 & 13	2.70
1.4	p = 9-12	0.26
1.5	p = 9	0.05

The estimated errors in the calculation of E_6 and E_{LS} are also $\sim .5$ MeV, and so a crude estimate of the accuracy of the energy expectation value is 1 MeV. On the other hand the variational wavefunction we use may not be general enough. First we minimize E by making limited variations in $f^p(r)$, second we do not include any f^{9-14} correlations that v^{9-14} may induce, and third we have no three-body correlation operators in our Ψ_v . Improvements in Ψ_v could lower the energy by, and this is a possibly unreliable guess based on calculations done with oversimplified models,²¹⁾ about 1 MeV. So we feel that our results give reliable upper bounds, but the true energy may be up to 2 MeV below our results.

F. Results of Reid and v_{14} Models

Most of the calculations use only three variational parameters d , d_t and α . We assume:

$$d^c = d^\sigma = d^\tau = d^{\sigma\tau} = d^b = d^{b\tau} = d, \quad (3.96)$$

$$d^t = d^{t\tau} = d_t. \quad (3.97)$$

At some test points we let d^b and $d^{b\tau}$ differ from d , but this did not produce an appreciable ($> .1$ MeV) lowering of energy. Since v^c and v^q do not have spin and isospin operators we take:

$$\alpha^c = \alpha^q = 1, \quad (3.98)$$

$$\alpha^\sigma = \alpha^\tau = \alpha^{\sigma\tau} = \alpha^t = \alpha^{t\tau} = \alpha^b = \alpha^{b\tau} = \alpha^{q\sigma} = \alpha^{q\tau} = \alpha^{q\sigma\tau} = \alpha. \quad (3.99)$$

Again it was verified that taking α^t and $\alpha^{t\tau}$, or α^b and $\alpha^{b\tau}$ different from α does not have significant effect on $E(k_F)$, and the α^{bb} and $\alpha^{bb\tau}$ were simply set to unity in all calculations. The v^{bb} has a significant L^2 part which should not be quenched anyway.

At the equilibrium point of the v_{14} model a bigger set of variational parameters ($d, d_t, \alpha, \beta_\sigma, \beta_t, \beta_b$) was used:

$$f^P(r, \alpha, d, d_t, \beta^P) = \beta^P f^P(r, \alpha, d, d_t) \quad , \quad (3.100)$$

$$\beta^\sigma = \beta^\tau = \beta^{\sigma\tau} = \beta_\sigma \quad , \quad (3.101)$$

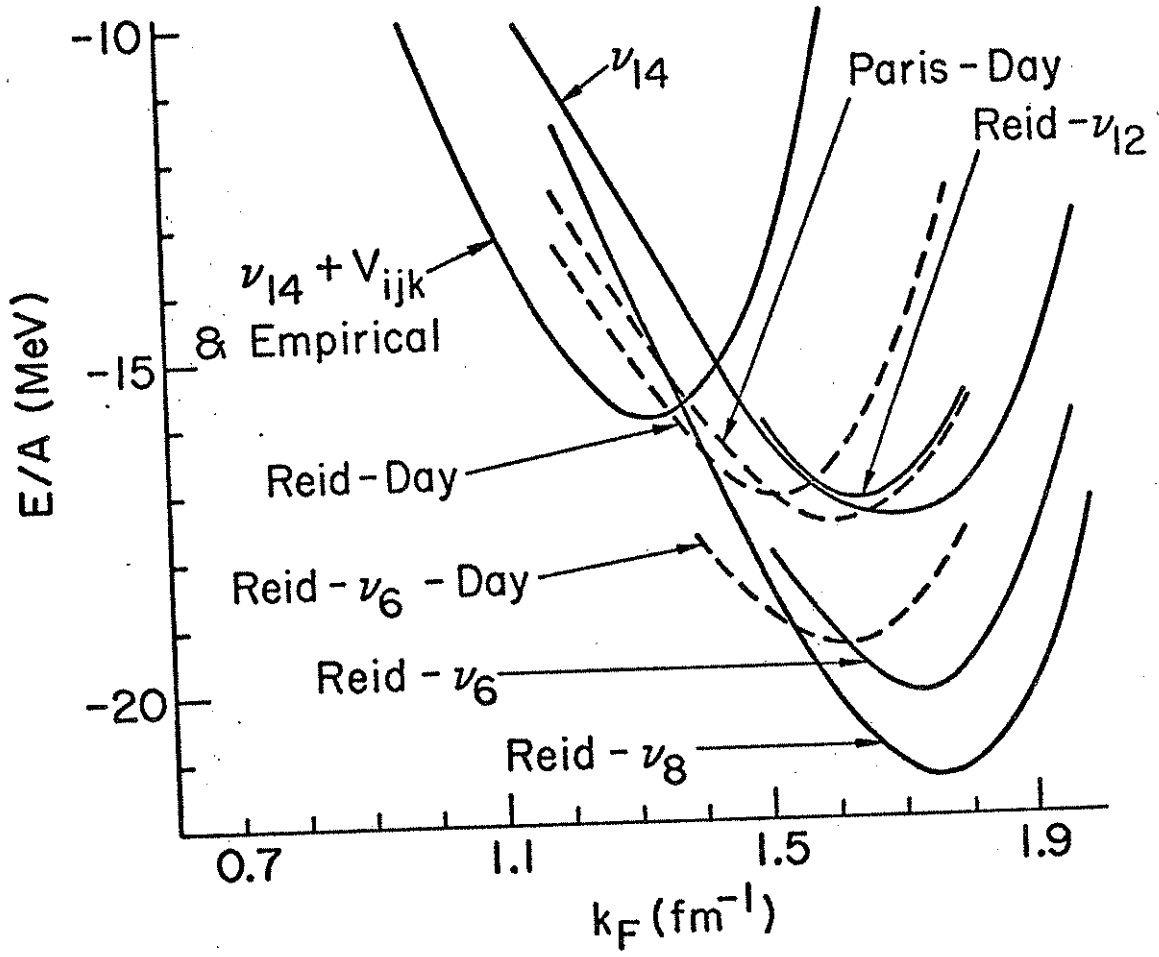
$$\beta^t = \beta^{t\tau} = \beta_t \quad , \quad (3.102)$$

$$\beta^b = \beta^{b\tau} = \beta_b \quad ; \quad (3.103)$$

fortunately the equilibrium values of β_p came out to be ~ 1 , suggesting that it is adequate to minimize $E(d, d_t, \alpha)$.

The calculated $E(k_F)$ are shown in Fig. 30. The Reid v_6 results are from ref. 26 and 51, while the Reid-Day results are from ref. 52. The Reid v_{12} $E(k_F < 1.5 \text{ fm}^{-1})$ is almost identical (within .2 MeV) of the v_{14} $E(k_F)$, though it saturates a little faster at $k_F > 1.6 \text{ fm}^{-1}$. The breakdown of the $E(k_F)$ is given in Table V. The Reid v_{12} variational results are in fair agreement with Day's Brueckner-Bethe results with the Reid-Day model. We may expect some differences between Reid-Day and Reid v_{12} models because they have different interactions in $^3P_0, ^3P_1, ^3D_2, ^3D_3$ and higher waves, however, a fraction of the difference may be in the method used to calculate $E(k_F)$.

The v^{9-14} give a repulsive contribution which helps reduce the over-binding of nuclear matter significantly. It also seems to reduce the equilibrium k_F by $\sim .1 \text{ fm}^{-1}$. But the calculated equilibrium k_F is much larger than the 1.33 fm^{-1} suggested by liquid drop fits. The curve labelled



v_{14} + TNI (three-nucleon interactions) in Fig. 30 has the correct equilibrium density ($k_F = 1.33 \text{ fm}^{-1}$), energy (-16 MeV), and compressibility (240 MeV).²⁾

There does not seem to be a big difference between the Reid v_{12} and the v_{14} models. Earlier, larger differences were found in the $E(k_F)$ given by Reid v_8 and various BJ- v_8 (Bethe-Johnson) models. However, v_8 models based on BJ ${}^3P_2 - {}^3F_2$ potentials give very repulsive phases in 3P_0 and 3P_1 states (Figs. 12, 13), and so are almost unrealistic. Reid v_{12} model is reasonably realistic, but still somewhat pedagogical, and its results should be taken accordingly. For example, there could be some effect of the stronger tensor force in the Reid v_{12} model, but it gets cancelled by that of the slightly weaker repulsion in 3P_0 and 3P_1 states, and does not show up in the comparison of the $E(k_F)$ of Reid v_{12} and v_{14} models.

Day's recent calculation⁶³⁾ with the Paris potential yields similar results with the v_{14} model. The Paris potential fits quite accurately the scattering data and gives phase shifts and deuteron properties that are similar to those given by the v_{14} models (Figs. 2-21). Day's results with the Paris potential are also shown in Fig. 30.

IV. THREE-NUCLEON INTERACTION CONTRIBUTIONS

Realistic two-nucleon interactions seem to overbind nuclear matter very significantly at $k_F > 1.5 \text{ fm}^{-1}$, whereas at low $k_F (< 1.3 \text{ fm}^{-1})$ they give an underbinding. The overbinding at $k_F > 1.5$ is certainly beyond any possible errors in the many-body calculations, while the underbinding at $k_F < 1.3 \text{ fm}^{-1}$ is not that overwhelming. However, we know that the realistic two-nucleon interactions leave light nuclei like triton⁵³⁾ and ${}^4\text{He}$ ⁵⁴⁾ underbound, and this strongly suggests the need for more attraction at low densities. In this Section we take a very phenomenological point of view, and add contributions of three nucleon interactions (TNI) to the v_{14} model to get the "correct" $E(k_F)$ around $k_F = 1.33 \text{ fm}^{-1}$.

To begin with let us ignore the spin-isospin dependence of the TNI; we will put in effect of its isospin dependence rather crudely. We hope that the TNI can be expanded as:

$$V_{123} = \sum_{\ell} \sum_{\text{cyc}} U_{\ell} u_{\ell}(r_{12}) u_{\ell}(r_{13}) P_{\ell}(\cos \theta_1) \quad , \quad (4.1)$$

where U_{ℓ} is a strength parameter, $u_{\ell}(r)$ are functions of interparticle distance, θ_i are the inner angles of the triangle $\vec{r}_1, \vec{r}_2, \vec{r}_3$, and \sum_{cyc} represents a sum of three terms obtained by cyclic rotation of indices 1, 2 and 3. At very high densities only the $\ell=0$ component of V_{123} will contribute. It must be repulsive and so we refer to it as TNR. The $\ell \neq 0$ components will give negative contributions to $E(k_F)$ through correlations, but these will saturate as density increases, and we refer to them collectively as TNA.

If one takes very seriously the indication of a "hole" in the ${}^3\text{He}$ nucleus,⁵⁵⁾ which two-nucleon interactions fail to give,²⁹⁾ a three-nucleon

P_2 interaction appears to be an attractive proposal to try out. A nucleon can be at the center of mass of the ^3He nucleus only when the three nucleons are in a line. The $\ell=2$ term of V_{123} can be very repulsive in this configuration, and attractive when the nucleons are at the corners of an equilateral triangle leaving a hole in the middle.

The two pion exchange TNI corresponding to field theoretical diagram has been studied,⁵⁵⁻⁵⁸⁾ and it does contain terms of type 4.1 with $\ell=2$ and $u_2(r) = T(r)$, where $T(r)$ is the radial shape of the one pion exchange tensor force:

$$T(r) = \left(1 + \frac{3}{\mu r} + \frac{3}{\mu^2 r^2}\right) \frac{e^{-\mu r}}{\mu r} (1 - \exp(-cr^2))^2, \quad (4.2)$$

$$\mu = 0.7 \text{ fm}^{-1}, \quad (4.3)$$

$$c = 2 \text{ fm}^{-2}. \quad (4.4)$$

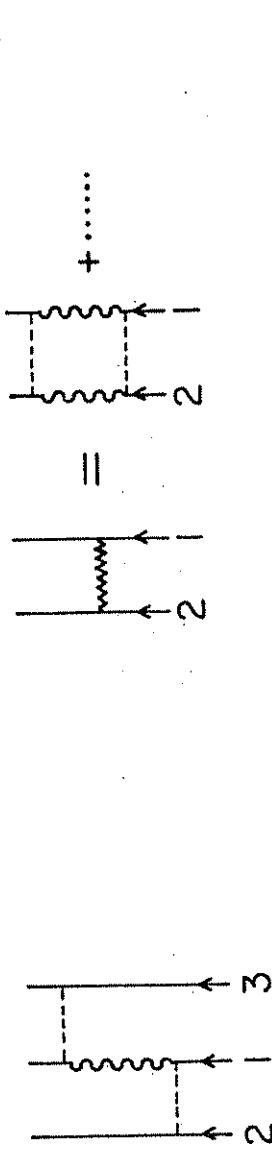
The cutoff in (4.2) is that in the v_{14} model; different authors generally use different cutoff's. The $\ell=2$ terms of (4.1) may possibly dominate TNA.

As a model for the $\ell=0$ TNR we consider separable diagrams involving isobar states.⁵⁹⁾ Their field theory analogs are very schematically illustrated in Figs. 31.2 and 31.3. This interaction requires the exchange of two pions between nucleons 1 and 2, and of other two pions between 1 and 3. We may thus take $u_0(r) = T^2(r)$.

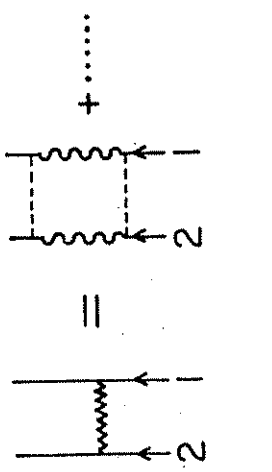
Let us recall that the v_{14} interaction model has three terms:

$$v_{14,ij} = v_{\pi} + v_{\text{I}} + v_{\text{S}} \quad (4.5)$$

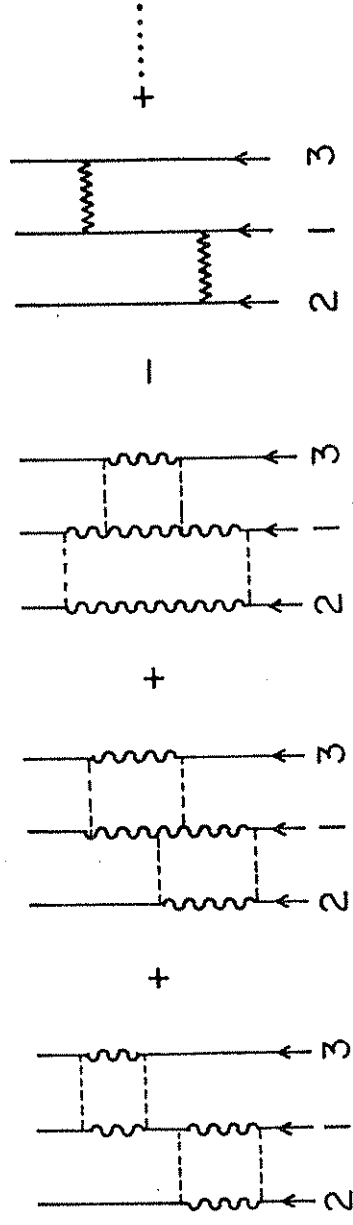
which respectively correspond to the one pion exchange, two pion exchange isobar box (illustrated in Fig. 31.2), and the short range core. The radial shape of v_{I} is taken to be $T^2(r)$ in accord with its assumed nature:



31.1



31.2



31.3

$$v_I = \sum_{p=1,14} I^p T^2(r_{ij}) O_{ij}^p, \quad (4.6)$$

and I^p are constants obtained by fitting the phase shifts. I^c is large and negative, and the rest $I^{p \neq c}$ are much smaller. The main effect of a TNR of type:

$$\sum_{\text{cyc}} U_0 T^2(r_{12}) T^2(r_{13}) \quad (4.7)$$

will be to weaken this attractive v_I , and we include it in the many-body calculation by making the two-nucleon interaction density-dependent:

$$v_{14}^{\text{TNR}} = v_{\pi} + v_I \exp(-\gamma_1 \rho) + v_S \quad (4.8)$$

We have chosen to use $\exp(-\gamma_1 \rho)$, instead of $(1-\gamma_1 \rho)$ the TNR gives, with the hope that it would take into account four and more body separable diagrams at very high densities. However, $\gamma_1 \rho$ is very small ($< .03$) in the region of nuclear densities, and whether one uses $\exp(-\gamma_1 \rho)$ or $(1-\gamma_1 \rho)$ hardly makes any difference.

The contribution of TNA will have the following characteristics. At low densities it will be proportional to ρ^2 , and it will saturate as ρ increases. The interaction 31.1, which we use as a model for TNA, has zero C-part because it leaves free τ_2 , τ_3 , σ_2 and σ_3 . It will contribute only when there are spin isospin correlations between 2 and 3 that close the ring. Thus, its contribution will be proportional to the expectation value of $(\tau_1 \cdot \tau_2)^2$:

$$\langle (\tau_1 \cdot \tau_2)^2 \rangle = 3-2 \left(\frac{N-Z}{A} \right)^2, \quad (4.9)$$

where N and Z is the number of neutrons and protons. The C-parts of spin

operators do not depend upon N and Z , so we will ignore them. A reasonable parametrization of the TNA contribution is then given by:

$$\text{TNA} = \gamma_2 \rho^2 \exp(-\gamma_3 \rho) \left(3 - 2 \left(\frac{N-Z}{A}\right)^2\right) . \quad (4.10)$$

We calculate $E(k_F, v_{14} + \text{TNR})$ with the interaction (4.8) by the variational method, and add the TNA contribution (4.10) to obtain the nuclear matter energy. The parameters γ_{1-3} are varied to obtain equilibrium $k_F = 1.33 \text{ fm}^{-1}$, $E_0 = -16. \text{ MeV}$, and $K = 240 \text{ MeV}$. Their values are:

$$\gamma_1 = 0.15 \text{ fm}^3 , \quad (4.11)$$

$$\gamma_2 = -700 \text{ fm}^6 \text{ MeV}, \quad (4.12)$$

$$\gamma_3 = 13.6 \text{ fm}^3 , \quad (4.13)$$

and the $E(k_F)$ obtained with these is shown by the curve labelled $v_{14} + \text{TNI}$ in Fig. 30.

Table IX gives the contributions of various interactions to the nuclear-matter energy. The interaction energies are defined as follows:

$$v_{14}\text{-interaction energy} = E(k_F, v_{14}) - T_F , \quad (4.14)$$

$$\text{TNI energy} = E(k_F, v_{14} + \text{TNR}) - E(k_F, v_{14}) + \text{TNA}. \quad (4.15)$$

They are not expectation values, because the wavefunction changes when the interaction is changed.

All the expectation values given in Table X are calculated with the $v_{14} + \text{TNR}$ wavefunction. However, since $\gamma_1 \rho$ is so very small there is little difference between v_{14} and $v_{14} + \text{TNR}$ wavefunction at nuclear matter density. Note that the TNA given by Eq. (4.10) is not an expectation value. There should be some kinetic energy of three-nucleon correlations,

Table IX

"Interaction Energies" in Nuclear Matter (MeV)

k_F (fm ⁻¹)	1.13	1.23	1.33	1.43	1.53
ρ (fm ⁻³)	.0975	.1257	.1589	.1957	.2419
T_F	15.89	18.82	22.01	25.44	29.12
v_{14}	-25.60	-30.36	-35.41	-40.57	-45.66
TNI	-3.89	-3.76	-2.59	-0.18	3.57
E	-13.60	-15.30	-15.99	-15.31	-12.97

Table X

"Expectation Values" in Nuclear Matter (MeV)

k_F (fm ⁻¹)	1.13	1.23	1.33	1.43	1.53
$\langle T \rangle$	27.54	32.79	38.72	45.33	52.62
$\langle v_\pi \rangle$	-20.69	-23.92	-27.26	-30.63	-33.94
$\langle v_I \rangle$	-94.31	-118.8	-148.9	-185.7	-230.0
$\langle v_S \rangle$	77.75	98.39	124.1	155.8	194.7
$\langle TNR \rangle$	1.41	2.24	3.52	5.40	8.15
TNA	-5.30	-6.00	-6.11	-5.58	-4.58

and a correction to $\langle v_{14} \rangle$ buried in it. Thus the expectation value of $\langle T \rangle$ could be a few MeV higher than listed in Table V; $2T_F$ is suggested as a reasonable estimate of $\langle T \rangle$ by the present work. The $\langle T \rangle$ is in fact measurable, and its measurement would be of great help in arriving at a correct theory of nuclear matter.

The TNA and TNR give much smaller contributions than the two-nucleon v_{14} . Microscopic calculations⁵⁸⁾ of TNA due to two pion exchange three-nucleon interaction of Fig.31.1 give ~ -2 to -3 MeV at equilibrium density, against our -6 MeV. These calculations certainly do not rule out larger TNA contribution. But it should be pointed out that we do not calculate $E(k_F, v_{14} + \text{TNR})$ exactly. As mentioned in Section II the variationally calculated $E(k_F, v_{14} + \text{TNR})$ could be 0-2 MeV too high, and the phenomenological TNA may in part be correcting for the differences between the variational Ψ_v and the exact Ψ .

The sum of separable diagrams involving isobar states should give some idea of the TNR contribution in matter. It is difficult to calculate it microscopically, for the required isobar-nucleon interactions are experimentally hard to study. Of the allowed $NN \rightleftharpoons NN$, $NN \rightleftharpoons N\Delta$, $N \rightleftharpoons \Delta\Delta$, $N\Delta \rightleftharpoons N\Delta$, $N\Delta \rightleftharpoons \Delta N$, $N\Delta \rightleftharpoons \Delta\Delta$, and $\Delta\Delta \rightleftharpoons \Delta\Delta$ only the $NN \rightarrow NN$, $NN \rightleftharpoons N\Delta$ and $NN \rightleftharpoons \Delta\Delta$ contribute significantly to the nucleon-nucleon scattering, but all are required to calculate TNR. Wiringa⁵⁹⁾ has attempted to calculate the sum of separable diagrams involving isobar states using the model of Niephaus, Gari and Sommer⁶⁰⁾ of transition potentials. Very preliminary results, which neglect $v^{p>6}$ $NN \rightarrow NN$ interactions, suggest that the sum of "isobar separable" diagrams is 1.42, 3.7, 7.9 MeV at $k_F = .9, 1.1$ and 1.3 fm^{-1} respectively. Our TNR contribution is smaller by approximately

a factor of two than these estimates. Recently Horikawa et al.⁶⁴⁾ have estimated the real part of Δ -nucleus optical potential U_{Δ} to be ~ -25 MeV, while the average nucleon-nucleus optical potential \bar{U}_N for occupied states is ~ -60 MeV. The Δ -percentage P_{Δ} in NM is estimated⁵⁹⁾ to be $\sim 6-7\%$. Thus the dispersion correction $P_{\Delta}(U_{\Delta} - \bar{U}_N) \sim 2.3$ MeV may account for the most of TNR.

The expectation values $\langle v_I \rangle$ and $\langle v_S \rangle$ are both quite large, but their sum is much smaller. The $\langle v_I \rangle$ and $\langle v_S \rangle$ individually will be very dependent on the two nucleon interaction model, and so their values should be regarded with some caution. In relativistic-mean-field theories, such as Walecka's,⁶¹⁾ the attraction $\langle v_I \rangle$ is attributed to a scalar field, and the kinetic energies are calculated with an effective mass $m^* = m_N + \langle v_I \rangle$. The m^* is smaller than m_N , and so generates larger kinetic energies which help to saturate nuclear matter. Any such relativistic effect that may exist in nuclear matter is also buried in the phenomenological TNR.

The present approach to TNI contributions in matter is very phenomenological and not aesthetically satisfactory. A better approach will be to assume a nuclear Hamiltonian:

$$H_{\text{nucl}} = -\frac{\hbar^2}{2m} \nabla_1^2 + \sum_{i < j} \sum_p v^p(r_{ij}) O_{ij}^p + \sum_{i < j < k} V_{ijk}, \quad (4.16)$$

and determine the important components of V_{ijk} by fitting the binding energies and form factors of light nuclei such as ${}^3\text{H}$, ${}^4\text{He}$. Some of the very neutron rich isotopes of helium (${}^6\text{He}$, ${}^8\text{He}$, etc.) may provide information on the three-neutron interaction. Techniques to obtain reasonable wavefunctions and calculate energies of few body systems with Hamiltonians such as (4.16), are being developed. In the meanwhile,

equations (4.8) and (4.10) define an effective Hamiltonian that fits the two-nucleon scattering data and nuclear matter properties, and it seems to have reasonable TNI contributions. We hope that it may be of use in studies of the equation of state of hot and cold nucleon matter, and the structure of nuclei and neutron stars.

V. ASYMMETRIC NUCLEAR MATTER

A. Statement of the Problem

In this Section we present our studies on the equation of state of cold asymmetric nuclear matter (ANM) characterized by the polarization parameter $\beta = (N-Z)/A$. Here N and Z respectively denote the number of neutron and protons, and $A = N+Z$. Neutron and symmetric nuclear matter are the limiting cases having $\beta=1$ and 0 respectively.

Following the notation of equations (3.54) and (3.57) we break down the energy $E(\rho, \beta)$ of ANM into the following terms:

$$E(\rho, \beta) = T_F + E_{2B} + W_O(MB) + W_C + W_S + U + v_F = W_F(MB) + TNA. \quad (5.1)$$

Here E_{2B} is the contribution of two-body clusters and TNA is the contribution of the attractive part of the TNI. The contribution of the repulsive part of TNI, is included in the terms E_{2B} through $W_F(MB)$. The values of these contribution in symmetric NM and pure neutron matter are given in Table XI at $\rho = .159$ (the assumed equilibrium density of symmetric NM) and $.35$ nucleons/fm³.

It is relatively simple to calculate the contribution of many-particle isospin correlations in the symmetric nuclear matter. One only needs to know, in this case, the C-part of the product of isospin operators. A further significant simplification occurs because only closed rings of isospin operators have a nonzero C-part, and if these rings are made up of single operator links, the order of operators is immaterial. All these simplifications are lost when we consider the $\beta \neq 0$ asymmetric matter. Calculations of $\beta=1$ neutron matter are simple because the isospin correlations can be completely eliminated in this case.

Table XI

$\rho(\text{fm}^{-3})$.159	.159	.35	.35
β	0	1.	0	1.
T_F	22.01	34.93	37.23	59.11
E_{2-b}	-36.89	-19.48	-44.10	-21.29
$W_O(\text{MB})$	- 3.40	- 2.05	- 8.18	- 3.32
W_C	2.74	1.99	1.81	1.28
W_S^*	5.07	1.53	9.51	2.28
$U+U_f+W_F(\text{MB})$.38	0.046	3.95	2.32
TNA	- 6.11	- 2.04	- 2.21	- 0.74
E_{TOT}	-16.00	14.94	- 1.99	39.64

The breakdown of nuclear and neutron matter energy.. The W_S^* is the sum of W_S , W_{CS} , $E_{LS}(\text{MB})$ and $E_Q(\text{MB})$.

With the hope of using the available $\beta=0$ and 1 results⁶⁷⁾ in the calculation of $E(\rho, \beta)$ we studied the β dependence of $E_{2B}(\rho, \beta)$ and $W_0(\text{MB}, \rho, \beta)$ numerically by calculating these at $\beta^2 = 0, .1, .2, \dots, .9$ and 1. To a surprisingly high accuracy the β -dependence of these terms is given by:

$$E_{2B}(\rho, \beta) \approx E_{2B}(\rho, 0) + \beta^2(E_{2B}(\rho, 1) - E_{2B}(\rho, 0)) , \quad (5.2)$$

$$W_0(\text{MB}, \rho, \beta) \approx W_0(\text{MB}, \rho, 0) + \beta^2(W_0(\text{MB}, \rho, 1) - W_0(\text{MB}, \rho, 0)) . \quad (5.3)$$

The calculated $E_{2B}(\rho, \beta)$ is given by Eq. (1.2) within .3% (.4%) at $\rho = .159$ (.35), while the calculated $W_0(\text{MB}, \rho, \beta)$ is reproduced by Eq. (1.3) within 0.4% and 16% at these densities. However $W_0(\text{MB}, \rho, \beta)$ is smaller than $E_{2B}(\rho, \beta)$ by an order of magnitude and so the $E_{2B}(\rho, \beta) + W_0(\text{MB}, \rho, \beta)$ can be approximated by a sum of β^0 and β^2 terms to an accuracy of .4% and 1.7% at $\rho = .159$ and $.35 \text{ fm}^{-3}$ respectively.

Calculations of the W_c and W_s in asymmetric nuclear matter are difficult. In symmetric nuclear matter the W_c and W_s are calculated with the help of chain equations that sum single operator chains having arbitrary lengths. These chain equations become very messy in asymmetric matter. However we can analyze the β -dependence of selected and hopefully important, three and four-body diagrams. Such an analysis suggests that W_c and W_s also do not have large β^4 or higher terms. The TNA has by definition only β^0 and β^2 terms, while the U , U_F and $W_F(\text{MB})$ are small and it may be reasonable to approximate their contribution by a sum of β^0 and β^2 terms.

Thus the main result of this study is that, at least at $\rho \leq .35 \text{ fm}^{-3}$, the energy of asymmetric nuclear matter may be well approximated by:

$$E(\rho, \beta) = T_F(\rho, \beta) + EI_0(\rho) + \beta^2 EI_2(\rho) . \quad (5.4)$$

The constants $EI_0(\rho)$ and $EI_2(\rho)$ can be obtained from existing results⁶⁷⁾ on the $E(\rho)$ of symmetric nuclear and neutron matter.

The $EI_0(\rho)$, $EI_2(\rho)$ and the symmetry energy $E_{\text{sym}}(\rho)$ are reported in Section 5B. Section 5C reports the two-body Euler-Lagrange equations for asymmetric matter, and the calculation of $E_{2B}(\rho, \beta)$. The generalization of FHNC equations to the case of asymmetric matter and the calculation of $W_0(\text{MB}, \rho, \beta)$ is reported in Section 5D. Section 5E analyzes the β dependence of simple W_c and W_s diagrams.

B. Results

The interaction energy of nuclear matter is defined as:

$$EI(\rho, \beta) = E(\rho, \beta) - T_F(\rho, \beta) . \quad (5.5)$$

Assuming validity of approximation (5.4) we have:

$$EI_0(\rho) = EI(\rho, 0) , \quad (5.6)$$

$$EI_2(\rho) = EI(\rho, 1) - EI(\rho, 0) . \quad (5.7)$$

The $EI_0(\rho)$ and $EI_2(\rho)$ are calculated using the $E(\rho, 0)$ and $E(\rho, 1)$ tabulated in ref. 67. Five point interpolations were used to obtain $E(\rho, \beta=0, 1)$ at the desired values of ρ . The $E_{\text{sym}}(\rho)$ is defined as:

$$E_{\text{sym}}(\rho) = \frac{1}{2} \left. \frac{\partial^2 E(\rho, \beta)}{\partial \beta^2} \right|_{\beta=0} , \quad (5.8)$$

and it is given by:

$$E_{\text{sym}}(\rho) = \frac{5}{9} T_F(\rho, 0) + EI_2(\rho) . \quad (5.9)$$

The $EI_0(\rho)$, $EI_2(\rho)$ and $E_{\text{sym}}(\rho)$ are tabulated in Table XII.

Table XII

ρ	EI_0	EI_2	E_{sym}
.0492	-18.37	9.54	15.13
.0676	-23.04	11.59	18.51
.0975	-29.49	14.39	23.22
.1257	-34.12	16.30	26.76
.1589	-38.01	17.73	29.96
.1975	-40.76	18.59	32.72
.2234	-41.75	18.76	34.11
.2515	-42.17	19.01	35.62
.2767	-41.99	18.66	36.36
.3034	-41.42	17.94	36.75
.3497	-39.74	17.34	38.02

The coefficients $EI_0(\rho)$ and $EI_2(\rho)$ of the interaction energy of nucleon matter, and the symmetry energy of nucleon matter.

The calculated symmetry energy at the equilibrium density ($\rho = .16 \text{ fm}^{-3}$) is 30 MeV. Empirically the symmetry energy is not very accurately determined. Its values range from 28-40 MeV¹⁾ in mass formulae. Our results for E_{sym} are in fair agreement with the results obtained by Fantoni and Rosati⁶⁷⁾ (31.1 MeV at $\rho = .17 \text{ fm}^{-3}$) with the semi-realistic OMY potential, and Siemens and Sjöberg⁶⁶⁾ (25-30 MeV at $k_F = 1.35 \text{ fm}^{-1}$) with the Reid potential and lowest order Brueckner theory.

C. Calculation of $E_{2B}(\rho, \beta)$

The variational calculations use a variational wavefunction:

$$\Psi_V(\rho, \beta) = \left\{ \prod_{i < j} \left[\sum_{p=1,8} f^P(r_{ij}, d, d_t, \alpha) O_{ij}^P \right] \right\} \phi(\rho, \beta) . \quad (5.10)$$

The variational parameters d , d_t and α should be varied in principle to minimize the $E(\rho, \beta)$. However, the equilibrium values of d , d_t and α are not too different in nuclear and neutron matter. For example at $\rho = .159 \text{ fm}^{-3}$ the equilibrium values of d , d_t and α in nuclear and neutron matter are respectively 2.15, 3.44 fm, .8 and 2.79, 3.44 fm, .8, and the neutron matter energy obtained with these two sets of d , d_t and α is 14.9 and 14.6 MeV respectively. In the following sections we neglect the β dependence of d , d_t and α and take their values from symmetric nuclear matter calculations. The results presented in Section 5B tacitly assume that the small effect of the β dependence of d , d_t and α on $E(\rho, \beta)$ is linear in β^2 .

The $f^P(d, d_t, \alpha)$ are calculated from two-body Euler-Lagrange equations 3.14 to 3.24 which depend upon the ϕ . Thus even for fixed values of d , d_t and α the f^P can depend upon β and ρ . The β and ρ dependence of the f^P equations is contained in the functions $\phi_{T,S}^X(r, \rho, \beta)$ given by

equations 3.8-3.11. Here $x = c, q$ or qq (for central L^2 and L^4), and T, S are the pair isospin and spin. In asymmetric matter we have two Fermi momenta k_{Fn} and k_{Fp} for neutrons and protons, and it is convenient to define functions $\Psi_{\lambda\mu}^x(T, S, r)$:

$$\Psi_{\lambda\mu}^x(T, S, r) = \frac{1}{\Omega^2} \sum_{k_\lambda < k_{F\lambda}} \sum_{k_\mu < k_{F\mu}} (\psi^*(\vec{k}_\lambda, \vec{k}_\mu) - (-1)^{T+S} \psi^*(\vec{k}_\mu, \vec{k}_\lambda)) O_{12}^x \psi(\vec{k}_\lambda, \vec{k}_\mu), \quad (5.11)$$

$$\psi(\vec{k}_\lambda, \vec{k}_\mu) = \exp(i(\vec{k}_\lambda \cdot \vec{r}_1 + \vec{k}_\mu \cdot \vec{r}_2)), \quad (5.12)$$

where λ and μ can be n or p for neutrons and protons. The $\phi_{T,S}^x(r, \rho, \beta)$ are given by:

$$(\phi_{T,S}^x(r, \rho, \beta))^2 = (\Psi_{np}^x(T, S, r))^2 + T\{(\Psi_{nn}^x(T, S, r))^2 + (\Psi_{pp}^x(T, S, r))^2\}.$$

The explicit forms of $\Psi_{\lambda\mu}^x(T, S, r)$ are given below:

$$(\Psi_{\lambda\mu}^c(T, S, r))^2 = \frac{1}{4} \rho_\lambda \rho_\mu \{1 - (-1)^{T+S} \ell_\lambda \ell_\mu\}, \quad (5.13)$$

$$(\Psi_{\lambda\mu}^q(T, S, r))^2 = \frac{1}{4} \rho_\lambda \rho_\mu \left\{ \frac{r^2}{10} (k_{F\lambda}^2 + k_{F\mu}^2) - (-1)^{T+S} \frac{1}{2} \vec{r} \cdot \vec{\nabla} \ell_\lambda \ell_\mu \right\}, \quad (5.14)$$

$$\begin{aligned} (\Psi_{\lambda\mu}^{qq}(T, S, r))^2 = & \frac{1}{4} \rho_\lambda \rho_\mu \left\{ r^4 \left(\frac{1}{70} (k_{F\lambda}^4 + k_{F\mu}^4) + \frac{1}{25} k_{F\lambda}^2 k_{F\mu}^2 \right. \right. \\ & \left. \left. + \frac{r^2}{5} (k_{F\lambda}^2 + k_{F\mu}^2) - (-1)^{T+S} \frac{1}{2} (\vec{r} \cdot \vec{\nabla})^2 \ell_\lambda \ell_\mu \right\}. \end{aligned} \quad (5.15)$$

Here ℓ_λ is the familiar Slater function $\ell(k_{F\lambda} r)$.

The $f^D(\rho, \beta)$ are obtained by solving the Eq. 3.14-3.24 with the above $\phi_{T,S}^x$. They do not exhibit significant β dependence. The important correlations, such as f^c or $f^{t\tau}$ change by $< 2\%$ in going from $\beta=0$ to 1.

Nevertheless this β -dependence is taken into account in the following calculations.

In symmetric nuclear matter only the C-parts of operator products contribute. In asymmetric matter terms linear in O_{ij}^τ also contribute. We define this term as the T_{ij} -part of the ΠO^P ,

$$\Pi O^P = C(\Pi O^P) + \sum_{i < j} T_{ij}(\Pi O^P) O_{ij}^\tau + \dots \quad (5.16)$$

The T_{ij} -parts, like the C-parts do not contain any σ or τ operators, and

$$T_{ij}(\Pi O^P) = \frac{1}{3} C(O_{ij}^\tau \Pi O^P) \quad (5.17)$$

With these definitions $E_{2B}(\rho, \beta)$ is given by:

$$\begin{aligned} E_{2B} = & \sum_{i,k=1,8} \sum_{j=1,14} \frac{\rho}{2} \int d^3r \langle C(f_{12}^i O_{12}^i H_{12}^j O_{12}^j f_{12}^k O_{12}^k) + O_{12}^\tau T_{12}(f_{12}^i O_{12}^i H_{12}^j O_{12}^j f_{12}^k O_{12}^k) \rangle_{dir} \\ & - \sum_{n=1,4} \frac{\rho}{8} \int d^3r \langle C(O_{12}^n f_{12}^i O_{12}^i H_{12}^j O_{12}^j f_{12}^k O_{12}^k) + O_{12}^\tau T_{12}(O_{12}^n f_{12}^i O_{12}^i H_{12}^j O_{12}^j f_{12}^k O_{12}^k) \rangle_{ex} \\ & + \sum_{n=1,4} \frac{1}{4} \rho \frac{\hbar^2}{m} \int d^3r \langle C(O_{12}^n f_{12}^i O_{12}^i \vec{v} f_{12}^k O_{12}^k) \cdot \vec{v} + O_{12}^\tau T_{12}(O_{12}^n f_{12}^i O_{12}^i \vec{v} f_{12}^k O_{12}^k) \cdot \vec{v} \rangle_{ex} \end{aligned} \quad (5.18)$$

The three integrals above correspond to the contributions of W_O diagrams 33.1 and 33.2 and W_F diagram 33.3 of Fig. 33 respectively. The C- and T_{12} -parts can be expressed as sum over terms containing $1, L^2, L^4 r \cdot \nabla$ and $L^2 r \cdot \nabla$ operators. The required expectation values $\langle \rangle_{dir}$ and $\langle \rangle_{ex}$ of these operators in asymmetric matter are given in Table XIII, where O_{12}^τ is abbreviated by τ .

The calculated $E_{2B}(\rho, \beta)$ at $\rho = .1589 \text{ fm}^{-3}$ is given in Table XIV. It is almost exactly linear in β^2 . The absence of significant β^4 terms in

E_{2B} can be understood as follows. The f^P 's have little β dependence, so the β dependence of E_{2B} must come from the expectation values in Table XIII. $\langle l \rangle_{dir}$ and $\langle \tau \rangle_{dir}$ do not have β^4 terms, while the β^4 terms in $\langle L^2 \rangle_{dir}$ and $\langle L^2 \tau \rangle_{dir}$ are very small as can be seen by expanding these in powers of β :

$$\langle L^2 \rangle_{dir} = 1 + \frac{5}{9} \beta^2 + \frac{5}{9} \frac{1}{27} \beta^4 + \dots \quad (5.19)$$

$$\langle L^2 \tau \rangle_{dir} = \beta^2 - \frac{1}{27} \beta^4 + \dots \quad (5.20)$$

The contribution of $\langle L^4 \rangle$ terms is very small and it does not give significant β^4 terms. So it is understandable that the direct part of E_{2B} has no significant $\beta^{n \geq 4}$ dependence.

The exchange part of E_{2B} involves l_c and l_τ functions which may be expanded in powers of β as follows. Let k_F denote the Fermi momentum of nuclear matter at density ρ , and $x = k_F r$. We get

$$l_c(x) = \sum_{n=0, \infty} \frac{1}{(2n)!} \frac{1}{3^{2n}} \beta^{2n} x^{6n-3} \left(\frac{1}{2} \frac{d}{dx} \right)^{2n} (x^3 l(x)) , \quad (5.21)$$

$$l_\tau(x) = \sum_{n=0, \infty} \frac{1}{(2n+1)!} \frac{1}{3^{2n+1}} \beta^{2n+1} x^{6n} \left(\frac{1}{2} \frac{d}{dx} \right)^{2n+1} (x^3 l(x)) . \quad (5.22)$$

The above can be rewritten as:

$$l_c(x) = l_0(x) + l_2(x) \beta^2 + l_4(x) \beta^4 + \dots , \quad (5.23)$$

$$l_\tau(x) = \beta l_1(x) + \beta^3 l_3(x) + \dots , \quad (5.24)$$

where $l_i(x)$ are functions independent of β . Since the l_c and l_τ are multiplied by short ranged functions with a typical range of ~ 1.5 fm their main contribution comes from small distances. However $l_{i \geq 2}(x)$ are quite small at small r as can be seen from Fig. 32, and hence the exchange part of E_{2B} is also quite linear in β^2 .

Table XIII

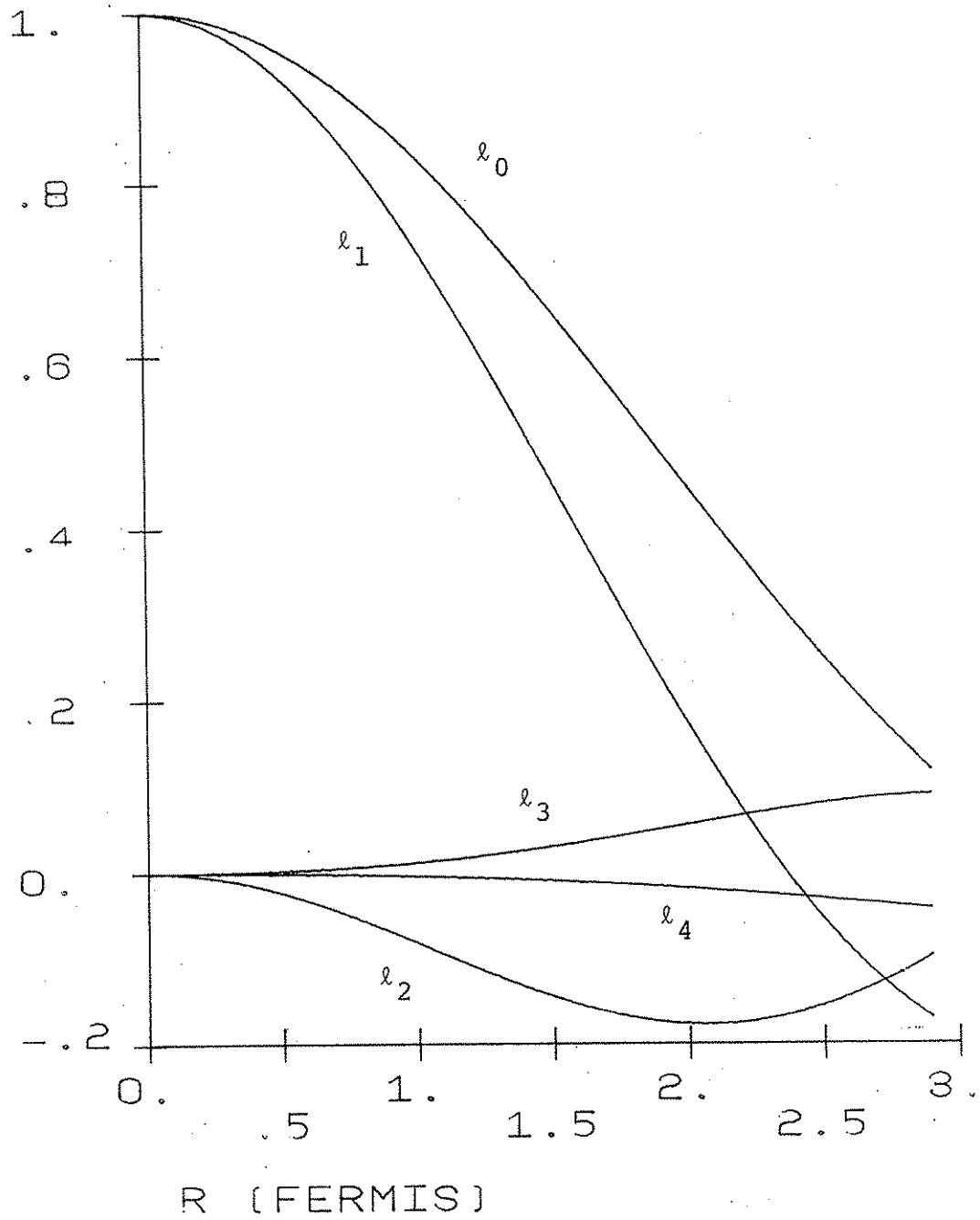
$$\begin{array}{ll}
y_n = \rho_n / \rho & , \quad y_p = \rho_p / \rho \\
l_c = y_n l_n + y_p l_p & , \quad l_\tau = y_n l_n - y_p l_p \\
\langle 1 \rangle_{\text{dir}} = 1 & , \quad \langle \tau \rangle_{\text{dir}} = \beta^2 \\
\langle L^2 \rangle_{\text{dir}} = \frac{r^2}{5} (y_n k_{Fn}^2 + y_p k_{Fp}^2) & , \quad \langle L^2_\tau \rangle_{\text{dir}} = \frac{r^2}{5} \beta^2 (y_n k_{Fn}^2 - y_p k_{Fp}^2) \\
\langle L^4 \rangle_{\text{dir}} = 2 \langle L^2 \rangle_{\text{dir}} + A+B & , \quad \langle L^4_\tau \rangle_{\text{dir}} = 2 \langle L^2_\tau \rangle_{\text{dir}} + A-B \\
A = \frac{12}{175} r^4 \{ y_n^2 k_{Fn}^4 + y_p^2 k_{Fp}^4 \} & \\
B = \frac{1}{175} r^4 y_n y_p \{ 5(k_{Fn}^4 + k_{Fp}^4) + 14 k_{Fn}^2 k_{Fp}^2 \} & \\
\langle 1 \rangle_{\text{ex}} = l_c^2 & , \quad \langle \tau \rangle_{\text{ex}} = l_\tau^2 \\
\langle L^2 \rangle_{\text{ex}} = \langle \vec{r} \cdot \vec{\nabla} \rangle_{\text{ex}} = \frac{1}{2} \vec{r} \cdot \vec{\nabla} l_c^2 & , \quad \langle L^2_\tau \rangle_{\text{ex}} = \langle \vec{r} \cdot \vec{\nabla} \rangle_{\text{ex}} = \frac{1}{2} \vec{r} \cdot \vec{\nabla} l_\tau^2 \\
\langle L^4 \rangle_{\text{ex}} = 2 \langle L^2_{\vec{r} \cdot \vec{\nabla}} \rangle_{\text{ex}} = \frac{1}{2} (\vec{r} \cdot \vec{\nabla})^2 l_c^2 & , \quad \langle L^4_\tau \rangle_{\text{ex}} = 2 \langle L^2_{\vec{r} \cdot \vec{\nabla}} \rangle_{\text{ex}} = \frac{1}{2} (\vec{r} \cdot \vec{\nabla})^2 l_\tau^2
\end{array}$$

The expectation values of L^n and τL^n operators.

Table XIV

β^2	E_{2B}	W_0 (MB)	$E_{2B} + W_0$ (MB)	$A + B\beta^2$
0	-36.88	-3.08	-39.97	*
.1	-35.14	-3.02	-38.17	-38.13
.2	-33.40	-2.95	-36.36	-36.29
.3	-31.65	-2.88	-34.54	-34.45
.4	-29.90	-2.81	-32.71	-32.61
.5	-28.13	-2.74	-30.88	-30.77
.6	-26.36	-2.67	-29.03	-28.93
.7	-24.57	-2.60	-27.18	-27.09
.8	-22.77	-2.53	-25.31	-25.25
.9	-20.96	-2.46	-23.41	*
.99	-19.29	-2.39	-21.68	-21.76

The calculated E_{2B} and W_0 (MB) at $\rho = .159 \text{ fm}^{-3}$ at various values of β^2 . The coefficients A and B of the last column are determined from $E_{2B} + W_0$ (MB) at $\beta^2 = 0$ and .9.





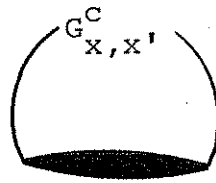
33.1



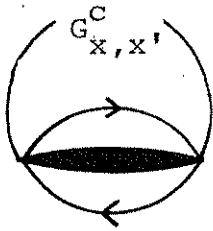
33.2



33.3



33.4



33.5



33.6

D. Calculation of Central Correlation Chains and W_0 (MB)

The central correlation chains are treated in the FHNC approximation. In asymmetric matter we must keep track of neutron and proton exchange loops separately. This is done by classifying the chains as: G_{dd}^n , G_{de}^n , G_{de}^p , G_{ee}^{nn} , G_{ee}^{np} , G_{ee}^{pp} , G_{cc}^n and G_{cc}^p . The subscripts, d for direct, e for closed exchange loop and c for incomplete chain of exchanges, specify the exchange patterns at the ends of the chain. The superscripts, n for neutron and p for proton, specify the type of exchange loops at the ends. The G_{de}^n has a neutron exchange loop at one end; G_{ee}^{np} has a neutron loop at one end and a proton loop at the other, and G_{cc}^p has incomplete proton exchange chain etc.

The derivation of the equations for the G's is quite straightforward, and hence we merely give the results. In the following equation λ, μ can be n or p.

We define the generalized Slater functions:

$$L_\mu = -l_\mu + 2G_{cc}^\mu ; \quad (5.25)$$

and partial distribution functions:

$$g_{dd} = (f^c)^2 \exp(G_{dd}) , \quad (5.26)$$

$$g_{de}^\mu = g_{dd} G_{de}^\mu , \quad (5.27)$$

$$g_{ee}^{\mu\lambda} = g_{dd} (G_{de}^\mu G_{de}^\lambda + G_{ee}^{\mu\lambda} - \frac{1}{2} L_\mu^2 \delta_{\lambda\mu}) , \quad (5.28)$$

$$g_{cc}^\mu = \frac{1}{2} g_{dd} L_\mu ; \quad (5.29)$$

and the link functions:

$$X_{dd} = g_{dd} - G_{dd} - 1 , \quad (5.30)$$

$$X_{de}^{\mu} = g_{de}^{\mu} - G_{de}^{\mu} , \quad (5.31)$$

$$X_{cc}^{\mu} = \frac{1}{2} (g_{dd}^{-1}) L_{\mu} , \quad (5.32)$$

$$X_{ee}^{\lambda\mu} = g_{ee}^{\lambda\mu} - G_{ee}^{\lambda\mu} . \quad (5.33)$$

The integral operators that join links at neutron or proton vertices are given by:

$$\Theta_{\mu}(X(r_{ik}); Y(r_{kj})) = \rho_{\mu} \int d^3 r_k X(r_{ik}) Y(r_{kj}) . \quad (5.34)$$

The chain equations are obtained as:

$$G_{dd} = \sum_{v=n,p} [\Theta_v(X_{dd} + X_{de}^v; g_{dd}^{-1}) + \Theta_v(X_{dd}; g_{de}^v)] , \quad (5.35)$$

$$G_{de}^{\mu} = \sum_{v=n,p} [\Theta_v(X_{dd} + X_{de}^v; g_{de}^{\mu}) + \Theta_v(X_{dd}; g_{ee}^{v\mu})] , \quad (5.36)$$

$$G_{ee}^{\lambda\mu} = \sum_{v=n,p} [\Theta_v(X_{ed}^{\lambda} + X_{ee}^{\lambda v}; g_{de}^{\mu}) + \Theta_v(X_{ed}^{\lambda}; g_{ee}^{v\mu})] , \quad (5.37)$$

$$G_{cc}^{\mu} = \Theta_{\mu}(X_{cc}^{\mu}; g_{cc}^{\mu}) . \quad (5.38)$$

These chain functions are used to calculate the FHNC contribution to W_0 (MB) represented by diagrams of type (33.4, 33.5) of Fig. 33. The main contribution of these diagrams is thought to come from terms having i, j and $k \leq 6$. The terms having i, j or $k > 6$ give relatively smaller contribution to W_{2B} , and we neglect their contribution to W_0 (MB) in the present work.

With the l_c, l_r, y_p and y_n of Table XIII we define:

$$G_{c,de} = y_n G_{de}^n + y_p G_{de}^p , \quad (5.39)$$

$$G_{c,ee} = y_n^2 G_{ee}^{nn} + y_p^2 G_{ee}^{pp} + 2y_p y_n G_{ee}^{np}, \quad (5.41)$$

$$G_{\tau,ee} = y_n^2 G_{ee}^{nn} + y_p^2 G_{ee}^{pp} - 2y_p y_n G_{ee}^{np}, \quad (5.42)$$

$$L_c = y_n L_n + y_p L_p, \quad (5.43)$$

$$L_\tau = y_n L_n - y_p L_p, \quad (5.44)$$

$$h^c = \exp(G_{dd}^c). \quad (5.45)$$

The contribution of W_0 (MB) diagrams 33.4 and 33.5 of Fig. 33 is given by:

$$\begin{aligned} W_0^{(MB)}{}_{33.4} = & \frac{\rho}{2} \sum_{i,j,k=1,6} \int d^3r \{ C(f^i_0 f^j_0 f^k_0) \\ & \times \{ h^c [1 + 2G_{c,de} + G_{c,ee} + (G_{c,de})^2] - 1 \} \\ & + T(f^i_0 f^j_0 f^k_0) [h^c [\beta^2 + 2G_{\tau,de} + G_{\tau,ee} + (G_{\tau,dc})^2] - \beta^2] \} \end{aligned} \quad (5.46)$$

$$\begin{aligned} W_0^{(MB)}{}_{33.5} = & -\frac{\rho}{8} \sum_{i,j,k=1,8} \sum_{n=1,4} \int d^3r \{ C(O^n f^i_0 f^j_0 f^k_0) (h^c L_c^2 - \ell_c^2) \\ & + T(O^n f^i_0 f^j_0 f^k_0) (h^c L_\tau^2 - \ell_\tau^2) \}. \end{aligned} \quad (5.47)$$

The calculated W_0 (MB) at $\rho = .159 \text{ fm}^{-3}$ is given in Table XIV, it is quite linear in β^2 .

Note that the W_0 (MB) in Table XI differs from that in Table XIV at $\beta = 0$ and 1. In the calculation of nuclear and neutron matter⁶⁷⁾ we include i) some of the terms having one or more of i, j and $k = 7, 8$, and ii) single operator rings in the links of FHNC.⁹⁾ Both these small effects are neglected here.

E. β -Dependence of W_c and W_s

The three-body diagrams give the largest contribution to W_c and W_s , and hence we first discuss their β -dependence. Any product Π of any number of O_{12} , O_{23} and O_{31} operators can be reduced by repeated use of the Pauli identity to the form:

$$\begin{aligned} \Pi = C(\Pi) + \sum_{i < j \leq 3} T_{ij}(\Pi) \tau_i \tau_j + B \tau_1 \cdot \tau_2 \times \tau_3 \\ + \text{terms having } \sigma_{i=1,3} \text{ operators.} \end{aligned} \quad (5.48)$$

In direct diagrams the $\langle \Pi \rangle$ is simply

$$\langle \Pi \rangle = \langle C(\Pi) \rangle + \beta^2 \sum_{i < j \leq 3} \langle T_{ij}(\Pi) \rangle ; \quad (5.49)$$

the $\tau_1 \cdot \tau_2 \times \tau_3$ gives zero contribution. Hence, to the extent the β dependence of the f^P can be neglected, the contributions of all three-body direct W_c and W_s diagrams have only β^0 and β^2 terms.

Exchange three body diagrams involve the functions l_c and l_t , and in principle their contribution can have $\beta^{n \geq 4}$ terms. However they appear to be small. For example the contribution of the important W_c exchange diagram 33.6 of Fig. 33, is given by ($j, p = \sigma$ or t)

$$-\frac{1}{8} \rho^2 A^j \int_{12}^c v_{12}^j \tau_{12}^p \tau_{23}^p \tau_{13}^p (3l_c^2 - l_t^2)_{13} d^3 r_{12} d^3 r_{13} . \quad (5.50)$$

To extract the β dependence we expand $3l_c^2 - l_t^2$ in powers of β^2 :

$$3l_c^2 - l_t^2 = 3l_0^2 + (6l_0 l_2 - l_1^2) \beta^2 + (3l_2^2 - 2l_1 l_3 + 6l_0 l_4) \beta^4 . \quad (5.51)$$

The function multiplying β^4 is much smaller than that multiplying β^2 in the above expansion, and so we may expect these contributions to have only β^0 and β^2 terms. At $k_F = 1.33 \text{ fm}^{-1}$ and $r < 2 \text{ fm}$ the coefficient

of β^4 in (5.51) is $< 5\%$ of that of the β^2 term.

It can be shown that in three-body W_c or W_s diagrams with exchanges, the β^4 terms can come only through the $l_i \geq 2$ functions. The contribution of such diagrams has a product of operators Π that can be reduced to the form 5.48. It is convenient to include in this product the spin exchange operators $\frac{1}{2}(1+\sigma_i \cdot \sigma_j)$, but treat the isospin exchange explicitly. One then has to consider the eight different possibilities in which the particles 1, 2 and 3 in the right hand Ψ are nnn, nnp, npn, pnn, ppp, ppn, pnp and npp. The contribution for any given possibility can be written as an integral containing the β -dependence via the y_n, y_p, l_n and l_p . The sum of the contributions of all the eight possibilities can be expressed, as is done to obtain Eq. (5.50), with an integral containing l_c, l_τ and β . To the extent all but l_0 and l_1 can be neglected the contribution has only β^0 and β^2 terms.

Four-body W_c and W_s diagrams can give β^4 terms. However, their contribution is small (~ 1 MeV), and so their β^4 terms should also be small. The β -dependence of four-body spin-isospin and tensor-isospin direct single operator chain diagrams is easy to calculate with the following method. The β -dependence comes from the product Π of the four $\tau_i \cdot \tau_j$ operators in the chain. The contribution depends upon the order of the four $\tau_i \cdot \tau_j$ operators in Π , and the total contribution is the sum of their contributions in all possible orders. Let us consider the simple order:

$$\begin{aligned} & \tau_1 \cdot \tau_2 \tau_2 \cdot \tau_3 \tau_3 \cdot \tau_4 \tau_4 \cdot \tau_1 \\ & = \tau_{1i} \tau_{1\ell} \tau_{2i} \tau_{2j} \tau_{3j} \tau_{3k} \tau_{4k} \tau_{4\ell} \end{aligned} \quad (5.52)$$

In asymmetric matter the $\langle \tau_i \tau_j \rangle$ is given by the matrix Q_{ij}

$$\langle \tau_i \tau_j \rangle = Q_{ij} = \begin{matrix} 1 & i\beta & 0 \\ -i\beta & 1 & 0 \\ 0 & 0 & 1 \end{matrix}, \quad (5.53)$$

$$\langle \tau_j \tau_i \rangle = Q_{ij}^*, \quad (5.54)$$

and the contribution of term (5.52) is given by $\text{Tr}(Q^* Q Q Q)$.

Both Q and Q^* can be diagonalized simultaneously to the form:

$$\begin{matrix} 1 & 0 & 0 \\ 0 & 1-\beta & 0 \\ 0 & 0 & 1+\beta \end{matrix} \quad \text{and} \quad \begin{matrix} 1 & 0 & 0 \\ 0 & 1+\beta & 0 \\ 0 & 0 & 1-\beta \end{matrix},$$

and so the Tr of a $(n-s)$ Q matrices and s Q^* matrices is given by:

$$\text{Tr}(Q^{n-s} (Q^*)^s) = 1 + (1+\beta)^s (1-\beta)^{n-s} + (1-\beta)^s (1+\beta)^{n-s}. \quad (5.55)$$

The expectation value of a product of n $\tau_a \cdot \tau_b$ operators forming an SOR in any order has the form (5.55) with a value of s , in range 1 to $n-1$ determined by the order. Thus the expectation value of the symmetrized product is given by:

$$\langle S(\tau_1 \cdot \tau_2 \tau_2 \cdot \tau_3 \dots \tau_n \cdot \tau_1) \rangle = \sum_{s=1, n-1} P_s^n (1 + (1+\beta)^s (1-\beta)^{n-s} + (1-\beta)^s (1+\beta)^{n-s}), \quad (5.56)$$

where P_s^n gives the probability of all orders whose expectation value contains s Q^* matrices. The P_s^n can be obtained from the recursion relation:

$$P_n^s = \frac{1}{n-1} [s P_s^{n-1} + (n-s) P_{s-1}^{n-1}], \quad (5.57)$$

and

$$P_0^2 = P_2^2 = 0, \quad P_1^2 = 1. \quad (5.58)$$

Equation (5.56) gives the β -dependence of four-body spin-isospin and tensor-isospin direct single operator rings as:

$$\langle S(\tau_1 \cdot \tau_2 \tau_2 \cdot \tau_3 \tau_3 \cdot \tau_4 \tau_4 \cdot \tau_1) \rangle = 3 - \frac{8}{3} \beta^2 + \frac{2}{3} \beta^4 . \quad (5.59)$$

The coefficient of β^4 is non zero, but it is reasonably small. Hence we may expect that the order of magnitude of the β^4 term is probably smaller than the contribution of four-body terms (which is ~ 1 MeV at $k_F = 1.33 \text{ fm}^{-1}$). Earlier calculations^{65,66} also find that the β^4 term in nuclear matter energy at $k_F = 1.33 \text{ fm}^{-1}$ is less than 1 MeV.

REFERENCES

1. At. data and Nuclear Tables 17, 5-6 (1976).
2. D. H. Youngblood, Bull. Am. Phys. Soc. 23, 42 (1978).
D. H. Youngblood, C. M. Rozsa, J. M. Moss, D. R. Brown and J. D. Bronson, Phys. Rev. Lett. 39, 1188 (1977).
3. M. H. Kalos, Phys. Rev. A2, 250 (1970)
M. H. Kalos, D. Levesque, L. Verlet, Phys. Rev. A9, 2178 (1974).
4. H. A. Bethe, Annual Rev. Nucl. Sci. 21, 93 (1971).
5. B. D. Day, Rev. Mod. Phys. 39, 719 (1967).
6. B. D. Day, Rev. Mod. Phys. 50, 495 (1978).
7. R. Jastrow, Phys. Rev. 98, 1479 (1955).
8. V. R. Pandharipande and K. E. Schmidt, Phys. Rev. A15, 2488 (1977).
9. V. R. Pandharipande and R. B. Wiringa, Rev. Mod. Phys. 51, 821 (1979).
10. E. Feenberg, Theory of Quantum Liquids, Academic N.Y. (1969).
11. J. W. Clark, Prog. in Part. and Nucl. Phys. Vol. 2, ed. D. Wilkinson Pergamon, Oxford (1979).
12. K. A. Brueckner, C. A. Levinson and H. M. Mahamoud, Phys. Rev. 95, 217 (1954).
13. J. Goldstone, Proc. Roy. Soc. (London) A239, 267 (1957).
14. R. V. Reid, Ann. Phys. (N.Y.) 50, 411 (1968).
15. B. H. Brandow, Phys. Rev. 152, 863 (1966).
16. H. A. Bethe, Phys. Rev. 138 B, 804 (1965).
17. B. D. Day, Phys. Rev. 151, 826 (1966).
18. B. D. Day, Phys. Rev. 187, 1269 (1969).
19. K. R. Lassey and D. W. Sprung, Nucl. Phys. A177, 125 (1971).
20. J. M. Van Leeuwen, J. Groeneveld, de Boer, Physica 25, 792 (1959).

21. K. E. Schmidt and V. R. Pandharipande, Nucl. Phys. A238, 240 (1979).
22. H. A. Bethe, invited talk at the Urbana workshop on Nuclear and Dense Matter (unpublished) (1977).
23. V. R. Pandharipande and R. B. Wiringa, Nucl. Phys. A266, 269 (1976).
24. R. B. Wiringa and V. R. Pandharipande, Nucl. Phys. A299, 1 (1978).
25. R. B. Wiringa and V. R. Pandharipande, Nucl. Phys. A317, 1 (1979).
26. R. B. Wiringa and V. R. Pandharipande, Phys. Lett. (1981) in press.
27. J. C. Owen, Ann. Phys. (New York) 118, 373 (1979).
28. R. B. Wiringa, Nucl. Phys. A338, 57 (1980).
29. J. Lomnitz-Adler and V. R. Pandharipande, Nucl. Phys. A342, 404 (1980).
30. M. Lacombe, B. Loiseau, J. M. Richard, R. Vinh Mau, J. Cole, P. Pires, R. de Tournell, preprint (1979).
31. H. Primakoff, Phys. Rev. 53, 938 (1938).
32. G. E. Brown, A. M. Green and W. J. Gerare, Nucl. Phys. A115, 435 (1968).
33. B.H.J. McKellar and R. Rajaraman, Mesons in Nuclei, eds. M. Rho and D. H. Wilkinson, North-Holland (1979).
34. G. E. Brown and A. D. Jackson, The Nucleon-Nucleon Interaction, North-Holland (1976).
35. A. M. Green and P. Haapakoski, Nucl. Phys. A221, 429 (1974).
36. T. Hamada and I. D. Johnston, Nucl. Phys. 34, 382 (1962).
37. C. N. Brussel, A. K. Kerman and B. Rouben, Nucl. Phys. A124, 624 (1969).
38. R. A. Arndt, R. H. Hackman and L. D. Roper, Phys. Rev. C15, 1002 (1977).
39. R. A. Arndt, Private Communication (1978) (as quoted in Ref. 3).

40. D. V. Bugg, J. A. Edgington, C. Amster, R. C. Brown, C. J. Oram and K. Shakarchi, *J. of Phys.* G4, 1025 (1978)
D. V. Bugg, J. A. Edgington, W. R. Gibson, N. Wright, N. M. Stewart, A. S. Clough, D. Axen, G. A. Ludgate, C. J. Oram, L. P. Robertson, J. R. Richardson and C. Amsler, preprint (1979).
41. G. E. Brown, A. D. Jackson and T.T.S. Kuo, *Nucl. Phys.* A133, 481 (1969).
42. A. C. Phillips, *Rept. on Prog. in Phys.* 40, 905 (1977).
43. R. A. Smith and V. R. Pandharipande, *Nucl. Phys.* A256, 327 (1976).
44. H. E. Conzett, F. Hinterberger, P. von Rossen, F. Seiter and E. J. Stephenson, *Phys. Rev. Lett.* 43, 572 (1979).
45. H. Arenhövel and W. Fabian, *Nucl. Phys.* A282, 397 (1977).
46. S. Galster, H. Klein, J. Moritz, K. H. Schmidt, D. Wegener and J. Bleckwenn, DESY report 71/7 (1971).
47. R. G. Arnold, B. T. Chertok, E. B. Dally, A. Grigorian, C. L. Jordan, W. P. Schütz, R. Zdarko, F. Martin and B. A. Mecking, *Phys. Rev. Lett.* 35, 776 (1975).
48. S. Blatnik and N. Zovko, *Acta Physica Austriaca* 39, 62 (1974).
49. H. J. Weber and H. Arenhövel, *Phys. Reports* 36C, 277 (1978).
50. H. A. Bethe and M. B. Johnson, A230, 1 (1974).
51. B. D. Day, *Nucl. Phys.* A328, 1 (1979).
52. B. D. Day, Invited talk given at the Topical Meeting on the Meson Theory of Nuclear Forces and Nuclear Matter, Bad Honnef (1979).
53. R. A. Brandenburg, Y. E. Kim and A. Tubis, *Phys. Rev.* C12, 1368 (1975).
54. H. Kümmel, K. H. Lührmann and J. G. Zabolitzky, *Phys. Rept.* 36C, 1 (1978).

55. I. Sick, Int. Conf. on Few Body Problems and Nuclear Forces, Graz (1978).
56. G. E. Brown and A. M. Green, Nucl. Phys. A137, 1 (1969).
57. B. A. Loiseau, Y. Nogami and C. K. Ross, Nucl. Phys. A165, 601 (1971).
58. S. A. Coon, M. D. Scadron, P. C. McNamee, B. R. Barrett, D.W.E. Blatt and B.H.J. McKellar, Nucl. Phys. A317, 242 (1979).
59. R. B. Wiringa, private communication.
60. G.-H. Niephaus, M. Gari and B. Sommer, Phys. Rev. C20, 1096 (1979).
61. J. D. Walecka, Ann. Phys. 83, 491 (1974).
62. S. Fantoni and S. Rosati, Nuovo Cimento A25, 593 (1975).
63. B. D. Day (to be published in the Proceedings of the Second International Conference on Recent Progress in Many Body Theories, Mexico City) (1981).
64. Y. Horikawa, M. Thies and F. Lenz, Nucl. Phys. A256, 327 (1976).
65. S. Fantoni and S. Rosati (Nuovo Cimento) in press.
66. P. J. Siemens, Nucl. Phys. A141, 225 (1970)
O. Sjöberg, Nucl. Phys. A222, 161 (1974).
67. B. Friedman and V. R. Pandharipande, to be published.

VITA

Born in Athens, Greece on April 26, 1952, Isaac Elias Lagaris received his bachelor's degree from the University of Ioannina in Ioannina, Greece in August 1975. He entered the University of Illinois in January 1976, where he has been teaching assistant and research assistant. He received the Master of Science degree from the University of Illinois in May, 1977.